# 43

# **Telescopes**

43.1	Introduction 726	
43.2	Refracting Telescopes 727	
43.2.1	Achromatic Refractor Telescopes 727	
43.2.2	Apochromatic Refractor Telescopes 730	
43.2.3	Apochromatic Telescopes Without Anomalous Dispersion Glasses	742
43.3	Reflecting Telescopes 744	
43.4	Single-mirror Reflecting Telescopes 745	
43.4.1	Spherical Mirror 745	
43.4.2	Parabolic Mirror (Newton Telescope) 745	
43.5	Two-mirror Reflecting Telescopes 746	
43.5.1	Cassegrain Telescope 746	
43.5.2	Ritchey–Chretien Telescope 750	
43.5.3	Dall–Kirkham Telescope 750	
43.5.4	Pressmann–Camichel Telescope 751	
43.5.5	Gregorian Telescope 751	
43.5.6	Schwarzschild Aplanatic Telescopes 753	
43.5.7	Couder Anastigmat 756	
43.5.8	Loveday Telescope 756	
43.6	Three-mirror Reflection Telescopes 758	
43.6.1	Paul–Baker Telescope 758	
43.6.2	Willstrop Mersenne–Schmidt Telescope 760	
43.6.3	Korsch Three-mirror, Single-axis Telescope 762	
43.6.4	Robb Three-mirror Telescope 763	
43.6.5	Korsch Three-mirror Four-reflection Telescope 764	
43.7	Other Three- and Four-mirror Reflecting Telescopes 765	
43.8	Two-mirror Schiefspiegler (Oblique Reflector) Telescopes 766	
43.8.1	Kutter Schiefspiegler 767	
43.8.2	Herrig Schiefspiegler 769	
43.8.3	Yolo Telescope 771	
43.9	Three-mirror Schiefspiegler Telescopes 772	
43.9.1	Kutter and Buchroeder Tri-Schiefspiegler 772	
43.9.2	Stevick–Paul Schiefspiegler 773	
43.9.3	Brunn Schiefspiegler 775	

Handbook of Optical Systems: Vol. 4 Survey of Optical Instruments. Edited by Herbert Gross Copyright © 2008 WILEY-VCH Verlag GmbH & Co. KGaA, Weinheim ISBN: 978-3-527-40380-6

43.14.9 Schupmann Medial Telescope 817
43.14.10 Schupmann Brachymedial 821
43.15 Telescopes with Field Correctors 821
43.15.1 Field-flattening Lens 822
43.15.2 Correctors for a Parabolic Mirror (Newton Telescope) 823

43.15.3	Correctors for a Spherical Mirror 825	
43.15.4	Corrector for Cassegrain and RC Telescopes	826
43.15.5	Focal Reducers 827	
43.15.6	Focal Extenders 828	
43.16	The Effects of Aperture Obscuration 829	
43.16.1	Central Obstruction 830	
43.16.2	Spider Obstruction 834	
43.17	Telescope Design Prescriptions 835	
43.18	Literature 861	

## 43.1 Introduction

Telescopes are used to gather light from a distant object and then to form a real image which is viewed using an eyepiece or is captured by a photographic film, CCD, or any other opto-electronic sensor. In this respect there is no fundamental difference from a "conventional" objective (e.g., used in photography when focussed at infinity), except that telescopes typically are characterized by long focal lengths, large apertures and comparatively narrow fields of view.

Notice that a telescope which is used in the reverse direction, i.e., when light is sent from the focal plane through the system and exits as a parallel beam, the system is then called a *collimator*.

Traditionally telescopes are used in conjunction with eyepieces to allow the visual observation of remote objects and to provide an enlarged view. The basic construction of a visual telescope is shown in figure 43-1. Two basic forms can be distinguished:

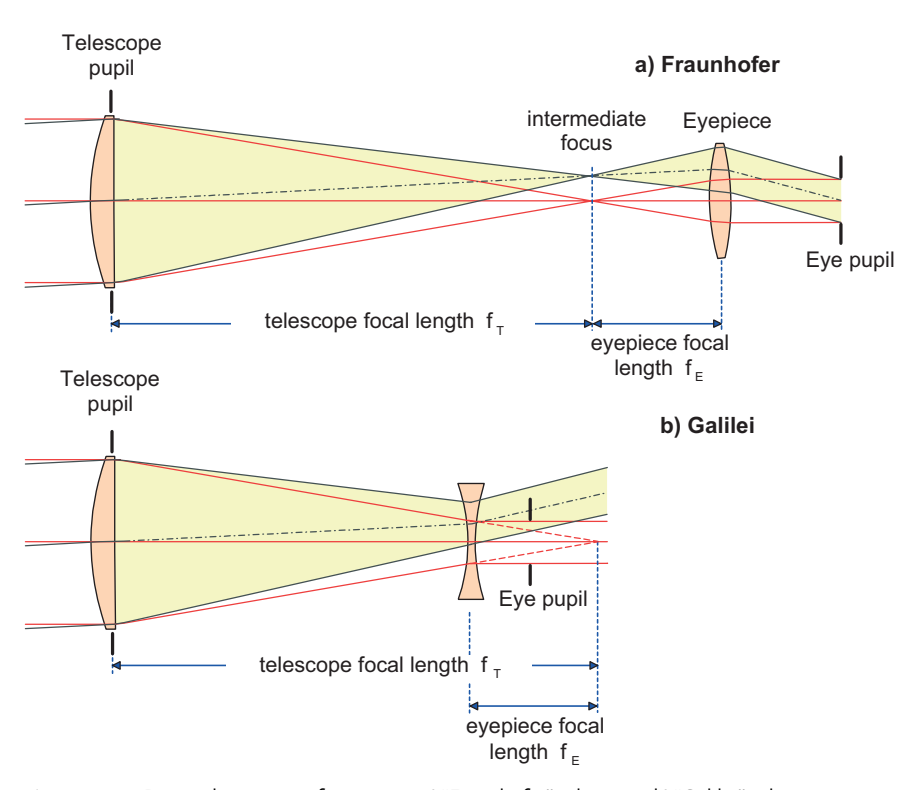


Figure 43-1: Basic telescope configurations: a) "Fraunhofer" telescope; b) "Galilei" telescope.

### Fraunhofer Telescope

In the Fraunhofer type, the image formed by an objective (lens, mirror or both) is imaged to infinity by an eyepiece with positive power. Parallel light rays enter the telescope and exit it on the eyepiece side. The human eye then observes the rays in a "relaxed" condition (i.e., accommodated to infinity).

#### Galilei Telescope

In the Galilei type, the image formed by an objective is imaged to infinity by an eyepiece with negative power. As in the Fraunhofer type, parallel light rays exit on the eyepiece side and the eye is relaxed.

The magnification of a visual telescope is given by

$$\Gamma_{\text{tel}} = \frac{f_{\text{T}}}{f_{\text{E}}} = \frac{D_{\text{EP}}}{D_{\text{AP}}} = \frac{w}{w'},$$
 (43-1)

where  $f_{\rm T}$  is the objective focal length,  $f_{\rm E}$  the eyepiece focal length,  $D_{\rm EP}$  the entrance pupil diameter of the objective (usually lens or mirror diameter),  $D_{AP}$  the exit pupil diameter, w the field angle in object space, and w' the field angle in image space (as seen by the eye).

The presentation and description of telescope designs in the following sections has been made as uniform and consistent as possible. In order to accomplish this, attempts have been made to ensure that:

- the design descriptions and performances are always referred to an entrance pupil diameter of 200 mm, whenever possible,
- an aperture ratio (F-number) F/10 to F/20 is assumed whenever possible,
- the object is always assumed to be at infinity, i.e., parallel beams enter the telescope,
- performance plots (e.g., spot diagrams, point spread functions) are always assumed to be on a flat image surface,
- gray-coded point spread function (PSF) plots are always given at a logarithmic scale in order to work out the faint effects of the side lobes.

# 43.2 **Refracting Telescopes**

#### 43.2.1

#### **Achromatic Refractor Telescopes**

By definition, achromatic telescopes are corrected for identical axial focus positions for two wavelengths, commonly referred to as blue and red. The other part of the visible spectrum which constitutes the "secondary spectrum" remains uncorrected. The definitions of primary, secondary and tertiary spectra are illustrated in figure 43-2.

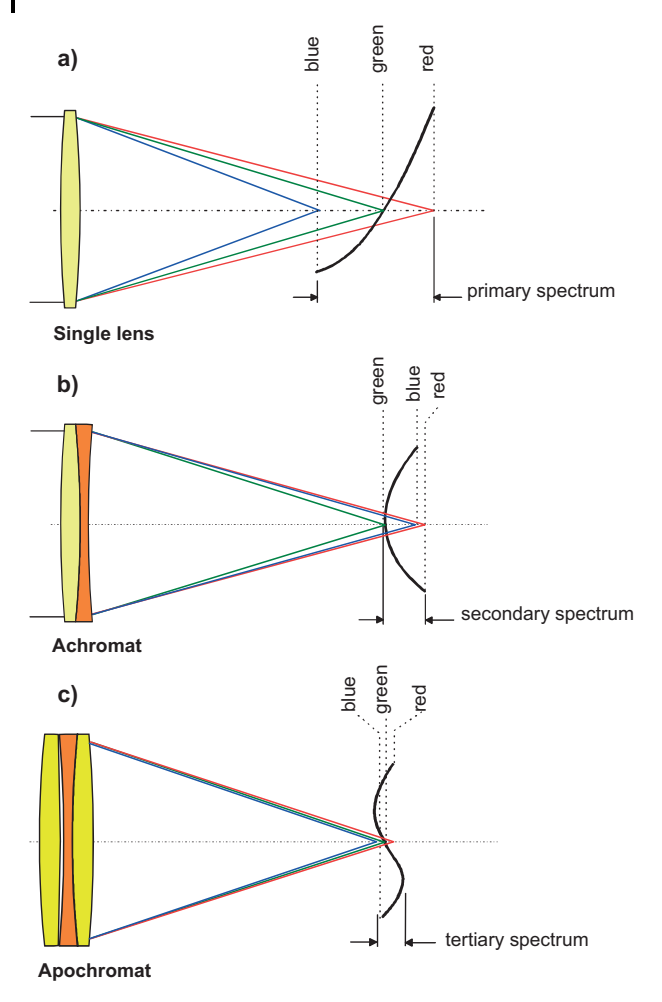


Figure 43-2: a) Primary, b) secondary and c) tertiary spectra (not to scale).

In this section we will be concerned in with refractors utilizing two lenses (and thus, two glass types) only, although solutions with three or more lenses are possible. Three conditions must be fulfilled: for power  $\Phi$ , Petzval sum P and longitudinal color Fl,

$$\Phi = \frac{1}{f} = \Phi_1 + \Phi_2 \,, \tag{43-2}$$

$$P = \frac{\Phi_1}{n_1} + \frac{\Phi_2}{n_2} \,, \tag{43-3}$$

$$Fl = \frac{\Phi_1}{v_1} + \frac{\Phi_2}{v_2} \,, \tag{43-4}$$

where v is the principal dispersion or Abbe number.

From the first and third condition of eqs. (43-2) to (43-4), we write

$$\frac{v_1}{v_2} = -\frac{\Phi_1}{\Phi_2}, \qquad \frac{n_1}{n_2} = \frac{\Phi_1}{\Phi_2}$$
 (43-5)

and finally

$$\frac{v_1}{v_2} = \frac{n_1}{n_2}$$
 (43-6)

This is the condition where the field curvature is corrected (P = 0). It requires glass types which have a high index at low primary dispersion v and vice versa. This relation explains, why "old" achromats exhibit a relatively high Petzval sum (i.e., a strong field curvature), since high-index crown glasses were not available prior to 1950 [43-2].

If we solve for the first and third condition of eqs. (43-2) to (43-4)

$$\Phi_1 = \frac{\frac{\Phi}{n_2} - P}{\frac{1}{v_2} - \frac{1}{v_1}},\tag{43-7}$$

we see that the powers of the individual lenses become smaller, the larger the difference  $\Delta v = |v_2 - v_1|$ . Thus if we want to design for a minimum Petzval sum (i.e., a larger radius of field curvature), we are limited to glasses which exhibit quite a small  $\Delta v$  value. Consequently, the relative powers are high and the more difficult will be the correction of spherical aberration, especially for low F-numbers. For this reason, a two-lens refractor achieves only moderate F-numbers when larger fields are desired.

Of more practical relevance is the requirement for zero longitudinal color. We solve for the first and third condition of eqs. (43-2) to (43-4)

$$\Phi_1 = \frac{\frac{\Phi}{v_2}}{\frac{1}{v_2} - \frac{1}{v_1}},\tag{43-8}$$

and from (43-2) we obtain the power of the second lens

$$\Phi_2 = \Phi - \Phi_1. \tag{43-9}$$

Equation (43-8) requires a pre-selection of the optical glasses depending upon whether it is the correction of the field curvature or chromatic aberration which is preferred. In general, the designer is interested in the amount of residual longitudinal color (the secondary spectrum) which is expressed in units of the focal length

$$\Delta f = \frac{\overline{P}_{F,e1} - \overline{P}_{F,e2}}{\nu_1 - \nu_2} = \frac{\Delta \overline{P}}{\Delta \nu} , \qquad (43-10)$$

where  $\bar{P}_{F,e}$  is the relative partial dispersion in the wavelength interval  $\lambda_F=486\,\mathrm{nm}$ to  $\lambda_e = 546 \, \text{nm}$  defined as [43-66]

$$\bar{P}_{F,e} = \frac{n_F - n_e}{n_F - n_C} \ . \tag{43-11}$$

The partial dispersion is used to express the variation of the refractive index in different parts of the optical spectrum. On a plot of  $\overline{P}$  versus v, eq. (43-10) is the slope of a line that is drawn between two chosen glasses. The amount of secondary residual chromatic aberration is proportional to the slope. As we will see in section 43.2.2, the glasses must have the same partial dispersion if we wish to reduce the secondary spectrum.

For "normal" achromats, i.e., when the glasses lie on the Abbe normal line, the chromatic variations  $\Delta f$  are about 0.05% for wavelengths between 486 nm and 650 nm.

#### 43.2.2

# **Apochromatic Refractor Telescopes**

Historically, the term apochromat was initially introduced by Abbe to mean color correction for three wavelengths and the correction of the sine condition for two colors [43-55]. This means correction of higher-order chromatic aberrations in addition to the axial secondary spectrum.

At this point it is worth clarifying any confusion about the meaning of apochromatism. Systems corrected for three colors in a restricted sense, i.e., those which are corrected for three colors in only the paraxial domain, have sometimes mistakenly been called apochromatic. But in the case of systems with large aperture, this implicit overemphasis on paraxial chromatism is out of place. It is useless to have paraxial chromatism at two, three or even four points of the spectrum, if one ends up with a system in which the spherical aberration varies considerably with the wavelength. This effect is commonly known as sphero-chromatism and is illustrated in figure 43-6. It must be considered during the design phase.

Another relaxed definition may be found in industrial applications, where - for the sake of promotion and sales – apochromatism is frequently defined as "to reduce the axial chromatic aberrations to a level which allows a significantly improved image performance compared with a standard achromat" [43-57]. This definition, however, does not necessarily imply a correction for three wavelengths.

In the following sections, however, in using the term apochromat, we will adhere to the strict correction for axial color for three wavelengths and with both spherical aberration and coma being achromatic (spherochromatism). Nothing is said about the transverse chromatic aberration. The term *superachromat* was introduced by Herzberger to mean that longitudinal chromatic aberration is corrected for four wavelengths [43-25]. We also require that spherical aberration and coma should be apochromatic for a superachromat.

The relations for correction of the paraxial spectrum at three wavelengths will be discussed in the next sections. From the thin-lens approximations, the following condition for perfect color correction of a thin lens doublet can be derived:

 $n_2(\lambda) = a + \beta \cdot n_1(\lambda)$ , which requires that the dispersion curves of two glasses must be related by a *linear* transformation [43-2]. This is not possible with an arbitrary wide wavelength range, and so residual chromatic aberrations will inevitably occur. We will see in section 43-13 about catadioptric designs, that there are special solutions which "imitate" the above requirement.

The design of apochromats and superachromats is the subject of an extensive amount of literature. A good discussion of different methods, unfortunately not entirely free of errors, is given by Mercado [43-54]. Furthermore, relevant publications of Herzberger, Mercado, Maxwell and Sigler [43-25, 43-51, 43-55, 43-74] are recommended.

#### Two-glass Apochromats

Considering only axial chromatic aberrations, the conditions for color correction at three wavelengths are:

$$\Phi = \Phi_1 + \Phi_2 \,, \tag{43-12}$$

$$\frac{\Phi_1}{\nu_1} + \frac{\Phi_2}{\nu_2} = 0, \tag{43-13}$$

$$\frac{\Phi_1}{\nu_1} \overline{P_1} + \frac{\Phi_2}{\nu_2} \overline{P_2} = 0. \tag{43-14}$$

We have three linear equations with two variables ( $\Phi_1$ ,  $\Phi_2$ ). Non-trivial solutions are obtained only with the additional requirement  $\overline{P}_1 = \overline{P}_2$ . The powers for the individual lenses are then

$$\Phi_1 = \frac{1}{1 - \frac{v_2}{v_1}} \Phi \quad \text{and} \quad \Phi_2 = \Phi - \Phi_1.$$
(43-15)

Note that the equation to the left is essentially identical to eq. (43-8). The glasses should have the same relative partial dispersion  $\overline{P}$  (i.e., they lie along a horizontal line in the  $\overline{P} - v$  diagram) but the difference in the primary dispersion  $v_1 - v_2$ should be as large as possible to keep the individual refractive powers low. This requires that at least one optical glass has anomalous partial dispersion, i.e., it deviates from the Abbe normal line (the green line in figure 43-3). Unfortunately, the range of possible glasses for two-glass apochromats is limited. Likely candidates are the fluor-crown, the phosphate-crown and the lanthanum-crown families and, in particular, crystals like calcium fluorite. Only the fluor-crown, phosphate-crown glasses (for example, the FK and PK family from the Schott catalog) and calcium fluorite, permit larger v-differences such that the powers of the lenses can be kept relatively small (see figure 43-3).

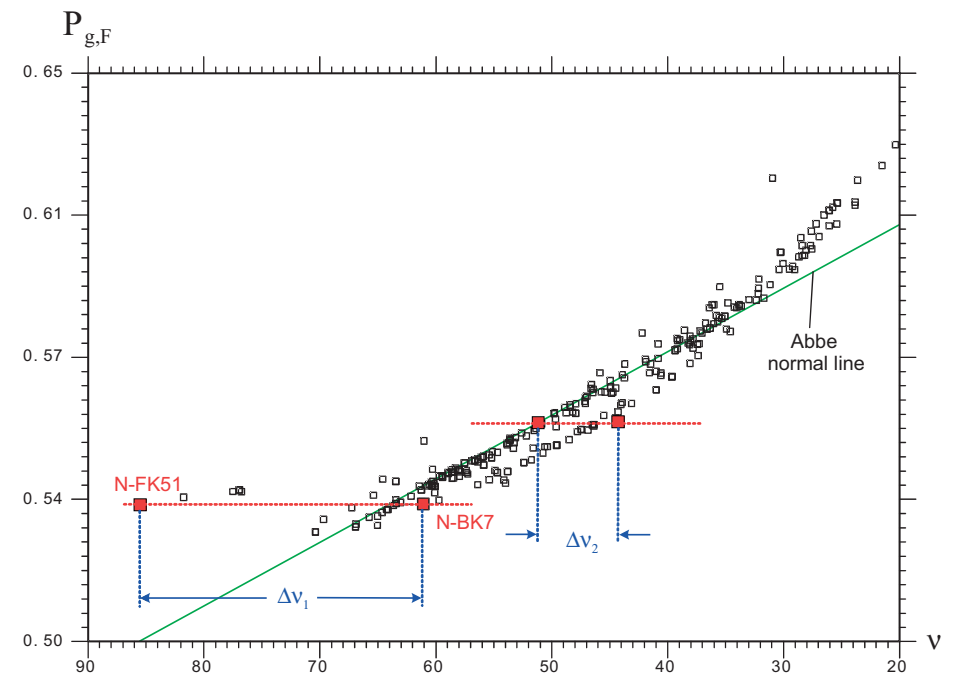


Figure 43-3: Glass selection for a two-lens apochromat in the  $\overline{P}-\nu$  domain. The lens powers depend on  $\Delta\nu$ . For example,  $\Delta\nu_1$  allows relatively small lens powers, while  $\Delta\nu_2$  requires larger powers, thus resulting in larger amounts of spherical aberration and spherochromatism.

#### **Design Examples**

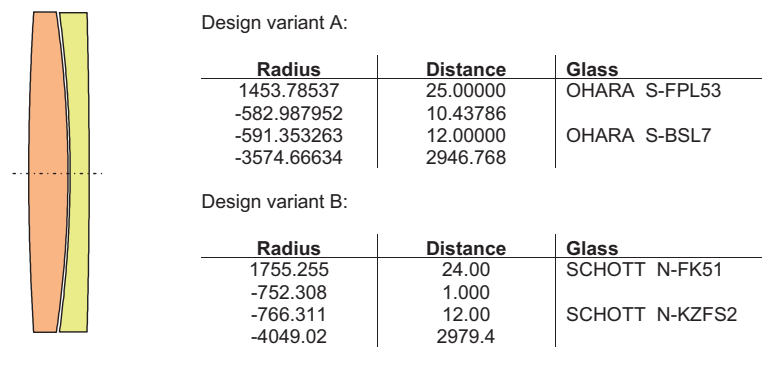
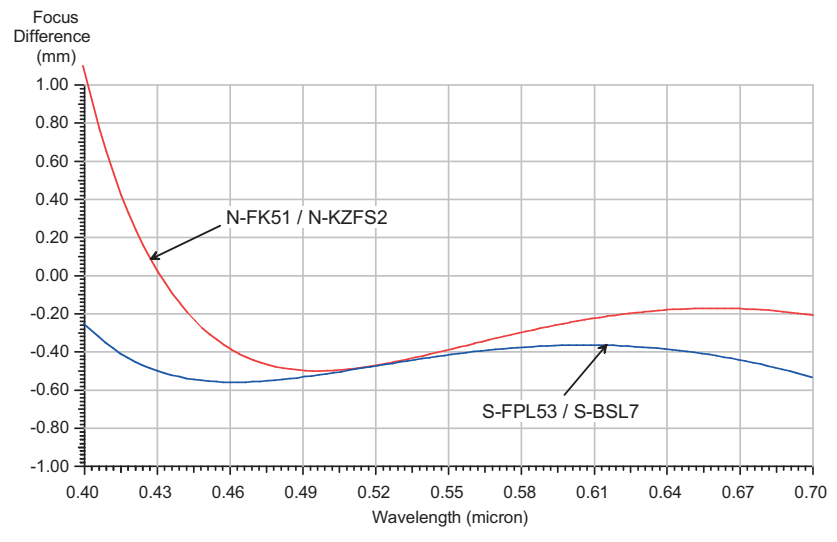
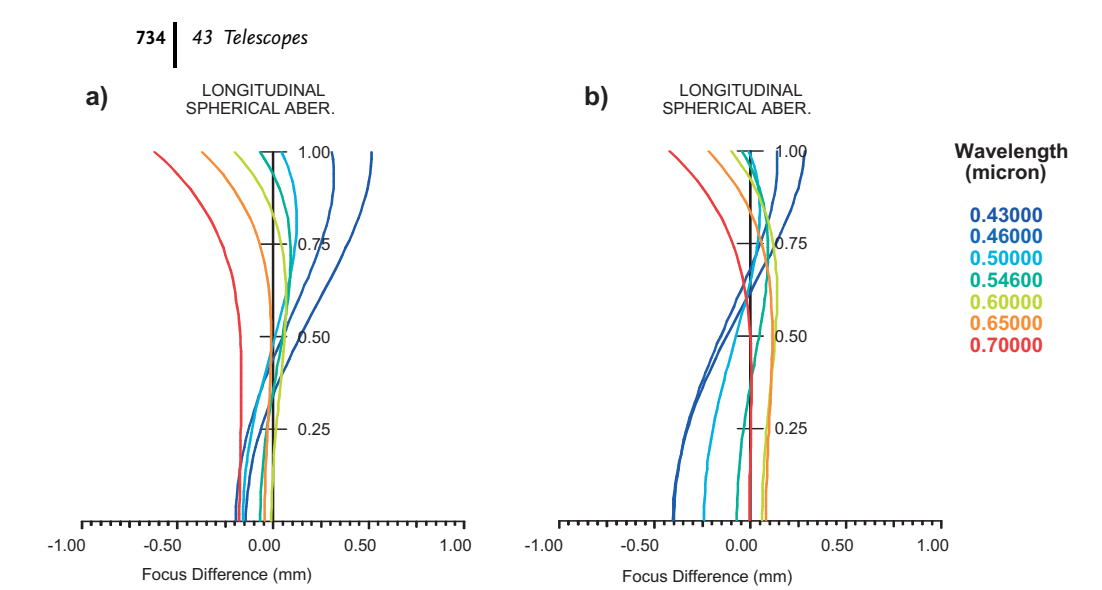


Figure 43-4: Design examples of F/15 apochromatic refractor objectives using only two glasses.



**Figure 43-5:** *Paraxial* logitudinal chromatic focus shift (secondary/tertiary spectrum) of the two apochromatic examples shown in figure 43-4.

The two apochromatic designs given in figure 43-4 nicely illustrate the effect of chromatic variation of the spherical aberration (spherochromatism). The longitudinal chromatic focus variations as depicted in figure 43-5 only consider *paraxial* effects, thereby neglecting higher-order effects. Figure 43-6(a) shows the longitudinal spherical aberration at seven discrete wavelengths over the visible spectrum. Whereas the paraxial focus difference is small and reflects the tertiary spectrum in figure 43-5 (blue curve), the spherical aberration varies significantly with wavelength when the paraxial domain is left (spherochromatism). A more balanced result is achieved if one deviates slightly from perfect (paraxial) apochromatism in favor of a higher-order spherical aberration variation (figure 43-6(b)). In air-spaced apochromats, adjusting the air space helps to reduce this effect.



**Figure 43-6:** Variation of longitudinal spherical aberration at seven discrete wavelengths. (a) Corrected for minimum paraxial chromatic aberration; (b) balanced aberrations in paraxial domain and at full aperture.

Figures 43-7and 43-8 show spot diagrams and diffraction point spread functions (PSF) of the two-glass designs presented in figure 43-4. As the secondary spectrum plot (figure 43-5) indicates, the S-FPL53/S-BSL glass combination yields a better correction of the longitudinal focus at shorter ("blue") wavelengths.

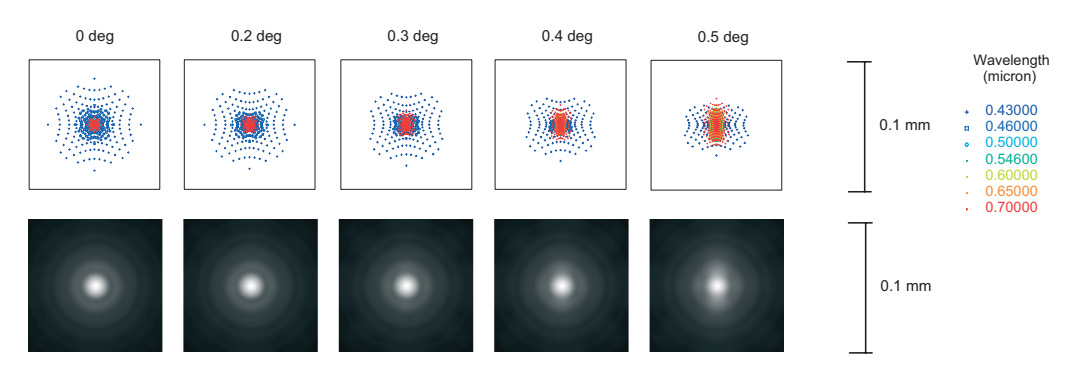
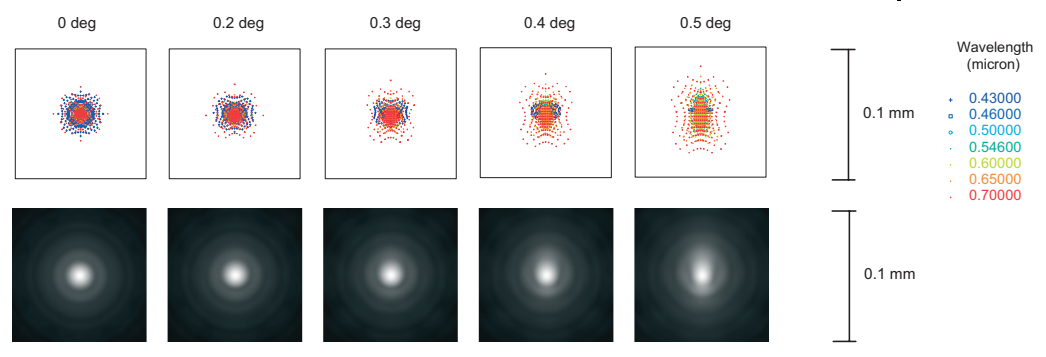


**Figure 43-7:** Spot diagram (top) and diffraction PSF (bottom) of a two-glass apochromatic refractor telescope. See variant A in figure 43-4.



Spot diagram (top) and diffraction PSF (bottom) of a two-glass apochromatic refractor telescope. See variant B in figure 43-4.

### Three-glass Apochromats

The conditions under which three lenses can be achromatized for three wavelengths are [43-21], [43-33]:

$$\Phi = \Phi_1 + \Phi_2 + \Phi_3 \,, \tag{43-16}$$

$$\frac{\Phi_1}{\nu_1} + \frac{\Phi_2}{\nu_2} + \frac{\Phi_3}{\nu_3} = 0, \tag{43-17}$$

$$\frac{\Phi_1}{\nu_1} \overline{P_1} + \frac{\Phi_2}{\nu_2} \overline{P_2} + \frac{\Phi_3}{\nu_3} \overline{P_3} = 0. \tag{43-18}$$

We have three equations with three variables. Solving for the individual powers we get

$$\Phi_1 = \frac{v_1(\overline{P}_3 - \overline{P}_2)}{N} \Phi, \qquad (43-19)$$

$$\Phi_2 = \frac{v_2(\overline{P}_1 - \overline{P}_3)}{N} \Phi, \qquad (43-20)$$

$$\Phi_3 = \frac{v_3(\overline{P}_2 - \overline{P}_1)}{N} \Phi, \qquad (43-21)$$

with

$$N = \nu_1(\overline{P}_3 - \overline{P}_2) + \nu_2(\overline{P}_1 - \overline{P}_3) + \nu_3(\overline{P}_2 - \overline{P}_1). \tag{43-22}$$

Equation (43-22) may be written as a determinant of the square matrix of the form

$$N = \operatorname{Det} \begin{bmatrix} 1 & v_1 & \overline{P}_1 \\ 1 & v_2 & \overline{P}_2 \\ 1 & v_2 & \overline{P}_3 \end{bmatrix} . \tag{43-23}$$

In applying eqs (43-19)-(43-22), it is desirable that the combination of optical glasses be selected not only to correct the chromatic aberration, but also to make the individual powers of the lenses small. Since N appears in the denominator of egs (43-19)–(43-21), the individual powers will be as weak as possible for a large value of N. Also, these equations imply a geometrical representation of N in the  $\nu - \overline{P}$  plot, where the quantity *N* may be interpreted as twice the area of the triangle defined by the three glasses. Thus it is desirable to have a large triangle area which will result in small powers within the three lens elements.

From a practical point of view, glass selection on the basis of equations of power can be rather cumbersome, although it may easily be implemented in computer code for rapid evaluation. If we look at the  $v-P_{\rm g,F}$  plot of real glasses, as given in figure 43-3, we see that most glasses fall into a narrow range with  $\Delta P/\Delta v$  being nearly constant. The few glasses which are away from the "normal" line (the socalled "Abbe" line) are usable as apochromats. The main obstacle is the small v difference which implies strong lens powers. In order to match for the partial dispersions, two glasses can be combined to simulate an equivalent partial dispersion. The element powers can be found from [43-20]

$$v_x = \frac{v_1(\overline{P}_2 - \overline{P}_3) + v_2(\overline{P}_3 - \overline{P}_1)}{\overline{P}_2 - \overline{P}_1}, \tag{43-24}$$

$$\Phi_3 = \frac{\nu_3}{\nu_3 - \nu_x} \,, \tag{43-25}$$

$$\Phi_2 = \frac{(1 - \Phi_3)(\overline{P}_3 - \overline{P}_1)\nu_2}{\nu_2(\overline{P}_3 - \overline{P}_1) + \nu_1(\overline{P}_2 - \overline{P}_3)},$$
(43-26)

$$\Phi_1 = 1 - \Phi_2 - \Phi_3 \,. \tag{43-27}$$

### **Design Examples**

#### Design variant A:



Radius	Distance	Glass
1330.126	13.33	SCHOTT N-K5
777.406	22.66	CaF2
-1314.439	13.33	SCHOTT N-BAK2
-3984.702	2971.23	

# Design variant B:



Radius	Distance	Glass
1185.592	25.00	OHARA S-BSL7
-1107.850	14.00	OHARA S-NBM51
388.704	0.50	
378.391	25.00	OHARA FTM8
-3442.665	2963.497	
-1036.701		

Glass selection derived from JP 57073713.

**Figure 43-9:** Sample designs of apochromatic refractor telescopes using three different glass types.

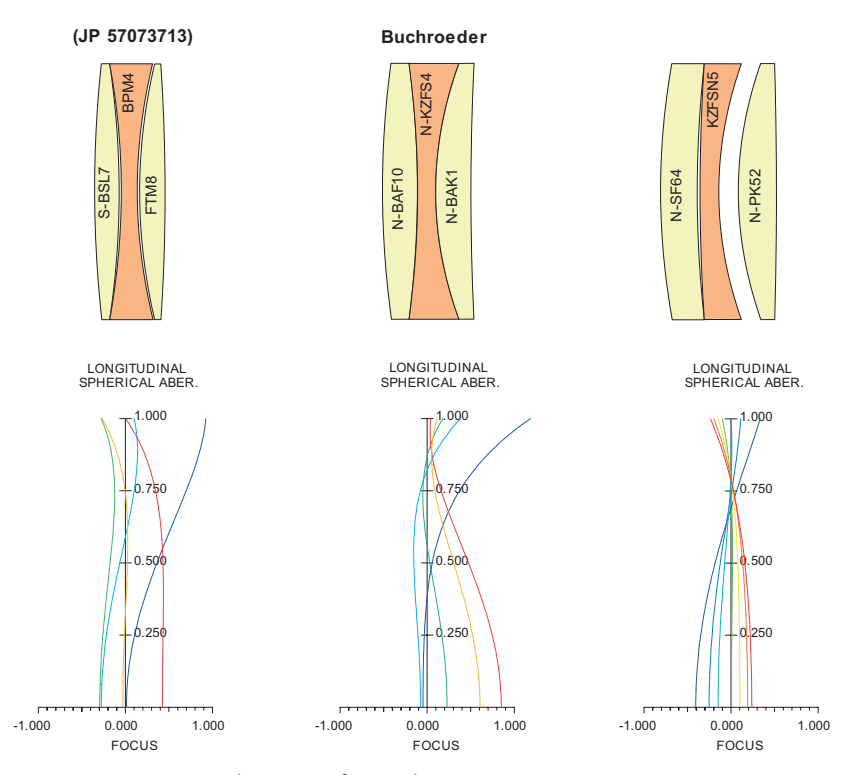


**Figure 43-10:** More apochromatic refractor objectives. Longitudinal aberrations are given for F10/2000 mm systems.

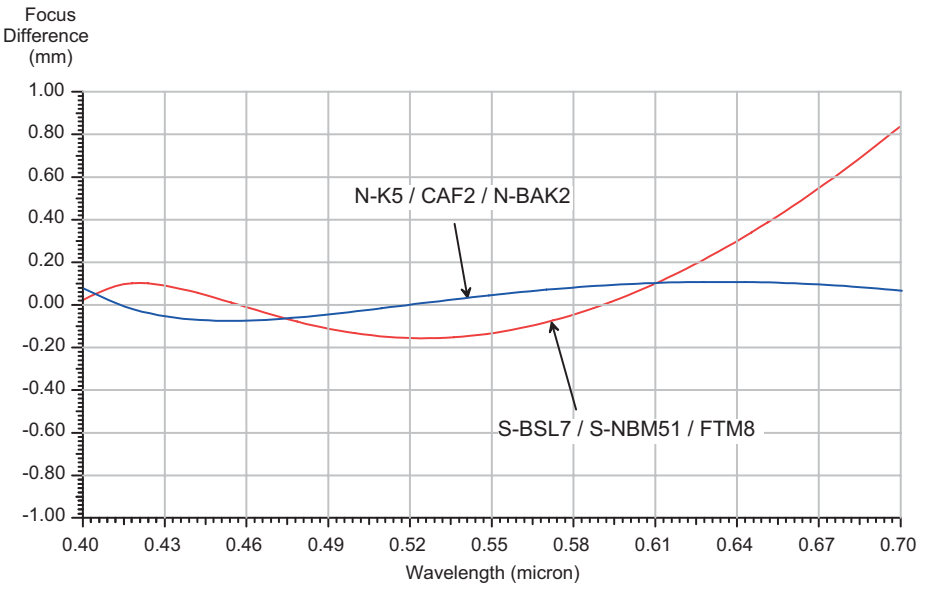


**Figure 43-11:** *Paraxial* logitudinal chromatic focus shift (secondary/tertiary spectrum) of the three-glass apochromatic examples shown in Fig. 43-9.

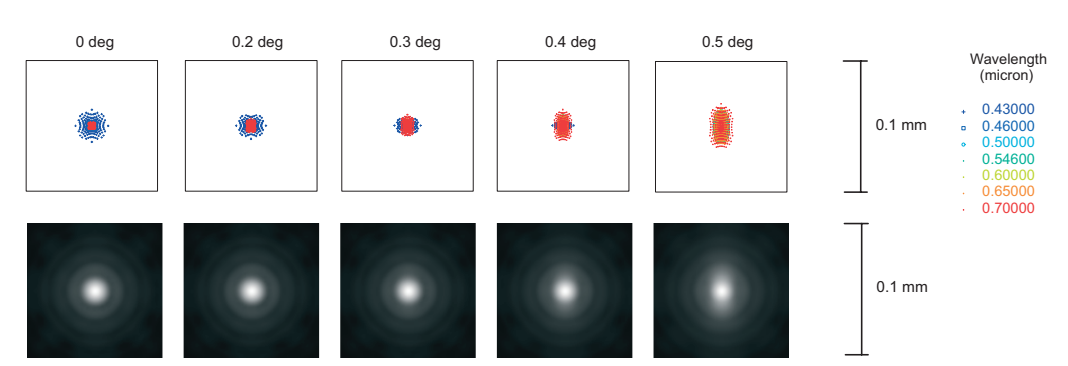


**Figure 43-12:** Spot diagram (top) and diffraction PSF (bottom) of a three-glass apochromatic refractor telescope according to variant A in Fig. 43-9.

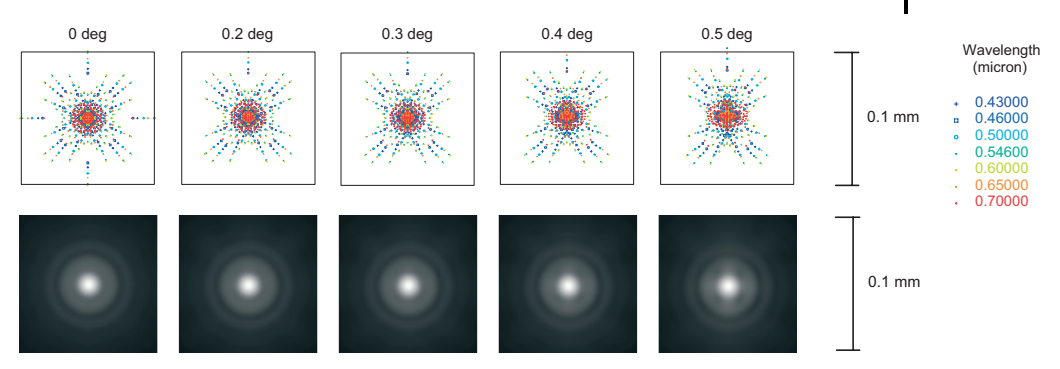


Figure 43-13: Spot diagram (top) and diffraction PSF (bottom) of a three-glass apochromatic refractor telescope according to variant B in Fig. 43-9.

# Superachromats

Following the definition of Herzberger [43-25], we require four wavelengths at a common focus for a superachromat. A better term for superachromat would be superapochromate, since it outperforms the apochromat but does not necessarily rival the achromate.

For a three-lens system corrected at four wavelengths, the relative partial dispersions at different wavelength intervals must match. We adopt eqs (43-16)–(43-17) and extend eq. (43-18) for two separate wavelength intervals, thus obtaining eqs (43-30) and (43-31):

$$\Phi = \Phi_1 + \Phi_2 + \Phi_3 \,, \tag{43-28}$$

$$\frac{\Phi_1}{v_1} + \frac{\Phi_2}{v_2} + \frac{\Phi_3}{v_3} = 0, \tag{43-29}$$

$$\frac{\Phi_1}{v_1} \overline{P_1}^b + \frac{\Phi_2}{v_2} \overline{P_2}^b + \frac{\Phi_3}{v_3} \overline{P_3}^b = 0, \tag{43-30}$$

$$\frac{\boldsymbol{\Phi}_1}{\boldsymbol{\nu}_1} \overline{\boldsymbol{P}_1}^{\mathrm{r}} + \frac{\boldsymbol{\Phi}_2}{\boldsymbol{\nu}_2} \overline{\boldsymbol{P}_2}^{\mathrm{r}} + \frac{\boldsymbol{\Phi}_3}{\boldsymbol{\nu}_3} \overline{\boldsymbol{P}_3}^{\mathrm{r}} = 0 \,, \tag{43-31}$$

where  $\overline{P_i}^b$  is the partial dispersion for a wavelength interval in the blue spectral range, here preferably  $\bar{P}_{g,F}$  for  $\lambda$ =435 nm – 486 nm and  $\overline{P_i}^r$  is the partial dispersion for the red spectral range, preferably  $\bar{P}_{c,C}$  for  $\lambda$ =587 nm – 656 nm. These wavelength regimes are suitable for correction of the visible spectral range between 450 nm and 650 nm. Equations (43-28) – (43-31) can be satisfied if and only if

$$N = \text{Det} \begin{bmatrix} 1 & \overline{P}_1^b & \overline{P}_1^r \\ 1 & \overline{P}_2^b & \overline{P}_2^r \\ 1 & \overline{P}_3^b & \overline{P}_3^r \end{bmatrix} . \tag{43-32}$$

Equation (43-32) requires that, in a plot of  $\bar{P}_{g,F}$  against  $\bar{P}_{c,C}$ , as shown in figure 43-14, the points for three glasses lie on a straight line.

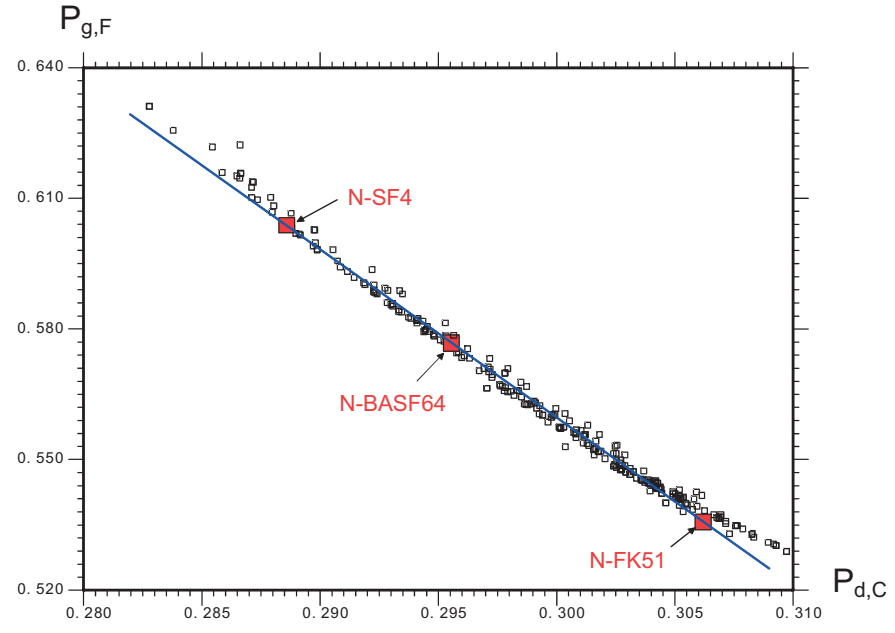
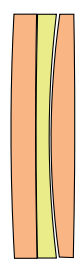


**Figure 43-14:** Glass selection for a three-lens superapochromat in the  $\bar{P}_{\rm g,F}-\bar{P}_{\rm c,C}$  domain. As an example, three glasses from the Schott catalogue which give superachromatic correction are shown

It should be emphasized that eqs (43-28)–(43-32) and the corresponding equations in section 43.2.2 only yield superapochromatic solutions in the *paraxial* domain. Higher-order aberrations, either monochromatic or polychromatic, are not accounted for in these equations. In particular, correcting chromatic variation of spherical aberration (*spherochromatism*) will often require deviation from the perfect paraxial solution in favor of balancing paraxial and higher-order aberrations. The following design is a good example of this effect.

### Superachromatic Refractor Design

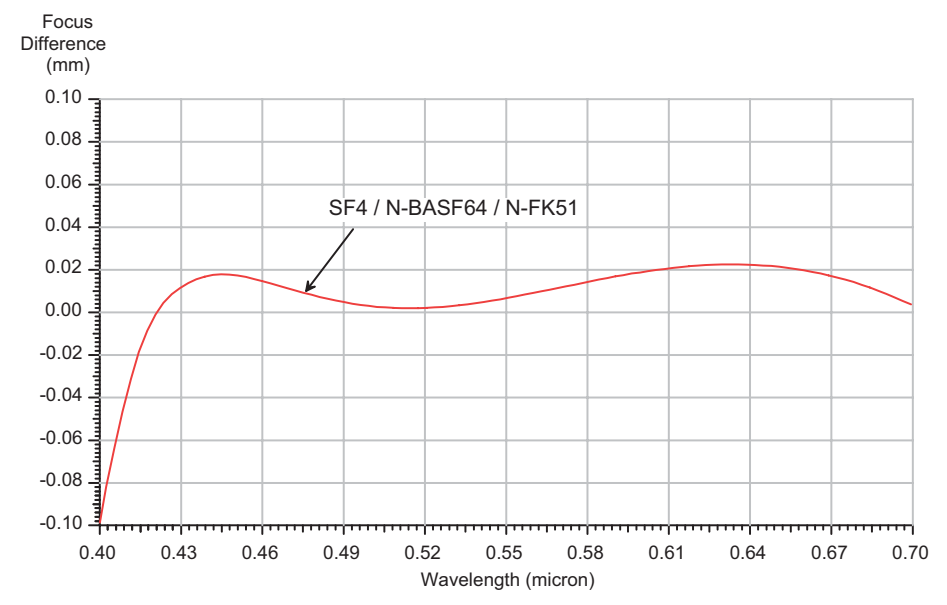
With reference to the glass selection shown in figure 43-14, a practical design example is given in figure 43-15 and following. As with all apochromatic designs presented in the previous sections, this design is super-apochromatic in the *paraxial* domain only, but suffers from significant chromatic variation of the spherical aberration.



# Super-apochromatic refractor telescope F20 / 4000mm:

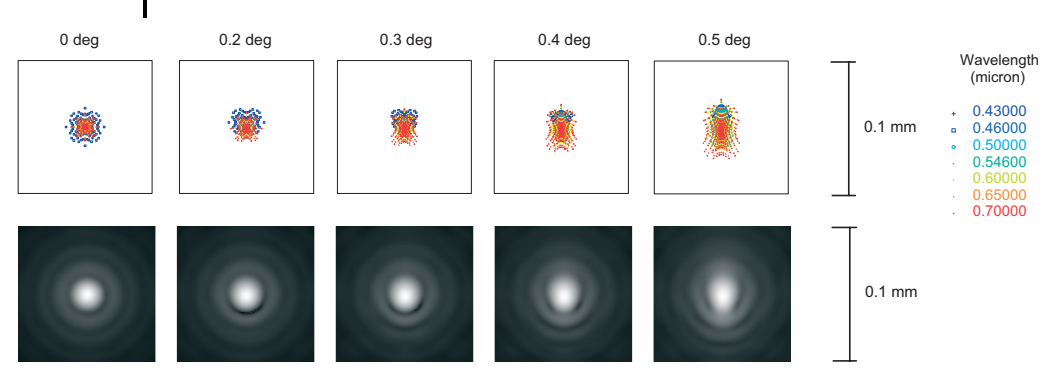
	1 =	1
Radius	Distance	Glass
1368.305	20.00	SCHOTT SF4
4439.544	0.538	
8076.334	10.00	SCHOTT N-BASF64
696.722	1.00	
664.250	20.00	SCHOTT N-FK51
-8666.846	3954.457	

Figure 43-15: Refractor telescope with superapochromatic correction in the *paraxial* domain.



**Figure 43-16:** Paraxial longitudinal chromatic focus of the superapochromatic refractor telescope given in figure 43-15.

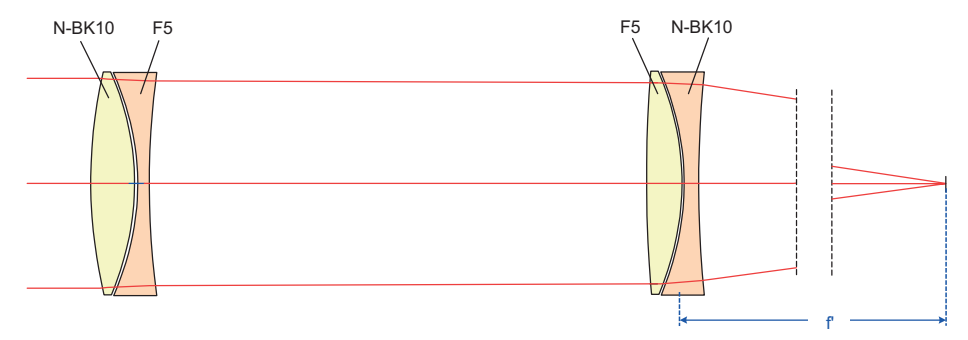




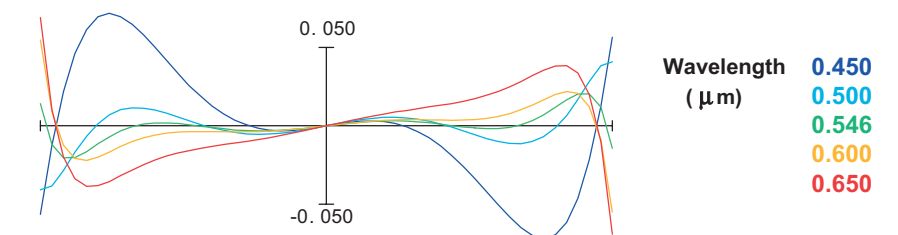
**Figure 43-17:** Spot diagrams and diffraction PSF of the superapochromatic refractor telescope given in figure 43-15.

# 43.2.3 Apochromatic Telescopes Without Anomalous Dispersion Glasses

As shown in section 43.2.2, at least one optical glass must have anomalous partial dispersion in order to correct for secondary longitudinal chromatic aberration. Several attempts have been made to avoid anomalous dispersion glasses because of their known practical problems (expensive, unavailable in larger dimensions, fragile, chemically unstable and difficult to polish). McCarthy [43-53] had already shown in 1945 that correction of the secondary spectrum can also be achieved using only normal dispersion glasses.



**Figure 43-18:** Apochromatic telescope using only glasses with normal dispersion, after McCarthy [43-53].



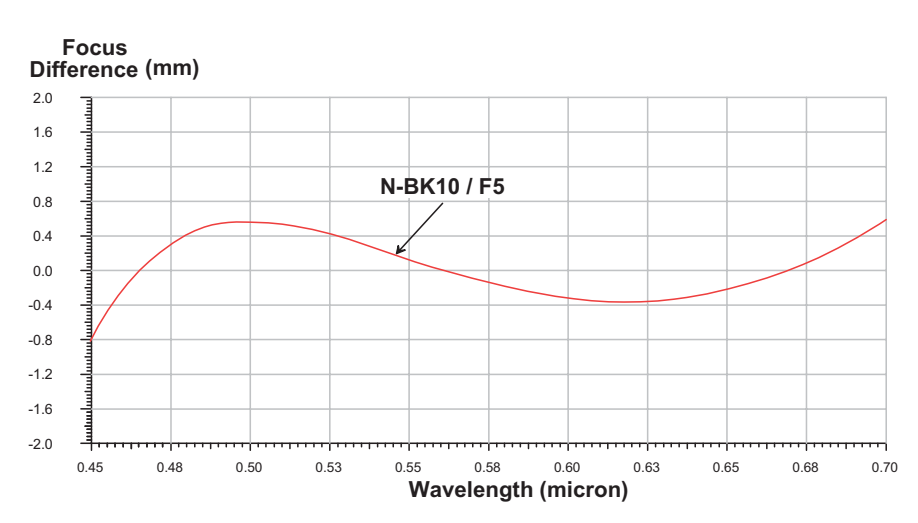


**Figure 43-19:** Transverse aberrations (a) and axial focus difference (b) of the McCarthy apochromatic telescope.

This lead to systems with sub-aperture correctors. If anomalous dispersion glasses are only used in lens groups with smaller diameters, the glass costs can be effectively reduced. Examples are given in figures 43-20 to 43-23.

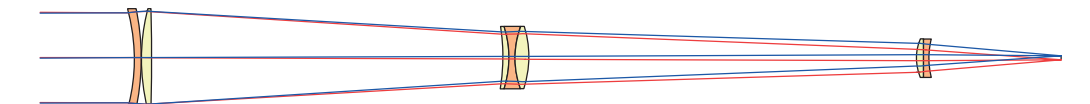


**Figure 43-20:** Apochromatic telescope with sub-aperture correctors and without anomalous dispersion glasses proposed by Duplov [43-16].

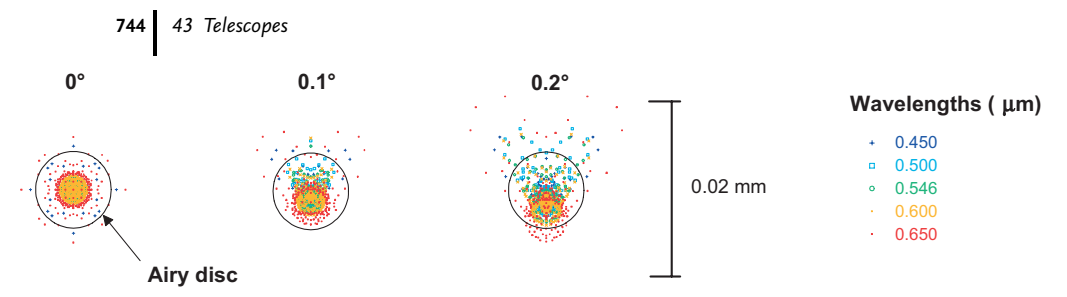
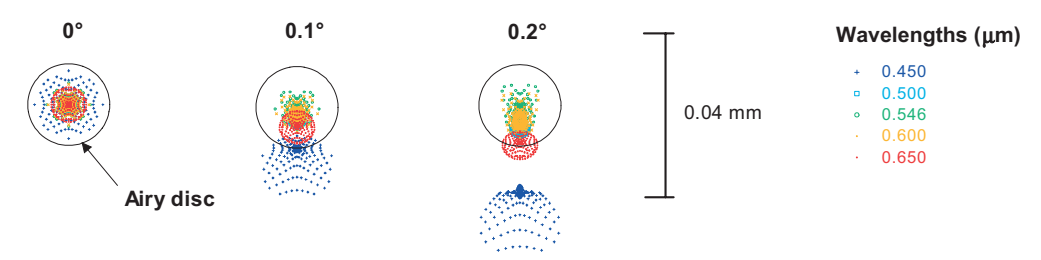


Figure 43-21: Spot diagram of the Duplov apochromatic telescope given for a F7/700 mm system.



Figure 43-22: Apochromatic telescope with sub-aperture correctors proposed by Sinnot [43-87]..



**Figure 43-23:** Spot diagram of the Sinnot apochromatic telescope using sub-aperture correctors given for a F14/2800 mm system.

# 43.3 Reflecting Telescopes

Purely reflecting telescopes can be grouped into two categories: compound telescopes and tilted component telescopes (TCTs). The latter group is also known as *Schiefspiegler*, a term first introduced by the German A. Kutter but nowadays widely accepted as a synonym for all forms of TCTs. A compound telescope is simply a sequence of imaging mirrors aligned on a common optical axis. It is evident that compound telescopes must have a central obscuration of the aperture. This effect is detrimental to image contrast and resolution, as explained in section 43.16, and is avoided in the numerous tilted component telescopes (TCT) or Schiefspiegler variants. The following survey of reflecting telescopes is grouped into single-, two-, three-, and four-mirror telescopes.

#### 43.4

# Single-mirror Reflecting Telescopes

#### 43.4.1

### Spherical Mirror

A spherical mirror is the most simple form of a reflecting telescope. Because the spherical aberration of a spherical mirror cannot be corrected, satisfying results can only be achieved by making the aperture ratio (F-number) as high as possible. Typically the aperture diameter is chosen small enough that the residual aberrations are below the diffraction limit (Airy diameter).

To third order, the longitudinal aberrations on a spherical mirror can be determined by

- spherical aberration: 
$$\Delta s_{\rm sph} = -\frac{1}{32 K^2} f$$
, (43-33)

- coma: 
$$\Delta s_{\text{coma}} = -\frac{3}{8 K} f \cdot \tan(w),$$
 (43-34)

where K is the aperture ratio (F-number) and f the focal length of the mirror, assuming the stop is at the mirror. Assuming that the image performance is to be diffraction limited (i.e., Strehl ratio > 0.8) the minimum focal length for a given mirror diameter *D* can be calculated without further derivation:

$$f_{\rm sph}^3 = \frac{D^4}{512.\lambda} \,, \tag{43-35}$$

$$f_{\text{coma}}^2 > \frac{D^2}{19.8 \ \lambda} \tan(w)$$
 (43-36)

Equation (43-35) indicates that an aperture ratio K > 10 is required to yield a near diffration limited performance if only spherical aberration is concerned.

#### 43.4.2

# Parabolic Mirror (Newton Telescope)

The limitations of the simple spherical mirror telescope can be avoided by having a parabolic-shaped mirror. This configuration is well known as the "Newton telescope" (figure 43-24). In order to obtain an accessible focus position, a flat folding mirror (M2) is placed into the beam. Although the Newton telescope provides a perfect image (no spherical aberration) on the optical axis, it suffers heavily from the field-dependent coma. Astigmatism and field curvature are also present in a Newton reflector, but coma is the most dominant aberration and overrules astigmatism and field curvature.





Figure 43-24: Newton telescope F10/2000 mm.

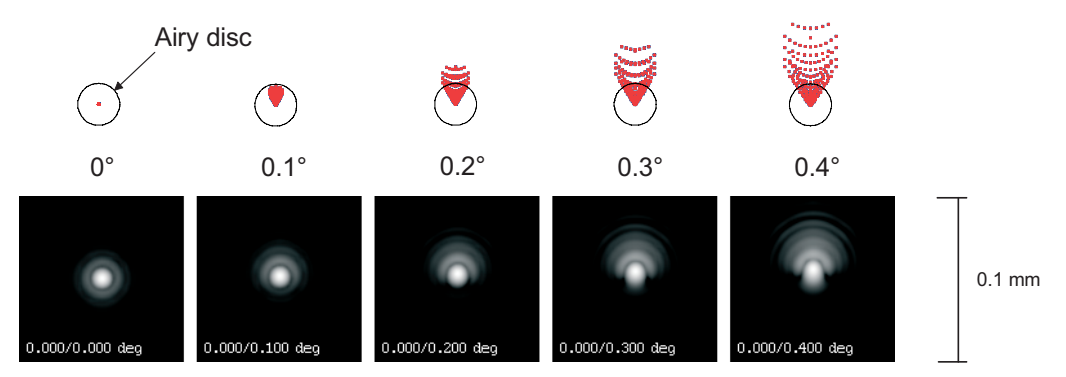


Figure 43-25: Spot and PSF performance of a F10/2000 mm Newton telescope.

# 43.5 Two-mirror Reflecting Telescopes

#### 43.5.1

#### Cassegrain Telescope

The Cassegrain form consists of a concave primary mirror and a convex secondary mirror as depicted in figure 43-26. Unlike the Gregorian telescope, the secondary lies inside the focus of the primary. Both mirrors are aspherical, the primary being of parabolic shape, the secondary hyperbolic.

Despite its optical "simplicity", there are so many different variants of the Cassegrain in terms of primary F-number, secondary magnification, back focal length or amount of central obscuration, that it is impossible to present all possible combinations in detail. Fortunately, a two-mirror compound telescope can be described by a few simple equations which will result in a well-corrected system.

The perfect (on-axis) imaging is due to the fact that each mirror provides a perfect image. The infinitely distant object is converted to a perfect real image by the parabolic shape of the primary. As shown in figure 43-27, the focal points of the hyperbola  $F_{H1}$  and the parabola  $F_{M1}$  coincide and the image of the primary becomes the (virtual) object of the secondary.

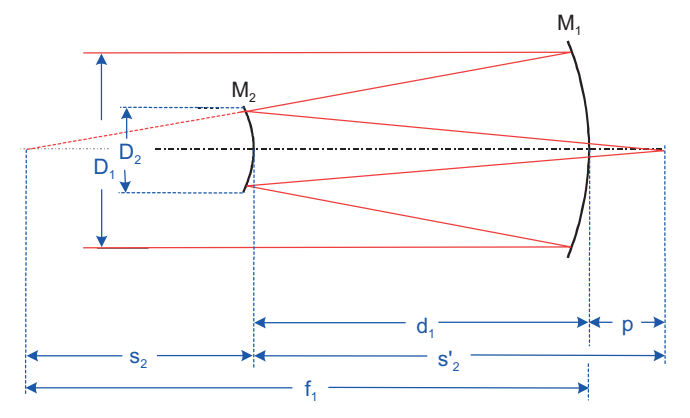
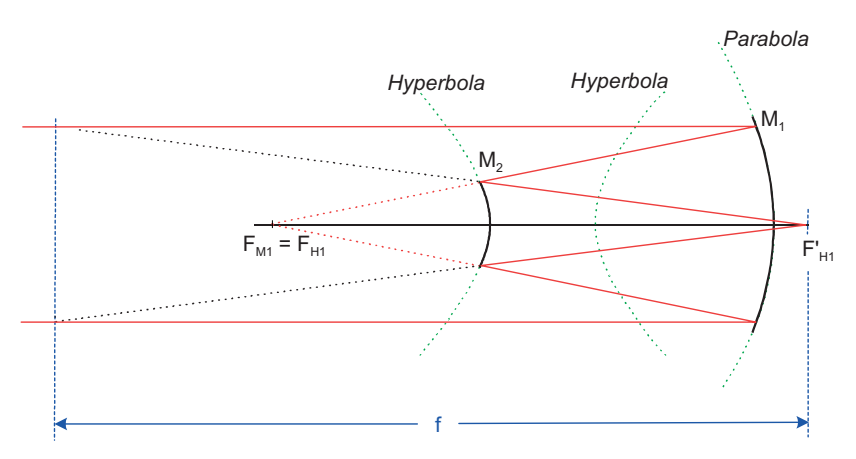


Figure 43-26: Paraxial parameters of the Cassegrain telescope.



**Figure 43-27:** The Cassegrain telescope formed by a combination of a parabolic and a hyperbolic mirror.

The optical design of a two-mirror compound telescope is completely defined by four parameters, the diameter of the primary, the position of the image behind the primary, the system F-number, and the axial separation of the mirrors. A fifth parameter will define the field of view.

With reference to figure 43-26 we chose an appropriate focal length  $f_1$  for the primary mirror which, together with  $D_1$ , defines the primary F-number. This is a fundamental design parameter, as the sensitivity of image quality to misalignment of the secondary mirror is strongly affected by the primary F-number. The fourth design parameter will be the distance p from the vertex of the primary mirror to the image (sometimes referred to as the *vertex back focus* or *working distance*).

Note that the sign of the mirror separation  $d_1$  is negative as the secondary mirror is to the left of the primary mirror. The primary and secondary focal lengths  $f_1$ ,  $f_2$  are also negative, as their radii of curvature are negative.

Selecting a suitable distance  $d_1$  between the primary and secondary mirror defines the secondary magnification,

$$m_2 = \frac{f}{f_1} = \frac{s'_2}{s_2} = \frac{p + d_1}{f_1 - d_1}.$$
 (43-37)

Conversely, choosing an appropriate secondary magnification  $m_2$  we can solve for the distance between primary and secondary mirror

$$d_1 = \frac{m_2 f_1 - p}{m_2 - 1}. (43-38)$$

The secondary magnification  $m_2$  is negative for a Cassegrain system and positive for a Gregorian system. With  $s'_2 = m_2 s_2$ , we obtain the curvature of the secondary mirror

$$\frac{2}{r_2} = \frac{1}{s_2'} + \frac{1}{s_2} = \frac{1}{m_2 s_2} + \frac{1}{s_2},\tag{43-39}$$

$$r_2 = \frac{2m_2s_2}{1+m_2} = \frac{2(p-d_1)}{1+m_2},\tag{43-40}$$

or with  $\Phi = 2/r$ 

$$\Phi_2 = \frac{1 + m_2}{m_2 s_2} \,. \tag{43-41}$$

For completeness, three other useful relations will be given if the focal lengths of the mirrors  $f_1, f_2$  and their axial separation  $d_1$  are known:

$$f = \frac{f_1 f_2}{f_1 - f_2 - d_1} \,, \tag{43-42}$$

$$\Phi = \Phi_1 + \Phi_2 - \Phi_1 \Phi_2 d_1, \tag{43-43}$$

$$s'_{2} = \frac{(f_{1} - d_{1})f_{2}}{f_{1} - f_{2} - d_{1}}.$$
(43-44)

We also note an important relationship between the field curvature and the secondary magnification

$$P = m_2 \Phi - \frac{1 + m_2}{p - d_1} \,, \tag{43-45}$$

where *P* is the third-order field-curvature coefficient (Petzval sum). Since the system focal length is high, i.e.,  $\Phi$  is low, the field curvature will be dominated by the secondary mirror. The radius of curvature of the image surface  $r_{\text{img}}$  is determined by the optical powers of the primary and secondary mirror,  $\Phi_1, \Phi_2$ 

$$\frac{1}{r_{\text{img}}} = \Phi_1 + \Phi_2 = \frac{1}{f_1} + \frac{1}{f_2} \,. \tag{43-46}$$

It is evident that equal curvatures for both mirrors will yield a flat field at the expense of a large central obstruction, which would be impractical. The diameter of the secondary mirror is obtained by

$$D_2 = \left(1 - \frac{d_1}{f_1}\right) D_1. \tag{43-47}$$

The linear central obscuration ratio is obtained by

$$e = \frac{D_2}{D_1} = \frac{s'_2}{f} = \frac{s'_2}{m_2 f_1}.$$
 (43-48)

It should be noted that eq. (43-48) refers to the minimum diameter of the secondary mirror, for which no loss of light (vignetting) for an axial field point occurs, but it does, however, exist at the edge of the field. If vignetting cannot be tolerated, the secondary must be oversized (depending on the field diameter at the focal plane). From section 43.16, it is evident that the central obstruction must be kept to a minimum for reasons of contrast and image sharpness.

Equation (43-48) shows the inverse proportionality of the obscuration ratio and the secondary magnification. Attempts to reduce the central obscuration will inevitably increase the secondary magnification if an accessible focus position behind the primary is required. Equation (43-45) indicates that a larger secondary magnification will also lead to stronger field curvature, thereby limiting the usable field of view. Finally, the aspherization and alignment sensitivity of the secondary mirror will be stronger with a larger secondary magnification.

Knowing all paraxial quantities, the conic constants of the mirrors can be determined. For the classical Cassegrain and Gregory forms, the primary mirror is of parabolic form  $(k_1 = -1)$ . The conic constant  $k_2$  of the secondary mirror is then a function of the secondary mirror magnification  $m_2$ 

$$k_2 = -\varepsilon^2 = -\left(\frac{m_2 - 1}{m_2 + 1}\right)^2,$$
 (43-49)

where  $\varepsilon$  is the numerical eccentricity of the conic surface. The secondary mirror of the Cassegrain form is a hyperbola.

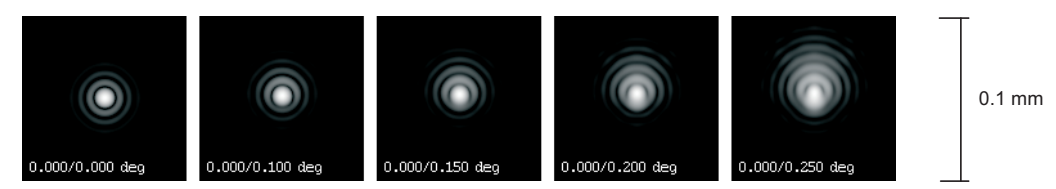


Figure 43-28: Diffraction PSF of a F10/2000 mm Cassegrain telescope. Performances are shown over a FOV of ±0.25°.

43.5.2

# Ritchey-Chretien Telescope

The Ritchey–Chretien (RC) form is an important modification of the Cassegrain telescope carried out by G.W. Ritchey and H. Chretien in 1910. They concluded that individual correction of primary and secondary mirrors is not required in a telescope of Cassegrain form. It is sufficient to have the final focus corrected.

The RC-solution eliminates the third- order coma of the Cassegrain telescope. Any optical system in which both spherical aberration and coma are corrected is called an aplanat. In other words, the RC system can also be called an aplanatic Cassegrain telescope. The main difference from the Cassegrain form lies in the aspherization of the mirrors. With reference to the definitions in section 43.5.1, the solution of the conic constants is

$$k_1 = -1 + \frac{2s_2}{d_1 m_2^3},\tag{43-50}$$

$$k_2 = -\left[\left(\frac{m_2 - 1}{m_2 + 1}\right)^2 + \frac{2f}{d_1(m_2 + 1)^3}\right]. \tag{43-51}$$

The only primary aberrations of the Ritchey–Chretien telescope are the field curvature and the astigmatism.

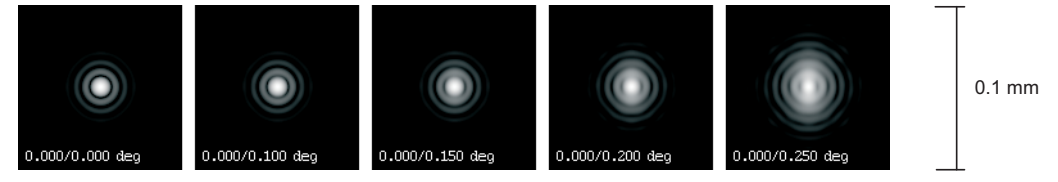


**Figure 43-29:** Diffraction PSF of a F10/2000 mm Ritchey–Chretien telescope. Performances are shown over a FOV of  $\pm 0.25^{\circ}$ .

#### 43.5.3

#### Dall-Kirkham Telescope

The Dall–Kirkham telescope is a variant of the Cassegrain telescope formed by utilizing a *spherical* secondary mirror, thus avoiding the difficulties involving a convex hyperbolic secondary of the classical Cassegrain telescope. The primary mirror is elliptical. However, the reduction in the manufacturing complexity is offset by an overly excessive coma (figure 43-30) that is  $(m^2+1)/2$  times larger than that of a Cassegrain telescope [43-67]. This narrows the usable field of view by the same factor

We omit the optical layout plot as it would be identical to the Cassegrain configuration (see figure 43-27), except for the conic constants of the mirrors.

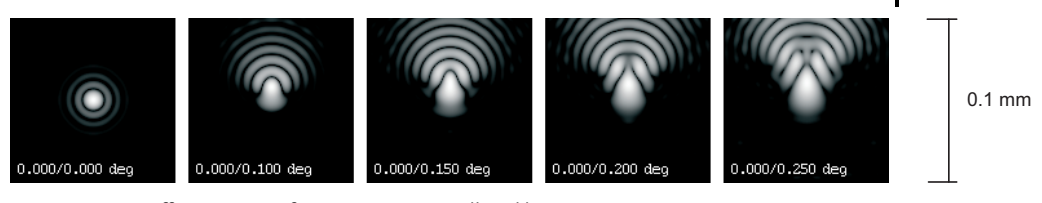


**Figure 43-30:** Diffraction PSF of a F10/2000 mm Dall–Kirkham telescope. Performances are shown over a FOV of ±0.25°.

#### 43.5.4

# Pressmann-Camichel Telescope

The Pressmann–Camichel telescope is another telescope which involves a reduction in the manufacturing complexity of the classical Cassegrain telescope. It utilizes a spherical primary mirror together with an oblate ellipsoid at the secondary.

In order to compensate for the strong spherical aberration of the primary mirror, the secondary mirror must be strongly deformed. As with the Dall–Kirkham telescope described in the previous section, the Pressmann–Camichel telescope suffers from strong coma and is therefore only usable over a very narrow field.

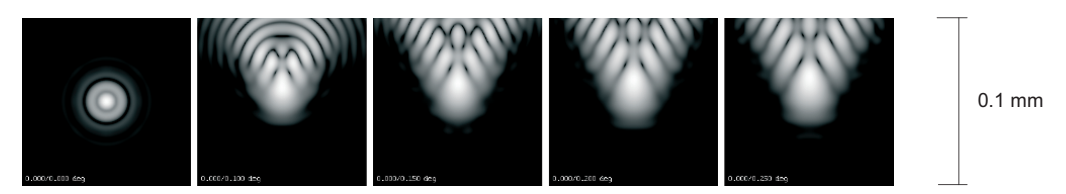


**Figure 43-31:** Diffraction PSF of a F10/2000 mm Pressmann–Camichel telescope. Performances are shown for a FOV of  $\pm 0.25^{\circ}$ .

#### 43.5.5

#### Gregorian Telescope

The equations shown for the Cassegrain telescope also apply for the Gregorian telescope, except that the secondary magnification  $m_2$  is positive. The Gregorian telescope is characterized by an intermediate focus and a concave secondary mirror outside the focus. This leads to a longer tube length compared to the Cassegrain telescope if the focal length and F-number of the primary mirror are kept constant.

As with the Cassegrain, the Gregorian has a parabolic primary mirror, but the secondary mirror is elliptical in its classical form. Other mirror shapes are possible to eliminate the strong coma of the classical Gregorian which leads to aplanatic forms similar to the Ritchey–Chretien telescope (see section 43.5.2). In the aplanatic form, image performance is greatly improved over the classical form (see figure 43-33). However, the primary mirror is most commonly used with the elliptical, which makes fabrication and testing more difficult.

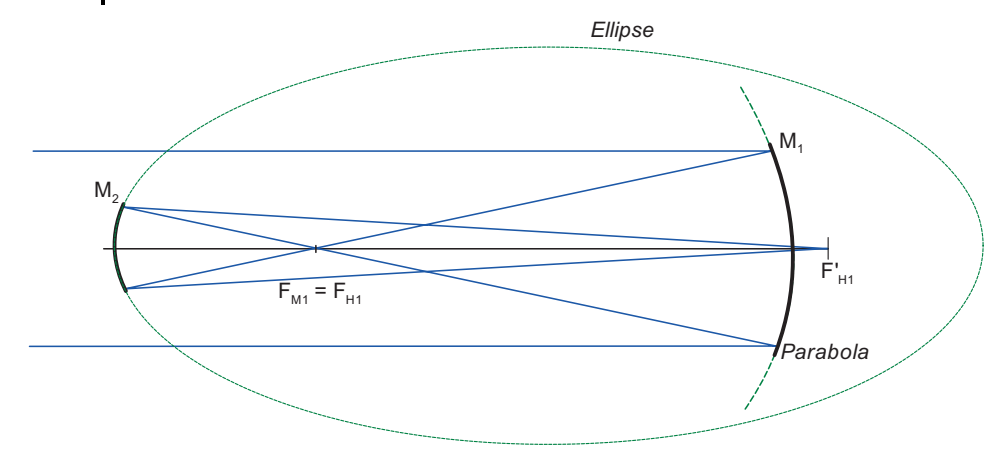


**Figure 43-32:** The Gregorian telescope formed by the combination of a parabolic and an elliptical mirror.

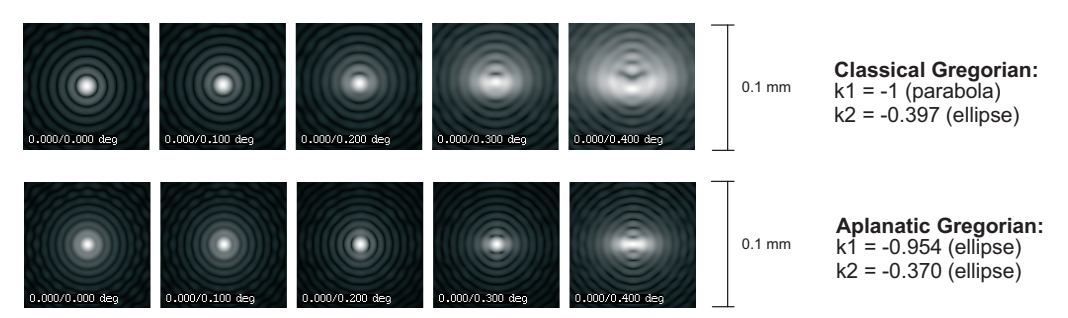


**Figure 43-33:** Diffraction PSF of the classical Gregorian telescope with parabolic primary (top) and aplanatic (bottom) form. Performances are shown for a F10/2000 mm system over a FOV of  $\pm 0.4^{\circ}$ .

The Gregorian telescope was very popular in the previous century, because it provided an erect image when used with an eyepiece, thus eliminating the need for image-reversing prism systems. The Gregorian telescope also has an outwardly curved focal surface which neatly matches with the eyepieces because they exhibit a field curvature in the opposite direction. In this way, the remaining astigmatism of an aplanatic Gregorian telescope could be almost fully compensated by the inherent astigmatism of the eyepiece, thus providing an equally sharp image both in the center and the field edge enabling better visual observation. For optimum performance, however, telescope and eyepiece must be optimized together as a single system.

Because the Cassegrain form is shorter, Gregorian telescopes are less interesting. There are only a few instances in which the Gregorian form is still used:

- in solar telescopes where access to the primary image is required
- for simplification of manufacture and test (all mirrors are concave)
- for the outwardly curved focal surface mentioned above.

An interesting modification of the Gregorian telescope is shown in figure 43-34. The light beam undergoes three reflection at two mirrors. Instead of forming an image behind the primary mirror, the radius of curvature of the secondary mirror is made larger so that an intermediate (uncorrected) focus is formed between M1 and M2. The light is reflected a second time at the primary mirror and the final focus is formed through a central opening in the secondary mirror.

As with the classical Gregorian, it can be designed to be aplanatic (both mirrors elliptical) or non-aplanatic (using a paraboloidal primary mirror). Due to the three reflections, the system can be built with lower F-numbers with only a marginal increase in tube length. The image performance of the three-reflection Gregorian is comparable with the classical form.

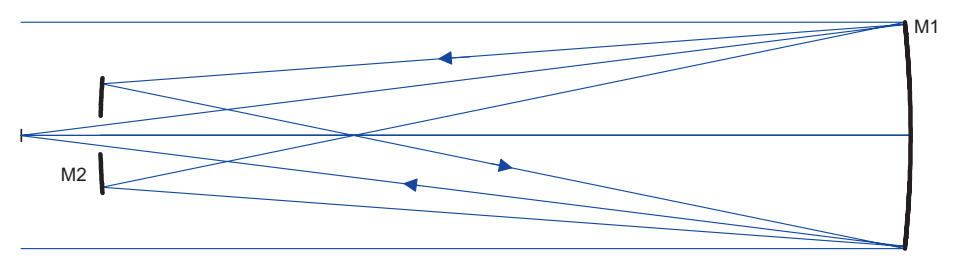


Figure 43-34: Gregorian telescope with three reflections.

#### 43.5.6

### Schwarzschild Aplanatic Telescopes

In 1905 Schwarzschild established the fundamental design equations for constructing aplanatic reflecting telescopes consisting of two mirrors [43-72]. These equations, here given in a form by Wilson [43-84], analytically describe the conic constants of the mirrors and are valid for any chosen geometry. Therefore they also include the Cassegrain and Ritchey–Chretien forms.

$$k_1 = -1 - \frac{2p}{d_1 m_2^3},\tag{43-52}$$

$$k_2 = -\left[ \left( \frac{m_2 - 1}{m_2 + 1} \right)^2 + \frac{2f}{d_1(m_2 + 1)^3} \right], \tag{43-53}$$

where p is the distance from vertex of primary mirror to focal plane,  $m_2$  is the secondary magnification,  $d_1$  the distance between mirrors, f the telescope focal length, and  $k_1, k_2$  are the conic constants.

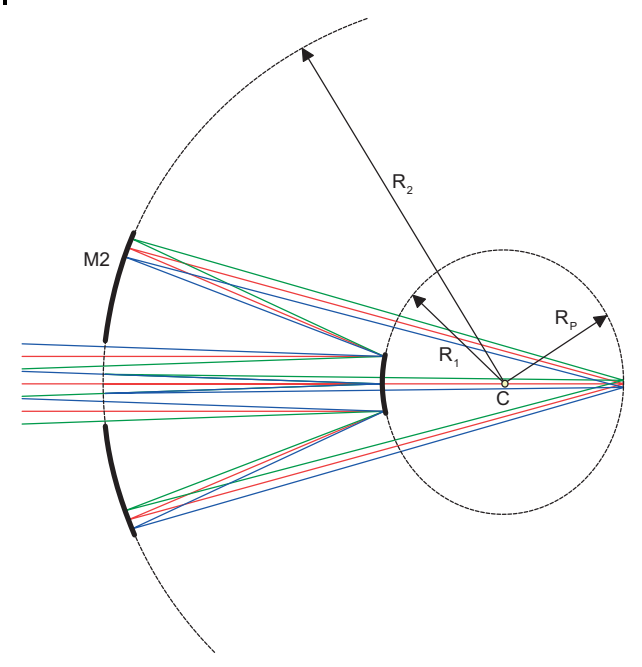


Figure 43-35: Construction of the concentric anastigmatic Schwarzschild telescope.

Schwarzschild also investigated two-mirror solutions which are able to correct the first four Seidel conditions (spherical aberration, coma, astigmatism, Petzval curvature). One such solution is shown in figure 43-36, but it leads to a totally unsuitable form for telescopes with large apertures [43-84].

Wilson [43-84] gives a thorough account of Schwarzschild's theory leading to this solution. The essential equations describing the construction parameter are summarized here:

$$R_1 = R_2 = f'\sqrt{2} \,, \tag{43-54}$$

$$d_1 = -\frac{R_1\sqrt{2}}{2}. (43-55)$$

Even though the system is "fast", it is not suitable for telescopic use because the secondary mirror is about 2.4 times larger than the primary mirror and both mirrors exhibit a relatively large linear obstruction ratio of 0.41. In spectroscopic applications, however, where "speed" is an issue, Schwarzschild's system can occasionally be found.

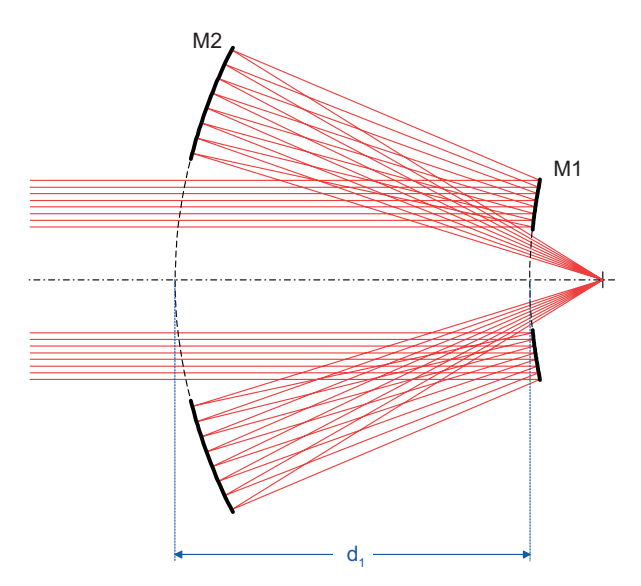


Figure 43-36: Schwarzschild's telescope corrected for the first four Seidel aberrations.

Having realized that no *practical* telescope form with two mirrors and correction of four Seidel aberrations is possible, Schwarzschild concentrated on aplanatic solutions (spherical aberration and comacorrected) with two mirrors [43-72], [43-84]. Figure 43-37 shows Schwarzschild's original aplanatic two-mirror telescope from 1905.

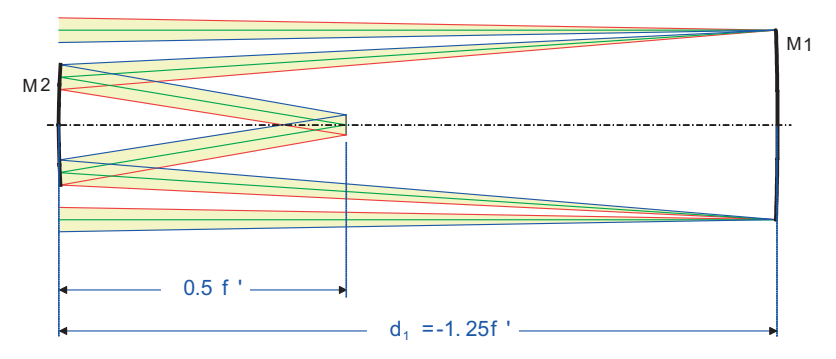


Figure 43-37: Aplanatic telescope from Schwarzschild (1905).

Again, this Schwarzschild telescope suffers from a very high linear obstruction ratio (>0.5) and an image position which is difficult to access. Also, effective baffling is almost impossible. Due to these drawbacks, the Schwarzschild telescope (figure 43-37) has no practical importance today, except that it is occasionally used as a feeder telescope in three-mirror and four-mirror configurations (compare with figures 43-48 and 43-51).

43.5.7

#### **Couder Anastigmat**

An interesting – and more practical – modification of Schwarzschild's anastigmatic telescope was proposed by Couder in 1926. He reduced the central obstruction by moving the secondary mirror further away from the primary mirror. The Couder telescope is therefore significantly longer than the Schwarzschild (compare with figure 43-37). The separation of the mirrors in the Couder telescope is 2f in comparison with 1.25f in the Schwarzschild anastigmat.

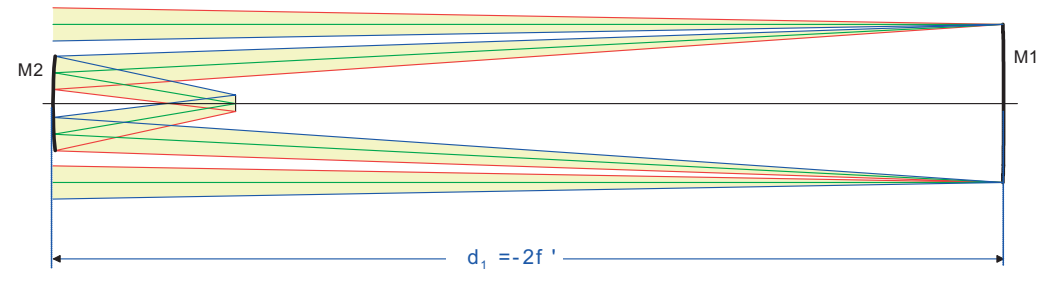


Figure 43-38: Couder's original telescope

The field curvature of the Couder telescope is higher than that for the Schwarzschild telescope because the magnification of the secondary mirror is higher. Field flattening can be obtained by a single lens with positive power close to the focal surface, similarly to the Schmidt telescope. Section 43.15.1 gives examples of field flatteners.

The major disadvantages of Schwarzschild's telescope, which is shown in figure 43-37, also apply to the Couder telescope. These are: difficult accessibility to the focal plane and poor baffling characteristics. In addition, its excessive length has prevented the wider use of this telescope type.

# 43.5.8 Loveday Telescope

Loveday [43-46] proposed another interesting telescope with two mirrors but three reflections. Both mirrors are parabolic in a confocal configuration, where the focal points of the mirrors coincide. The concept can be explained in two ways. Starting from the Cassegrainian form, the curvature of the secondary mirror is adjusted to give a parallel beam after M2 which is then reflected by the primary mirror. As discussed in section 43.6.2, mirrors M1 and M2 form a Mersenne-type telescope and a third mirror (i.e., the primary mirror) creates the final image at the original focal plane of the primary mirror. However, this configuration neatly mimics the underlying principle of the Paul–Baker, Mersenne–Schmidt and Willstrop telescopes in that an afocal two-mirror telescope in conjunction with a third imaging mirror

makes the similarity evident. The notable differences are that the third mirror (i.e., third reflection) in the Loveday telescope is exactly at the location of the primary mirror and is of parabolic shape (as opposed to a spherical tertiary in the original Paul-Baker telescope).

An almost identical two-mirror three-reflection telescope was patented earlier by Rumsey [43-64], but in his solution the primary focus and the final focus are at separate positions. This is probably only due to the dual use of the identical focal position. Loveday's telescope was named after him.

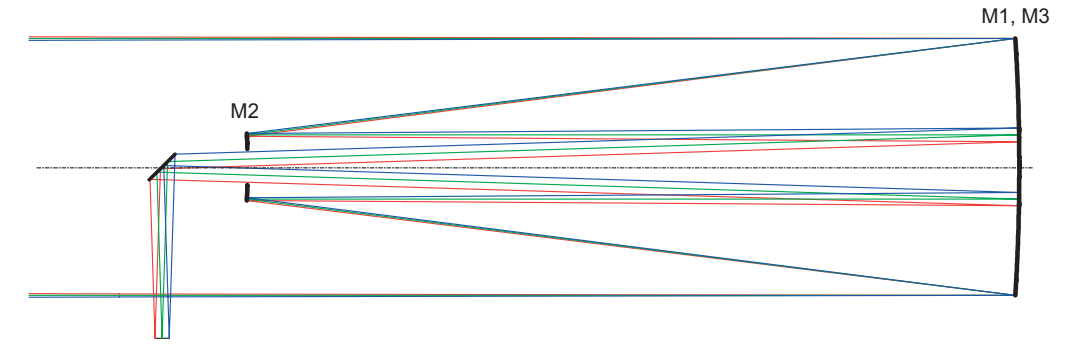


Figure 43-39: Loveday telescope.

# PSF at prime focus (F6/1200mm):

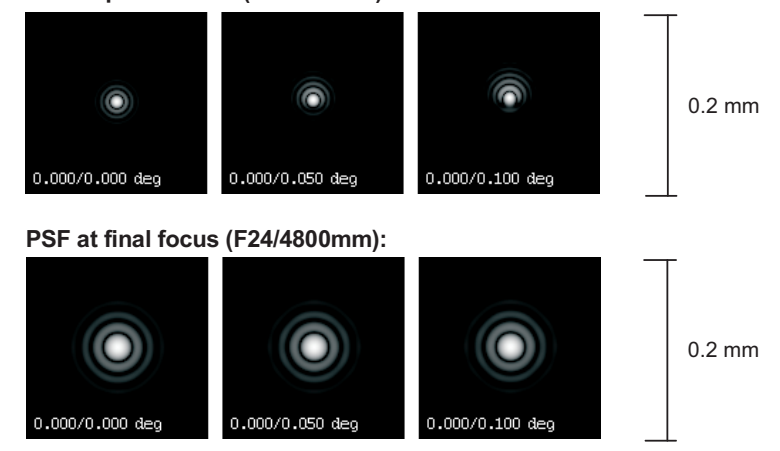


Figure 43-40: Diffraction PSF of the Loveday telescope shown in figure 43-39. Telescope parameters are F6/1200 mm for the primary and F24/4800 mm in the three-reflection case (after Rutten and van Venrooji [43-65]).

The Loveday telescope only allows a very small field of view, in the order of 0.2°, because otherwise the hole in the secondary mirror would rapidly exceed the dimensions of the secondary mirror itself. The optical performance of the Loveday telescope also suffers from coma, but at a very low level. Due to the small field and the slow speed in the three-reflection configuration it is essentially diffraction limited (figure 43-40).

A further feature which makes the Loveday telescope particularly interesting for amateur-sized telescopes is that it can be either used as a fast Newton telescope (if M2 is removed) or as a slow Newton telescope (with M2 inserted).

Wilson gives a simple relation of the final F-Number (FN) in the three-reflection case as a function of the primary F-Number  $FN_{primary}$  and the linear obstruction ratio  $R_{\rm obs}$  [43-84],

$$FN_{3-\text{refl}} = \frac{FN_{\text{primary}}}{R_{\text{obs}}}.$$
 (43-56)

# 43.6 Three-mirror Reflection Telescopes

Telescopes using three mirrors have been developed in order to overcome the inherent limitations of two-mirror systems. Schwarzschild demonstrated in his 1905 paper that it was impossible to correct a practical two-mirror system for the first four Seidel aberrations (spherical aberration, coma, astigmatism, field curvature) simultaneously [43-72], [43-84]. A notable exception is the two-mirror Schwarzschild system shown in figure 43-36. However, this would not be a practical solution for an astronomical telescope. Because the number of free parameters in a two-mirror system is limited (two radii, two conic sections), only the first two Seidel aberrations can be corrected. A detailed account of this limitation is also given by Wilson [43-84].

#### 43.6.1

#### Paul-Baker Telescope

In 1935 Paul devised a three-mirror telescope composed of a Cassegrain afocal telescope (mirrors M1 and M2 in figure 43-41) and a spherical tertiary mirror [43-59]. The Cassegrain afocal telescope converts an input beam of diameter D into a collimated output beam of diameter d. With a paraboloidal primary and secondary mirror this system is free from spherical aberration, coma and astigmatism to third order.

The spherical tertiary mirror is placed at a distance 2 R<sub>3</sub> from the vertex of the secondary mirror, i.e., the secondary mirror is at the center of curvature of the tertiary. This is a condition similar to a Schmidt camera if the stop is chosen at the secondary mirror. The tertiary mirror now adds spherical aberration to the system which may be compensated if the (paraboloidal) secondary mirror is replaced by a

spherical mirror. If  $R_2 = R_3$  the spherical aberrations of secondary and tertiary mirrors cancel each other and the system is free from spherical aberration to third order. Paul showed that this system is also free from third-order coma and astigmatism, albeit at a curved image surface with radius  $R_1/2$ .

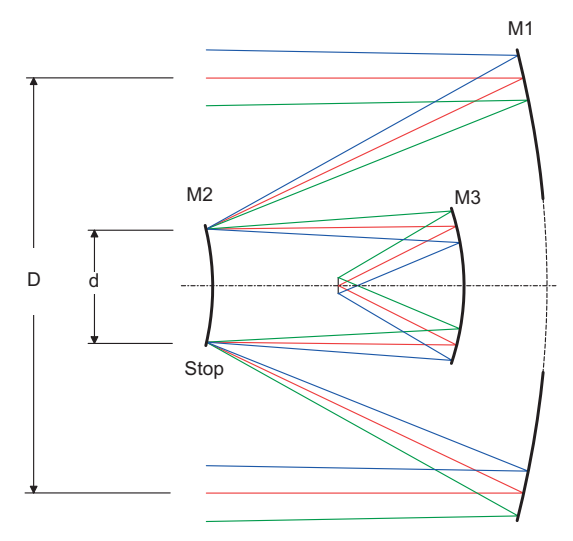


Figure 43-41: Paul-Baker telescope.

The original design by Paul, is one in which  $R_2 = R_3$  can be generalized to systems with  $R_2 \neq R_3$ . To understand this, we refer to the Schmidt condition formed by the tertiary mirror and the secondary mirror M2 located at the center of curvature of M3. The secondary mirror, when changed from a paraboloidal shape to a sphere, acts like the aspherical plate in a Schmidt system by pre-deforming the wavefront and thus compensating the inherent spherical aberration of the tertiary mirror. We may therefore change the conic constant of the secondary without introducing coma or astigmatism. The reader is encouraged to consult section 43.13.2 for information about the Schmidt telescope.

Baker [43-15] independently analyzed the condition for a flat image surface, i.e., zero Petzval curvature. From the general Petzval equation

$$\frac{1}{R_p} = \sum_{1}^{n} \frac{2}{R_n},\tag{43-57}$$

we obtain the image curvature

$$\frac{1}{R_p} = \frac{2}{R_1} \left[ 1 - \frac{f_1}{f_2} \left( 1 - \frac{R_2}{R_3} \right) \right]. \tag{43-58}$$

Requiring  $1/R_p = 0$  gives

$$\frac{R_2}{R_3} = 1 - \frac{R_2}{R_1} \,. \tag{43-59}$$

Despite the excellent imaging properties of the Paul-Baker telescope, only a few telescopes with this configuration have actually been built. This is probably connected with its disadvantages, of which the most evident ones are listed here.

- Limited space for instrumentation because the focal plane is "inside" the telescope tube.
- Relatively large central obscuration plus additional baffles to shield the tertiary mirror from light outside the FOV.
- Additional optical components, such as filters or atmospheric dispersion correctors, which reduce the image performance,
- Limited choice of overall focal length and focal ratio.

Further accounts of the Paul-Baker telescope are given by Schroeder [43-67] and Wilson [43-84].

#### 43.6.2

### Willstrop Mersenne-Schmidt Telescope

The three-mirror Mersenne-Schmidt telescope is based on a design first described in 1935 by Paul [43-59] and independently in 1945 by Baker [43-15]. The original Paul-Baker design, as discussed in section 43.6.1, consisted of a paraboloidal primary mirror and spherical shapes for secondary and tertiary mirrors. The system is corrected for spherical aberration, coma and astigmatism, albeit at a curved field. It covers a remarkable field-of-view (FOV) of 5° which bridges the gap between the limited FOV of the Cassegrain and Ritchey-Chretien telescopes (< 0.5°) and the wide fields achievable with the Schmidt telescope (> 10°).

Compared with the Schmidt telescope which is twice as long as its focal length and requires a refractive corrector (thus limiting its chromatic performance), the Paul-Baker is relatively compact. Its overall length is only about 38% of the system's focal length. Willstrop [43-85], [43-86] extended the Paul-Baker telescope by moving the tertiary mirror far behind the primary mirror. The focus is then formed at the vertex of M1 (see figure 43-42). The weakest feature of the Mersenne-Schmidt or Willstrop concept is the large linear obscuration ratio. For example, in Willstrop's proposal it amounts to 0.45 (excluding the oversizing required by baffles). The Wilstrop solution is characterized by the relations

$$d_1 = f_3 = f_2 = \frac{f_1}{2}. (43-60)$$

Superficially, the Mersenne-Schmidt (Paul-Baker, Willstrop) telescopes may be considered as an afocal Cassegrain combination (mirrors M1 and M2) and a focussing third mirror. The afocal Cassegrain form, where a parallel beam enters and leaves the system, was proposed first by Mersenne in 1636 and may also be considered as the first mirror telephoto system (see figure 43-43). Generally, the afocal Gregory or Cassegrain forms are considered to be Mersenne telescopes.

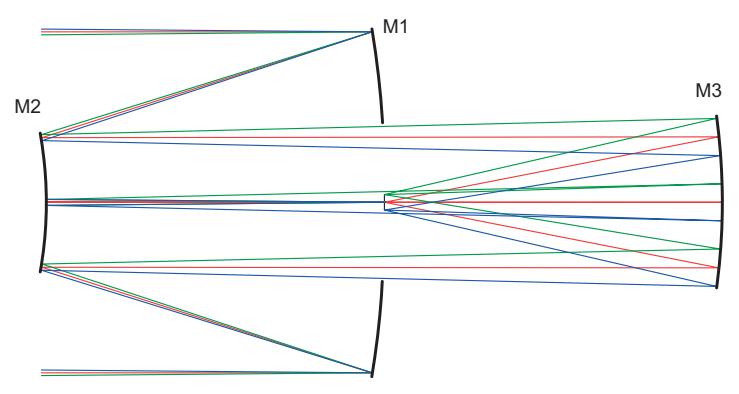
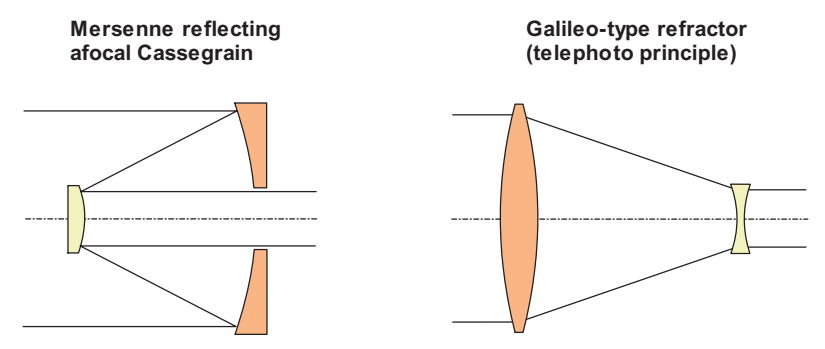


Figure 43-42: Optical layout of the flat-field Willstrop Mersenne–Schmidt telescope.



**Figure 43-43:** Mersenne design principle compared with a Galileo-type refracting telescope. Both systems also work as an afocal beam reducer, or if used in the reverse direction, as a beam expander.

The field can be flattened by changes in the radii of curvature of the secondary and tertiary mirror and by an ellipsoidal shape of the tertiary mirror, as shown by Baker and Willstrop [43-85] . The curvature of the image field is described by the Petzval curvature  $(1/R_p)$ . It is related to the radii of curvature  $R_i$  of the mirrors by

$$\frac{1}{R_{\rm p}} = \sum_{1}^{n} \frac{2}{R_{\rm i}}.$$
 (43-61)

If the system of the first two mirrors is to be afocal (Mersenne form), the center of curvature of the tertiary mirror coincides with the vertex of the secondary mirror. Furthermore, if the focal plane is kept at the vertex of the primary mirror, then we have

$$R_1 = -2f, \quad R_2 = 2(1-d)f, \quad R_3 = 2df,$$
 (43-62)

where *f* is the focal length of the primary mirror and *d* is the separation of the primary and secondary mirrors. The sign of a convex mirror is considered positive. The condition for a flat focal surface (eq. (43-61)) then leads to [43-85]

$$\frac{2}{-2f} + \frac{2}{2(1-d)f} + \frac{2}{-2df} = 0 ag{43-63}$$

or

$$\frac{d^2+d-1}{(d-d^2)f}=0. (43-64)$$

The solutions are

$$d = -1.618034$$
 and  $d = +0.618034$ .

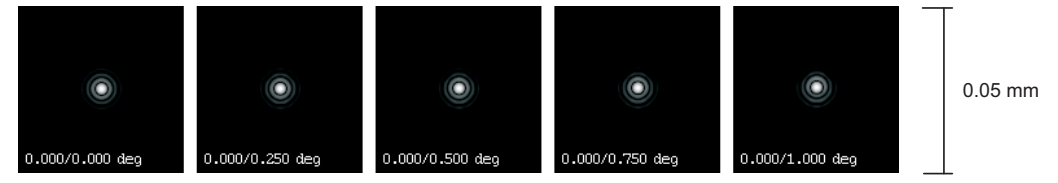


Figure 43-44: Diffraction PSF of a flat-field Mersenne–Schmidt telescope corresponding to Willstrop. Performances are shown for an F2.6/520 mm system over a FOV of  $\pm 1^{\circ}$ .

### 43.6.3

### Korsch Three-mirror, Single-axis Telescope

Relaxing the requirement of a collimated light beam between the secondary and tertiary mirror in the Mersenne telescope, now offers new possibilities in reflective telescope design. A flat-field design by Korsch [43-67] uses a slightly converging beam between the secondary and tertiary mirror (see figure 43-45). The focal plane is just outside the space occupied by the secondary mirror and therefore not easily accessible. All mirrors are hyperbolic which allow an excellent (diffraction limited) image quality over a field of 1.2°. A major drawback of this construction is the large obstruction by the tertiary mirror.

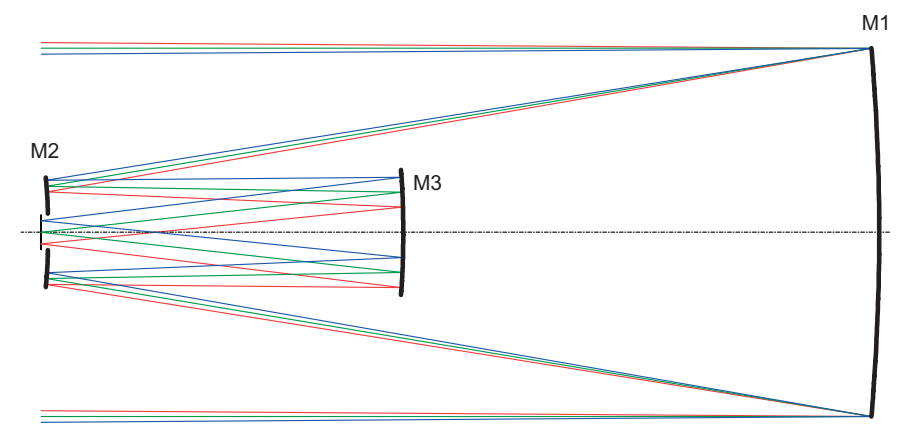


Figure 43-45: Korsch three-mirror telescope. All surfaces are aspherical.

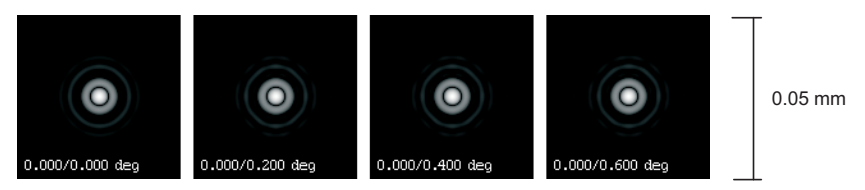


Figure 43-46: Diffraction PSF of the Korsch 3-mirror telescope at F4.5/900mm.

# 43.6.4 Robb Three-mirror Telescope

The three-mirror design by Robb is another example of the Mersenne type of construction but using a non-collimated light beam between the secondary and tertiary mirror. It offers a flat image over a field of 2°. All mirrors are hyperbolic with higher-order aspherical terms.

The image is near the primary mirror. Similar to the Korsch three-mirror telescope (figure 43-45) its main disadvantage is the large obscuration if the field size of 2°, as shown in figure 43-47, is fully utilized.

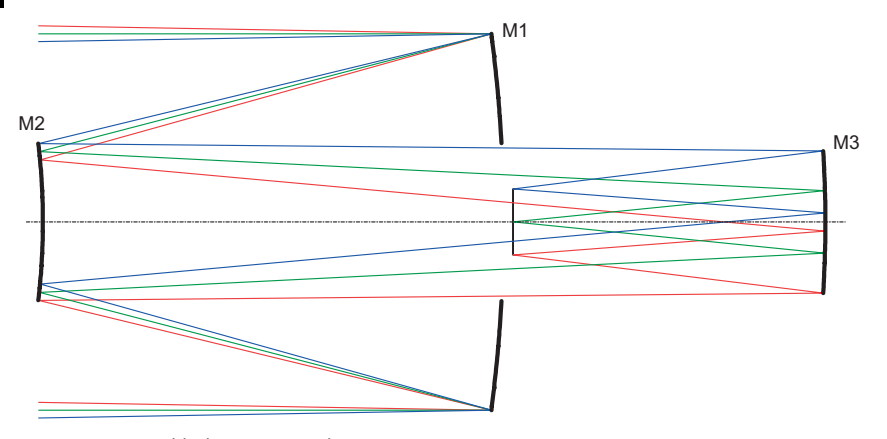


Figure 43-47: Robb three-mirror telescope.

# 43.6.5 Korsch Three-mirror Four-reflection Telescope

Wilson describes a three-mirror telescope attributed to Korsch with four reflections (figure 43-48). The first two mirrors form a Cassegrain telescope but with the focus between M1 and M2. The tertiary mirror is placed closely to the primary, and after reflection from M3, the secondary mirror is used a second time.

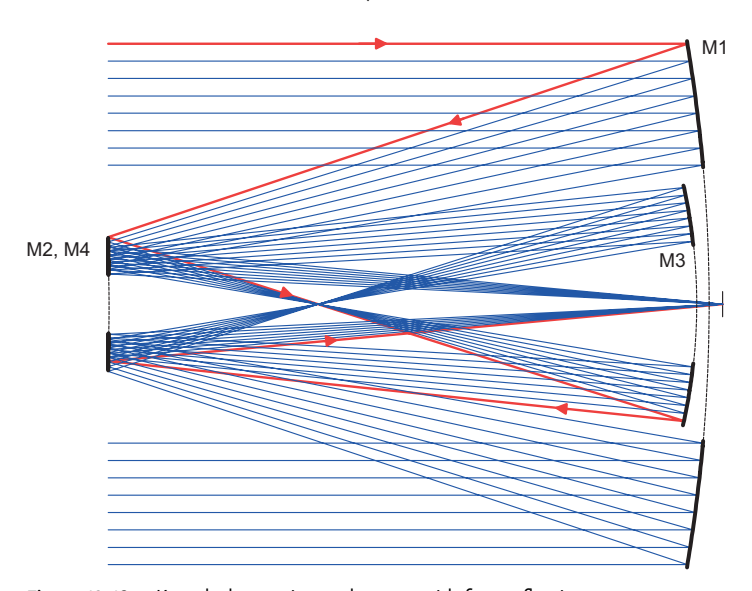


Figure 43-48: Korsch three-mirror telescope with four reflections.

The system can produce a diffraction-limited image over a 0.5° field of view for a 16 m aperture in connection with a Next Generation Large Space Telescope [43-84]. Wilson also pointed out a major problem with four-mirror or four-reflection telescopes. Because the standard coating for large mirrors is still aluminium which has a relatively low reflectivity (approx. 85% in the visible), the telescope transmittance after four reflections drops to about 50%. This value is even further reduced if obstruction effects are taken into account.

## 43.7 Other Three- and Four-mirror Reflecting Telescopes

Telescopes in the Earth's orbit need to be short and lightweight optical systems relative to their diameter to allow them to be cost effectively transported into space. For this kind of application, Beach [43-5] has proposed a four-mirror telescope which has its roots in the Baker–Paul and Mersenne configurations. The primary and secondary mirrors form a near-afocal Mersenne-type feeder system and the tertiary mirror, together with a fourth corrector mirror, perform the imaging. Without the fourth mirror the system would be analogous to the Loveday telescope.

All four mirrors are aspherical, which allows a diffraction-limited image performance over a field of view of  $\pm 0.5^{\circ}$  for apertures up to 1m, and an extremely short construction. The overall length is only 27% of the focal length. This compactness must be paid for by high asphericities of the primary and secondary mirror which requires advanced manufacturing capabilities. Beach proposes computer-controlled diamond turning with subsequent computer-controlled conformable lapping.

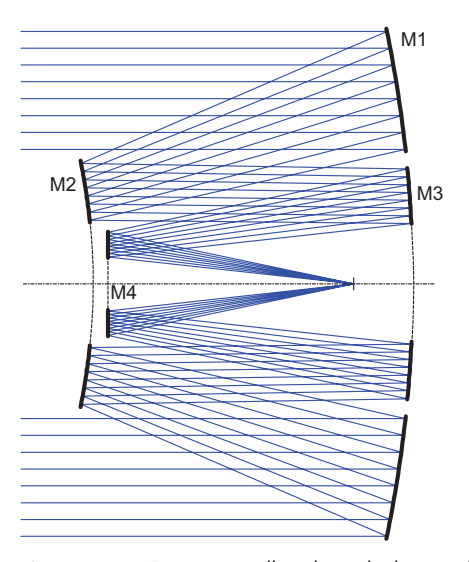


Figure 43-49: Four-mirror all-aspherical telescope for space application after Beach [43-5].

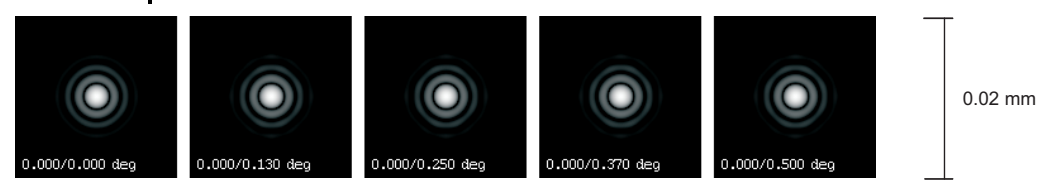


Figure 43-50: PSF of the four-mirror all-aspherical telescope for space application after Beach [43-5]. The PSF is given for a F2.4/ 2400 mm system. FOV =  $\pm 0.5^{\circ}$ .

The four-mirror four-reflection telescope shown in figure 43-51 uses a spherical primary mirror. Due to the intermediate image the entrance pupil is re-imaged onto the fourth mirror, which is not only advantageous for correction of the spherical aberration, but also allows effective stray light suppression. Mirrors M2-M4 are aspherical.

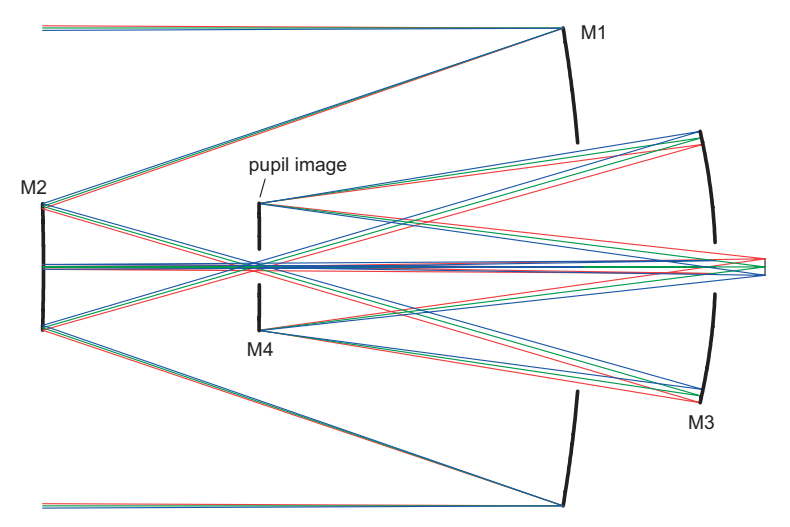


Figure 43-51: Four-mirror compound telescope [43-84].

## 43.8 Two-mirror Schiefspiegler (Oblique Reflector) Telescopes

The name "Schiefspiegler" is German and means "skew" or "oblique reflector". Schiefspiegler telescopes are also commonly known as tilted component telescopes (TCT).

Schiefspiegler telescopes are characterized by the property that they avoid obstruction by secondary mirrors as can be seen with Cassegrain and Ritchey-Chretien telescopes. This is achieved by inclining the primary mirror against the main viewing axis, or by using a centered system off-axis, and therefore allowing the secondary mirror to be moved out of the optical beam. Typically the secondary mirror is also inclined to correct for coma and astigmatism introduced by the tilted primary. Most Schiefspiegler telescopes exhibit a focal ratio of F/20 or higher in order to keep these defects at an acceptable level.

#### 43.8.1

### **Kutter Schiefspiegler**

The German Anton Kutter published his "Schiefspiegler" (oblique mirror) telescope design in 1953 [43-41], which itself was based on earlier work by Fritsch. Since then, the term Schiefspiegler has become the generic name for this type of telescope. It is composed of spherical mirrors only which can be made easily at low cost.

Basically, the design idea was derived from a Cassegrain construction as had already been proposed by Bode in the "Berliner Astronomisches Jahrbuch" in 1811. This concept may easily be understood if only eccentric (off-axis) sections of a centered, two-mirror telescope are used, as shown in figure 43-52.

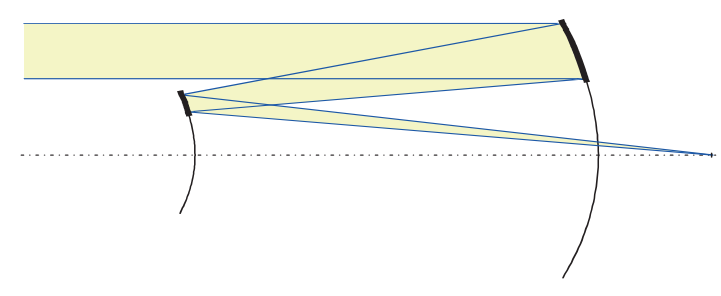


Figure 43-52: Evolution of Kutter's Schiefspiegler from the two-mirror compound telescope.

The main rationale was to avoid the central obstruction but still to obtain a simple design using spherical mirrors. However, when used off-axis, the mirrors are asymmetric and difficult to construct. Kutter made three important changes to facilitate manufacturing.

- He reduced the magnification of the secondary mirror. Typically, in Cassegrain or RC systems, the secondary magnification is between 2 and 4, while in a Schiefspiegler it is close to 1.7.
- He chose long radii of curvature for both mirrors, which helps to reduce aberrations. This resulted in large focal ratios, typically between 20 and 30. If the radius of the secondary is identical to the radius of the primary, manufacture and testing are simplified and a flat field is also achieved.
- The secondary mirror is tilted to further minimize aberrations.

Among the three variants given in Kutter's book, two of them are of particular interest:

The *coma-free* design requires a cylindrical or wedged corrector lens to eliminate the residual astigmatism. However, this corrector creates a noticeable field dependent lateral chromatic aberration. Despite the fact that the design would be very close to the diffraction limit in a monochromatic sense, it is the chromatic aberration of the corrector lens which limits the performance of this telescope.

The astigmatism-free or anastigmatic design tolerates some amount of coma but does not exhibit astigmatism. In addition, it does not require a corrector lens which is subject to the introduction of chromatic errors. The residual coma of the anastigmatic design is on the order of the Airy diameter.

The third solution, which Kutter denoted as "the golden mean", has the secondary mirror tilted between the anastigmatic and the coma-free system. Astigmatism and coma both exist but can be eliminated by placing a tilted plano-convex lens in the beam between the secondary mirror and the image. Since the power of this lens is weak, color aberrations are also small.

In the following analysis, we shall be concerned only with the anastigmatic design which is the most popular system. A detailed reasoning is given by Kutter [43-41] and a thorough analysis of coma correction and astigmatism is provided by Wilson.

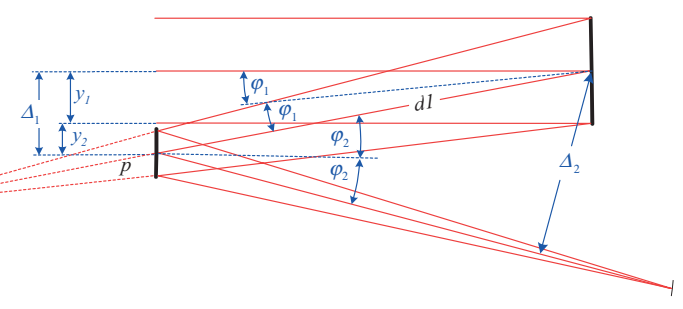


Figure 43-53: Schematics of the Schiefspiegler.

The tilt of the primary mirror is defined by the requirement of a non-obstructed aperture and is obtained by the simple trigonometric relation

$$\sin 2\varphi_1 = \frac{\Delta_1}{d_1} \,. \tag{43-65}$$

The tilt angle of the secondary mirror depends on the condition of corrected astigmatism. Without further derivation we write

$$\sin \varphi_2 = \sin \varphi_1 \frac{\gamma_1}{\gamma_2} \sqrt{\frac{r_2}{r_1}}.$$
 (43-66)

We have now obtained a telescope which is free from astigmatism but which suffers from coma. However, if the system is made long enough, coma can be reduced to a level which is close to the Airy disk. The Petzval sum will be zero (flat field) if the radius of curvature of each mirror is identical. Equation (43-66) then reduces to

$$\sin \varphi_2 = \sin \varphi_1 \frac{\gamma_1}{\gamma_2}. \tag{43-67}$$

As with many of the Schiefspiegler variants, the image plane is tilted with respect to the direction of the axial beam, thus limiting the usable field of view for visual applications (i.e., in conjunction with an eyepiece). For photographic applications, the film plane may also be tilted.

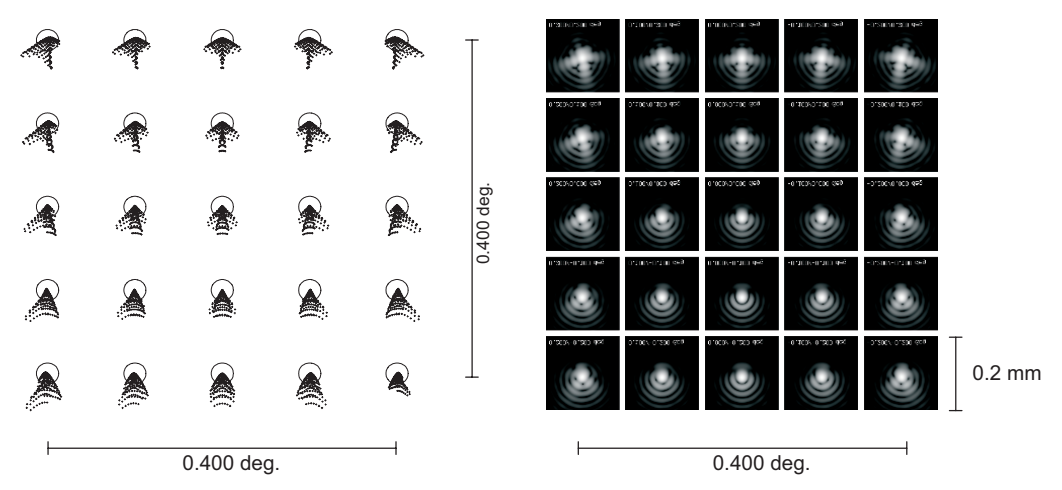


Figure 43-54: Spot performance of an anastigmatic Kutter Schiefspiegler at F29/5700 mm.

### 43.8.2 Herrig Schiefspiegler

A two-mirror telescope using only spheres, but with four reflections in a double-path configuration, was proposed by E. Herrig [43-24], as shown in figure 43-55. The first mirror is a convex sphere, the second one is concave. The image is created at a displaced location behind the primary mirror which gives an observational condition similar to a refractor telescope.

Due to the double-pass configuration, the telescope becomes very compact. The system provides excellent compensation for coma and astigmatism on a flat image surface. The image quality is nearly diffraction limited over a field-of-view of 0.4°. Even though the image surface is flat, it is slightly tilted with respect to the main beam. This effect can (and should) be compensated for photographic applications by tilting the film (or CCD) plane as well. However, this may degrade the sharpness for visual applications when the telescope is used in conjunction with an eyepiece.

An obvious disadvantage of this concept is that the mirror diameters need to be significantly oversized, even for a relatively small field of view. For example, the configuration shown in figure 43-55 is an unvignetted F/12 system with 0.4° FOV, but requires a primary mirror that is 1.5 times larger than the entrance aperture. The oversizing factor for the secondary mirror is approximately 1.4.

The Herrig telescope also presents difficulties in construction and testing because the radii of the mirrors are extremely large.

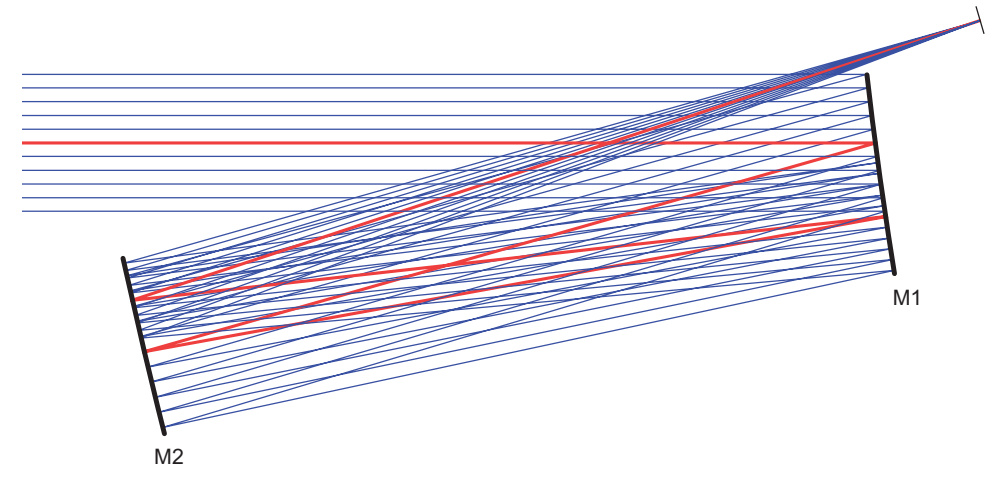


Figure 43-55: Herrig Schiefspiegler [43-24] comprising two spherical mirrors and four reflections.

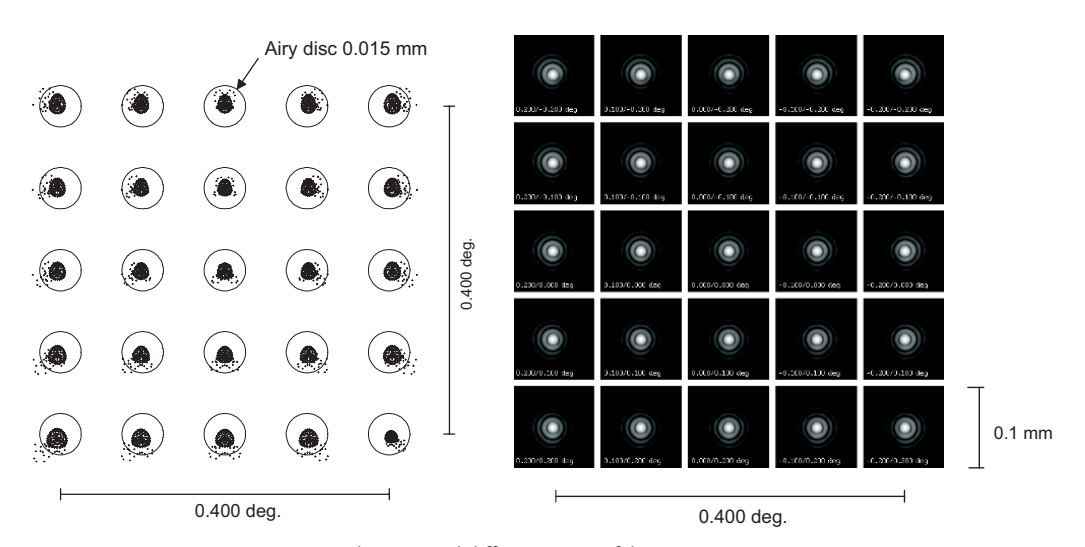
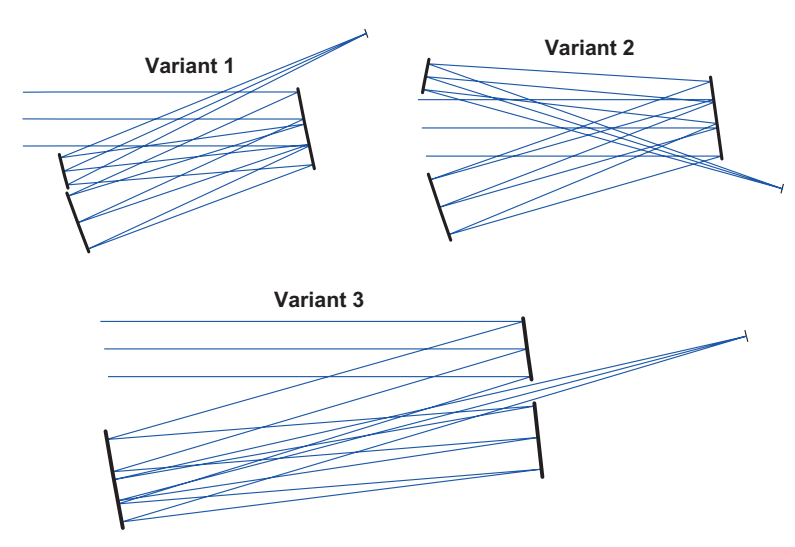


Figure 43-56: Spot diagram and diffraction PSF of the Herrig Schiefspiegler on a tilted focal plane. The square FOV is 0.4°. Telescope parameters: F11/2200 mm.

Variations of the Herrig telescope are possible, e.g., by replacing the common secondary mirror by two separate mirrors. This gives additional degrees of freedom for further optimizations and also new configurations (see figure 43-57).



**Figure 43-57:** Other configurations of the Herrig telescope using three mirrors in a double folded path.

## 43.8.3 Yolo Telescope

The Yolo telescope, named by the inventor Arthur S. Leonard, after a county in California, differs from a Schiefspiegler in that the light beams are folded in a X-shaped configuration and both mirrors are concave. The system power is almost evenly distributed among the two mirrors, that is, an F/12 system is composed of two mirrors each having a focal ratio of F/24.

The advantages of the Yolo system over the Kutter Schiefspiegler are smaller focal ratios, smaller image tilts, and a more compact form. The major drawback is that the Yolo design cannot be corrected for astigmatism. This is typically compensated for by the toroidal shape of the secondary mirror. Several methods have been employed in order to generate the desired form, for example, by use of a warping harness, by refining the correction of the secondary, or adding a cylindrical lens in the convergent beam close to the focus.

The design suffers from residual spherical aberration and also the astigmatism cannot be fully compensated using a toroidal mirror. Aspherizing the primary mirror in addition helps to further reduce these aberrations.

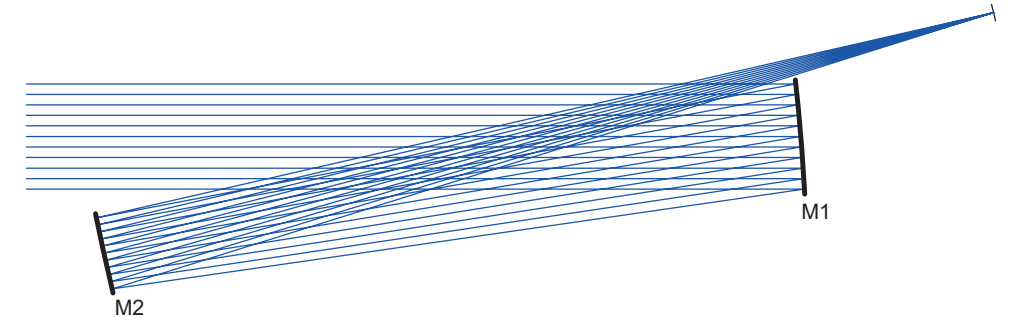
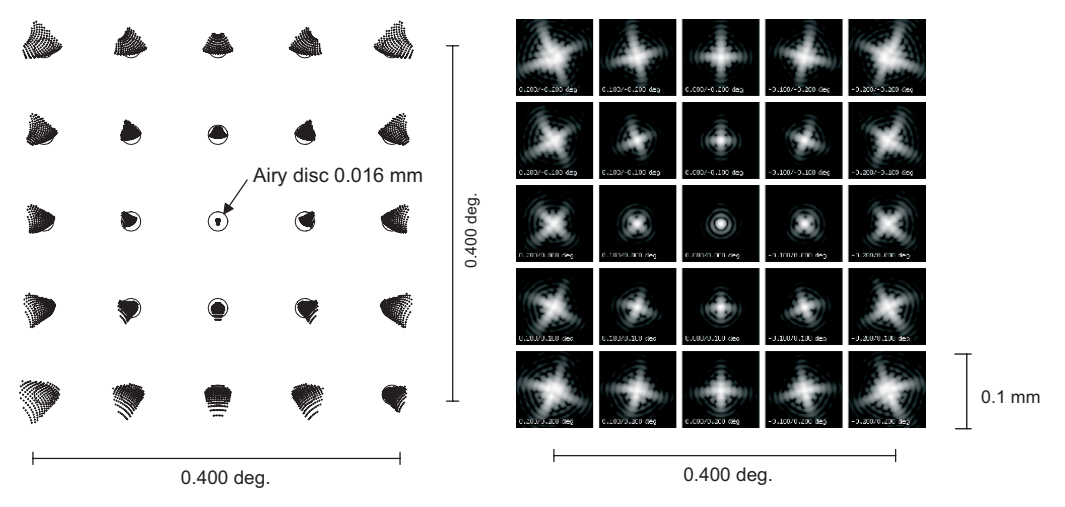


Figure 43-58: Yolo telescope.



**Figure 43-59:** Spot diagram and diffraction PSF of the Yolo Schiefspiegler on a tilted focal plane. The square FOV is 0.4°. Telescope parameters: F12.5/2500 mm.

# 43.9 Three-mirror Schiefspiegler Telescopes

### 43.9.1

### Kutter and Buchroeder Tri-Schiefspiegler

After the development of his two-mirror Schiefspiegler, Kutter added a third mirror in order to eliminate the inherent limitations of the classical two-mirror form, coma respectively astigmatism. A modern version with improved performance near to the diffraction limit over 0.4° field of view was then suggested by Buchroeder, as shown in figure 43-60.

Three-mirror Schiefspiegler telescopes can be successfully corrected up to apertures of approximately 300 mm, however, they are limited to large F-numbers (> F/12).

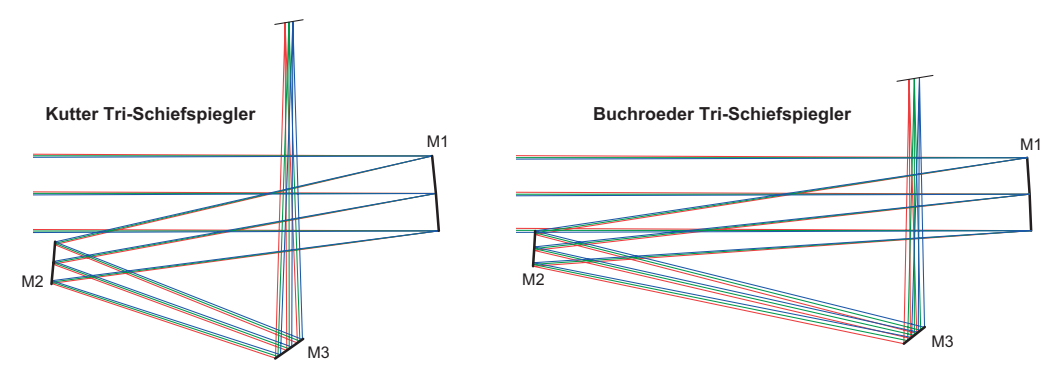
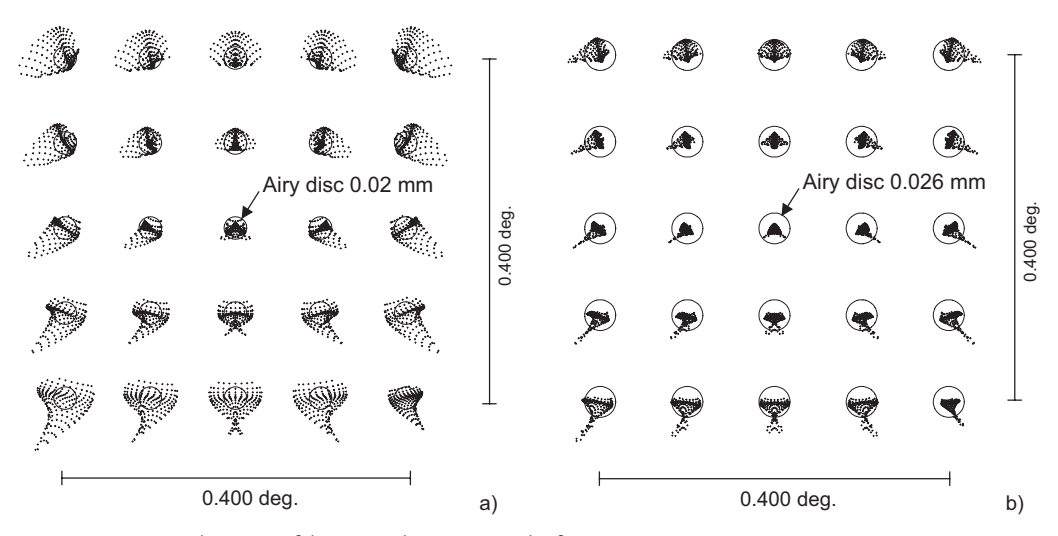


Figure 43-60: Kutter and Buchroeder three-mirror Schiefspiegler



**Figure 43-61:** Spot diagrams of the Kutter three-mirror Schiefspiegler (a) and the Buchroeder three-mirror Schiefspiegler (b) as given in figure 43-60.

# 43.9.2 Stevick-Paul Schiefspiegler

The telescope proposed by Stevick [43-78] is based on the original Paul three-mirror design (see section 43.6.1) but is using off-axis segments of the mirrors to get rid of the large obstruction inherent in the Paul design. He also moved the tertiary mirror

behind the primary mirror, so that the center of curvature of M3 coincides with the location of M2; a modification we have already seen with the Paul–Baker and Willstrop telescopes, in order to fulfill the condition for a flat field.

Stevick sought a solution for a telescope that could be built by amateurs, so he used only spherical surfaces, which resulted in a system with a long focal length. The system can only be used at relatively "slow" relative apertures of F/15 and higher. A fourth (flat) mirror was added to gain better access to the focal plane, which is tilted by about 9°. Despite its nearly diffraction limited performance over a field of about 0.5°, the large image plane tilt imposes practical limits for visual observation (i.e., when used in conjunction with an eyepiece), because the focal plane of the eyepiece is perpendicular to the main ray bundle.

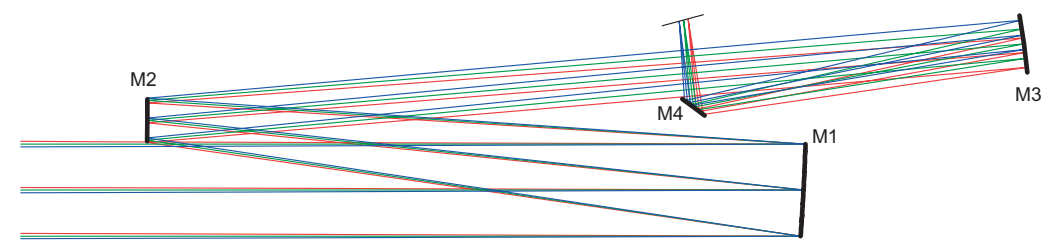


Figure 43-62: Stevick-Paul Schiefspiegler

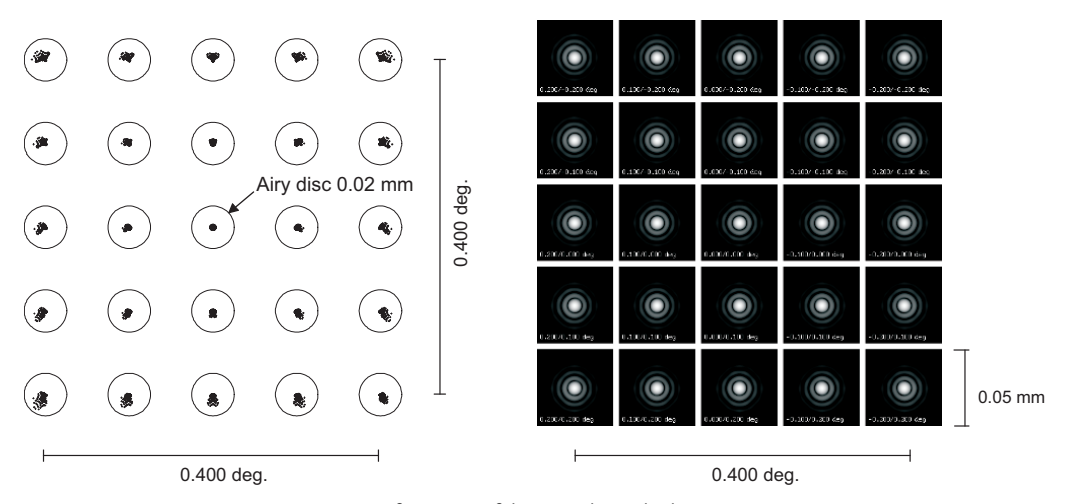


Figure 43-63: Image performance of the Stevick–Paul telescope, F14.5/2900 mm, FOV = 0.4°.

A modification of the Stevick–Paul telescope is given by Francis [43-18], who folded the beam path using an additional flat mirror between the secondary and tertiary mirrors, thus effectively using the polar axis in a German mount (figure 43-64). The image performance is comparable with the Stevick–Paul telescope.

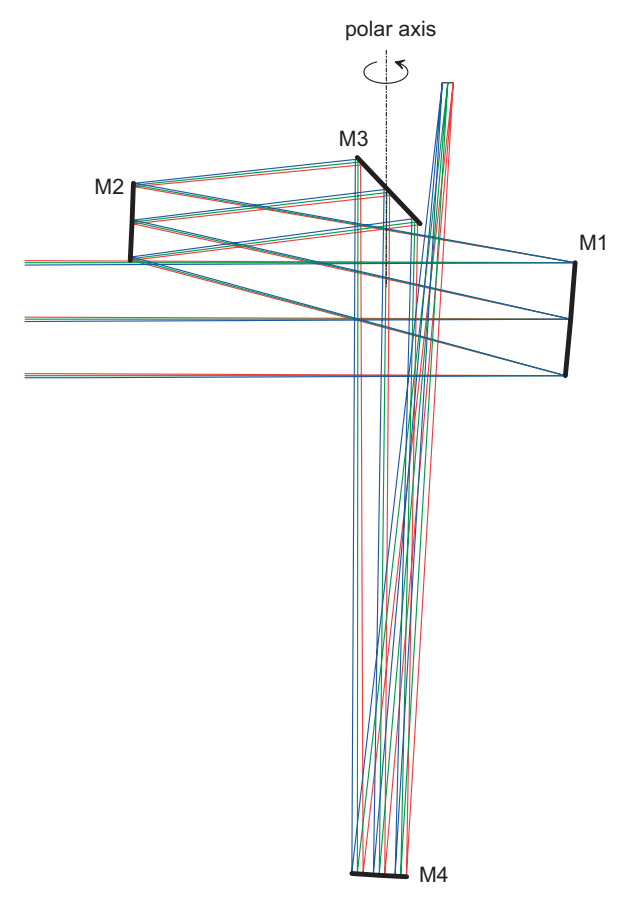


Figure 43-64: Modified Stevick—Paul Schiefspiegler by Francis, using an additional fold mirror (M3) and sending the light path down the polar axis in a German mount [43-18].

#### 43.9.3

### **Brunn Schiefspiegler**

A modification of the Stevick–Paul telescope was subsequently published by Brunn [43-8] (figure 43-65). The spherical mirrors are used at larger off-axis sections (or larger tilt angles, respectively) to free the space between the mirrors and gain a better accessibility of the focal plane. Because the mirrors are used at larger angles, a relative aperture of F/20 and higher is required to achieve near-diffraction-limited performance. At this aperture ratio, spots and diffraction PSF are comparable to the Stevick–Paul design (figure 43-64).

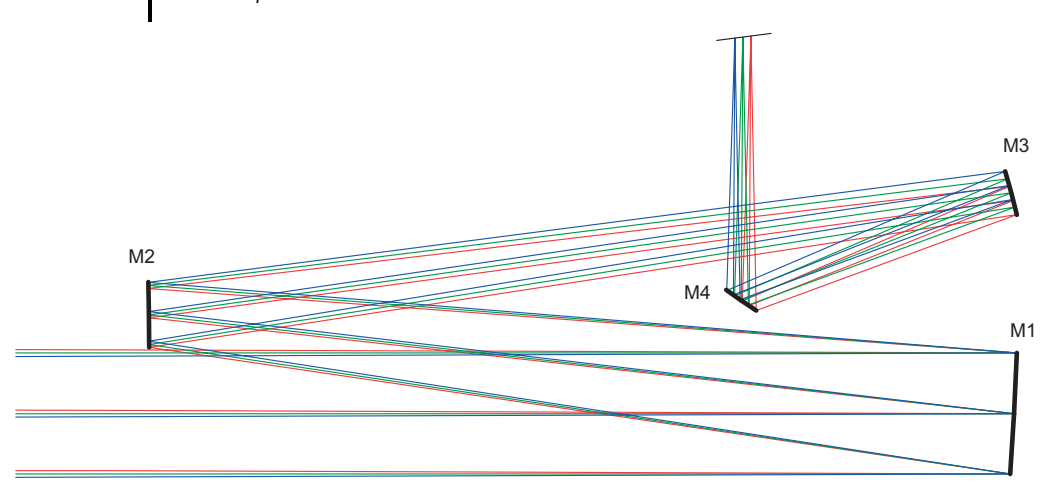


Figure 43-65: Brunn Schiefspiegler [43-8]

## 43.9.4 **Shafer Schiefspiegler**

This three-mirror design using only spherical mirrors was initially developed by Shafer as an infrared collimator [43-89] (figure 43-66). At reduced speed, however, aberrations can be controlled near to the Airy diffraction diameter over a field of ±0.2° in the visible spectrum. Shafer reports that field diameters up to 1.3° are possible without vignetting.

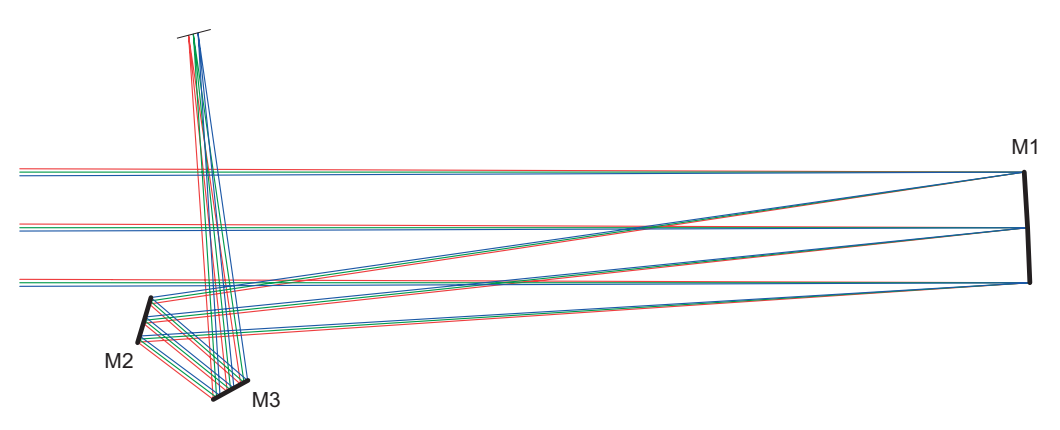


Figure 43-66: Shafer three-mirror Schiefspiegler.

### Solano Schiefspiegler

The Solano design is essentially based on the Yolo telescope (section 43.8.3), except that a third mirror close to the focal plane is added (figure 43-67). The tertiary mirror's optical power is opposite to the power of the secondary mirror which allows reduction of field curvature and an intrinsically better correction of off-axis aberrations.

Despite the fact that three mirrors are required, the major advantage of the Solano telescope over the Yolo design is that it utilizes only spherical mirrors. This property avoids the difficulty to fabricate the toroidal secondary mirror of the Yolo telescopes and therefore significantly reduces manufacturing efforts.

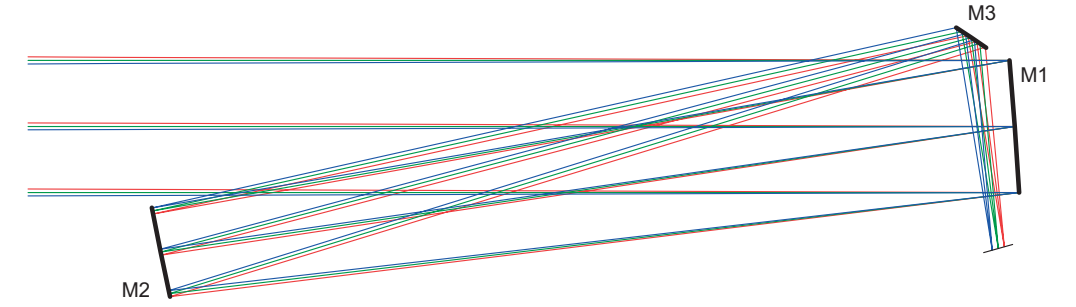


Figure 43-67: Solano three-mirror Schiefspiegler.

# 43.9.6 General Solutions for Three-mirror Schiefspiegler Telescopes

In a series of papers, Howard and Stone [43-27], [43-28], [43-29] attempted to design two-, three- and four- mirror oblique telescopes using spherical surfaces from the ground, i.e., without resorting to previous centered design forms and then used it off-axis for removal of obstructions, or by incrementally modifying existing centered designs and forcing out obstructions in small steps.

The approach of Howard and Stone is based on a Taylor expansion of Hamilton's point-angle mixed characteristic, where the coefficients of the Taylor expansion are functions of the system parameters. The configuration space found by this method is then searched by a global computer optimization routine (known as adapted simulated annealing, ASA). Because the mathematical derivation of their method does not fit into the scope of this book, the reader is referred to the corresponding papers [43-27]–[43-29].

The configurations found for three-mirror plane-symmetric telescopes are shown in figures 43-68 to 43-70 and in tables 43-1, 43-2. Also note the four-mirror solutions by Howard and Stone in section 43.10.4.

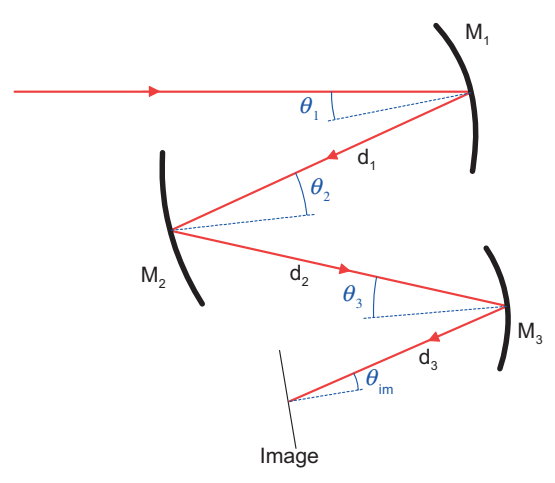


**Figure 43-68:** Parameter definitions for oblique three-mirror telescopes as shown in figures 43-69 and 43-70.

**Table 43-1:** General solutions A–F for tilted mirror telescopes using only spherical mirrors, according to Howard [43-28]. Construction data are given for 100 mm focal length and focal ratio F/10. Notice the sign conventions for radii, thicknesses and tilt angles given in section 43.17.

Parameter	Α	В	С	D	E	F
$\theta_1$ (°)	10.000	70.000	10.000	10.000	10.000	10.000
$\theta_2(°)$	4.000	70.000	-50.000	-24.000	30.000	52.000
$\theta_3$ (°)	-14.000	-70.000	-12.000	10.000	-18.000	28.000
$\theta_{im}(°)$	0.858	0.097	12.988	-9.685	10.521	-15.426
$d_1$ (mm)	-90.000	-90.000	-70.000	-70.000	-70.000	-70.000
$d_2$ (mm)	86.954	66.341	65.135	65.670	16.936	8.877
$d_3$ (mm)	-22.417	-33.000	-22.643	-34.512	-53.737	-54.029
$R_1$ (mm)	1000.0	-333.333	-333.333	-333.333	-333.333	-333.333
$R_2$ (mm)	180.832	103.124	-2728.7	-479.118	-327.671	-715.582
R <sub>3</sub> (mm)	340.368	90.979	105.603	-107.354	142.077	-187.196

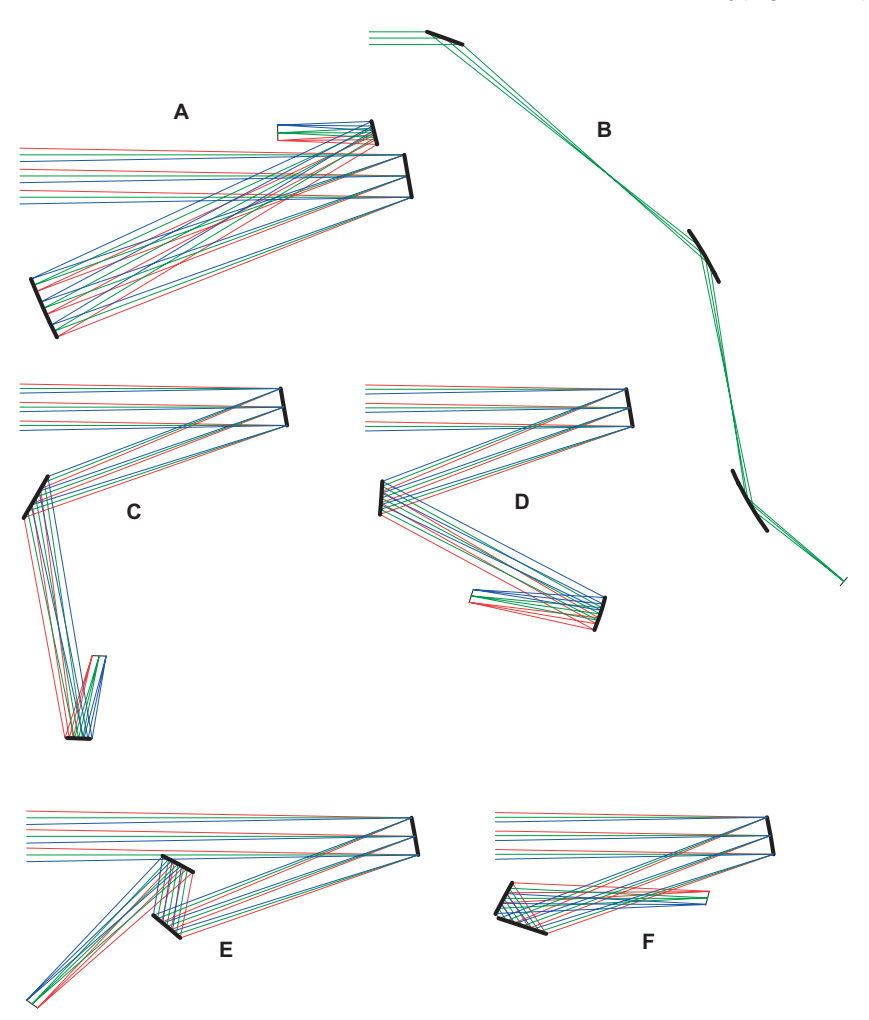


**Figure 43-69:** General solutions A–F for tilted mirror telescopes using only spherical mirrors, according to Howard [43-28].

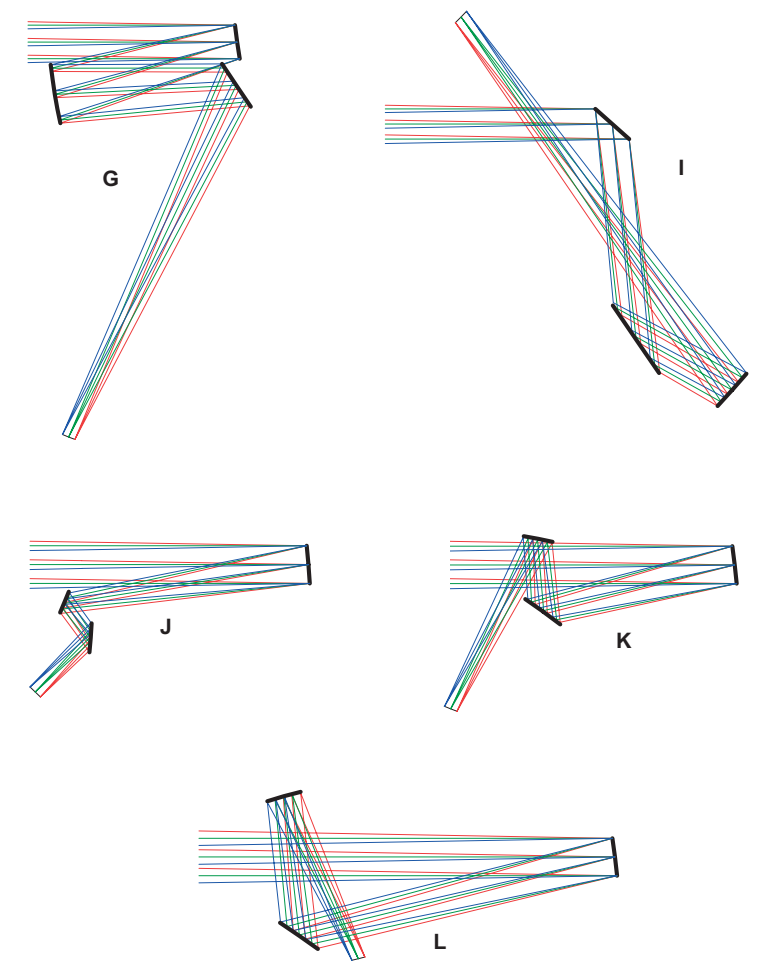


**Figure 43-70:** General solutions G–L for tilted mirror telescopes using only spherical mirrors, according to Howard [43-28].

**Table 43-2:** General solutions G–L for tilted mirror telescopes using only spherical mirrors, according to Howard [43-28]. Construction data are given for 100 mm focal length and focal ratio F/10. Notice the sign conventions for radii, thicknesses and tilt angles given in section 43.17.

Parameter	G	I	J	К	L
$\theta_1$ (°)	8.000	48.179	4.543	6.743	6.974
$\theta_2(°)$	-6.587	-62.712	-31.434	40.721	41.224
$\theta_3$ (°)	30.882	-12.493	49.364	-16.058	9.162
$\theta_{\scriptscriptstyle im}(°)$	3.463	10.056	1.134	4.882	-10.361
$d_1$ (mm)	-50.209	-47.257	-65.197	-51.983	-86.043
$d_2$ (mm)	48.086	24.207	11.152	18.718	36.790
$d_3$ (mm)	-103.369	-101.737	-20.544	-50.303	-47.174
$R_1$ (mm)	182.715	6622.52	-180.245	-277.239	-452.489
$R_2$ (mm)	142.939	-13084.3	-170.156	-1826.817	-3210.27
R <sub>3</sub> (mm)	2837.68	193.424	-298.113	-288.101	-157.778

# 43.10 Four-mirror Schiefspiegler

Numerous innovative multi-mirror designs employing only spherical mirrors and avoiding obscuration have recently been published by Shafer [43-73], [43-89], [43-98], [43-100]. Some of his most interesting designs with respect to telescopes are presented in the sext sections.

# 43.10.1 Shafer-Mersenne Telescope

In the design initially proposed by Shafer [43-98], an afocal front telescope of the Mersenne type and a Schwarzschild imaging telescope (similar to figure 43-36) are successively combined. Figure 43-71 shows the optical configuration in which an off-axis (eccentric) portion of the pupil is used to prevent obstruction. If only spherical mirrors are utilized, the usable field of view is very small.

A practical example of this system, albeit in an axial configuration with obscuration, is also discussed by Chung and Lee [43-99].

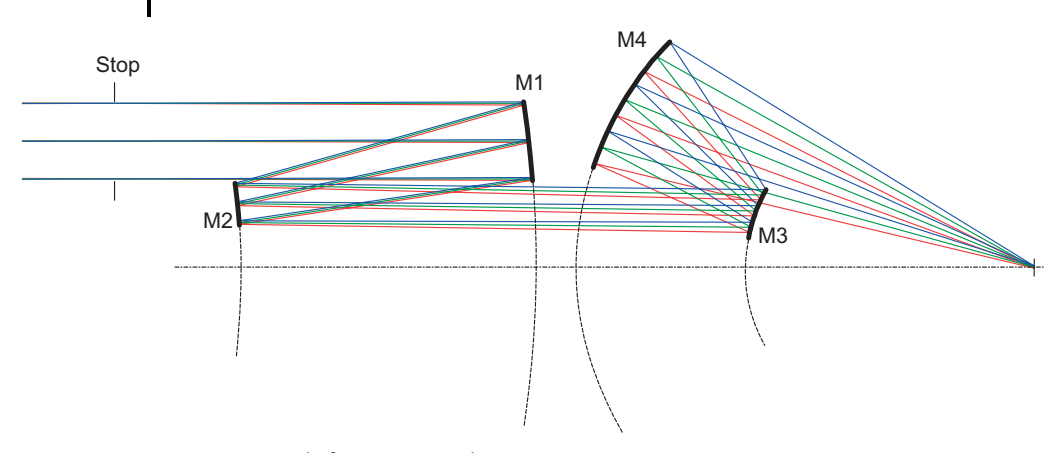


Figure 43-71: Shafer-Mersenne telescope.

# 43.10.2 Shafer Four- and Five-mirror Unobscured Telescopes

Another four-mirror telescope proposed by Shafer is shown in figure 43-72. Due to the double Z-folding of the optical beam a very compact design can be achieved. The maximum length in axial direction is only 1.2 times the focal length. Using only spherical mirrors, the system can be made nearly diffraction limited at an aperture ratio >F/8. Another interesting feature is that the beams at the focal plane are almost perfectly telecentric if the stop coincides with the secondary mirror.

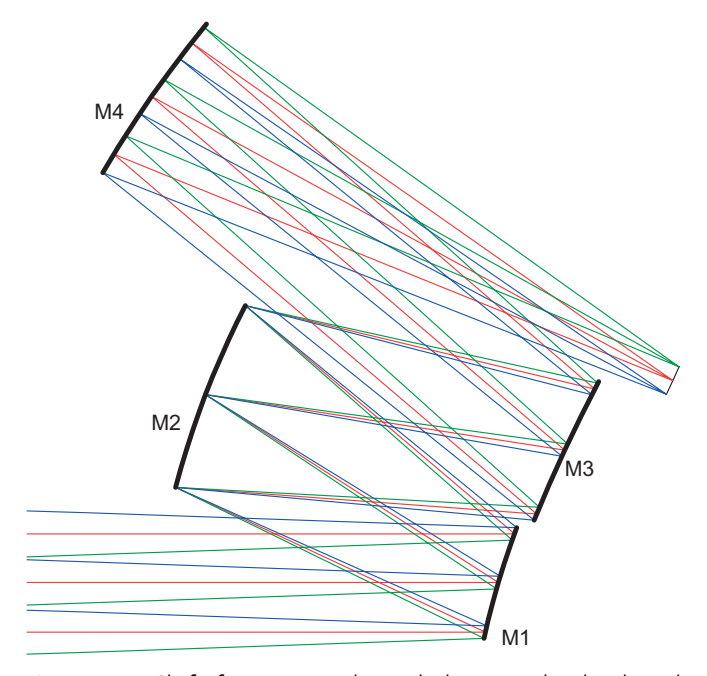


Figure 43-72: Shafer four-mirror unobscured telescope with only spherical surfaces.

The five-mirror telescope by Shafer shown in figure 43-73 uses only off-axis segments of mirrors by neatly combining well-known design principles already described in this chapter. The curved field of the spherical primary mirror is flattened by the secondary mirror M2 in a similar way to the field flattener lens described in section 43.15.1. The optical power of the lens is hereby replaced by a mirror. The tertiary mirror is essentially a folding mirror (with very large radius of curvature) to deflect the optical beams into an Offner relay system (mirrors M4 to M6). The Offner relay is a 1:1 imaging system and is known for its excellent imaging characteristics on a flat field.

With this configuration, practically diffraction limited performance can be achieved at fast focal ratios >F/5 over strip fields of 0.3° (in Y-direction) by 1° (in X-direction).

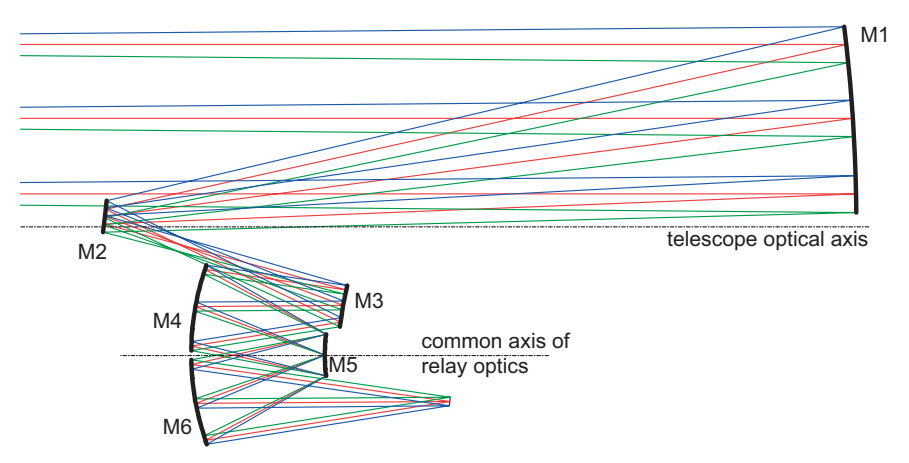


Figure 43-73: Shafer five-mirror telescope using an Offner-type relay optics [43-73].

# 43.10.3 Afocal Four-mirror Telescope

An afocal version of an unobscured four-mirror telescope proposed by Kebo [43-32] is shown in figure 43-74. The curvatures of revolution of all mirrors are aligned on a common optical axis, however, all mirrors are used at off-axis segments to avoid obstruction. The optical construction of the feeder telescope (M1, M2) is based on a Mersenne type, used at off-axis apertures. The mirror pairs (M1, M2) and (M3, M4) each form an afocal telescope. All mirrors must be aspherical in order to correct higher-order aberrations.

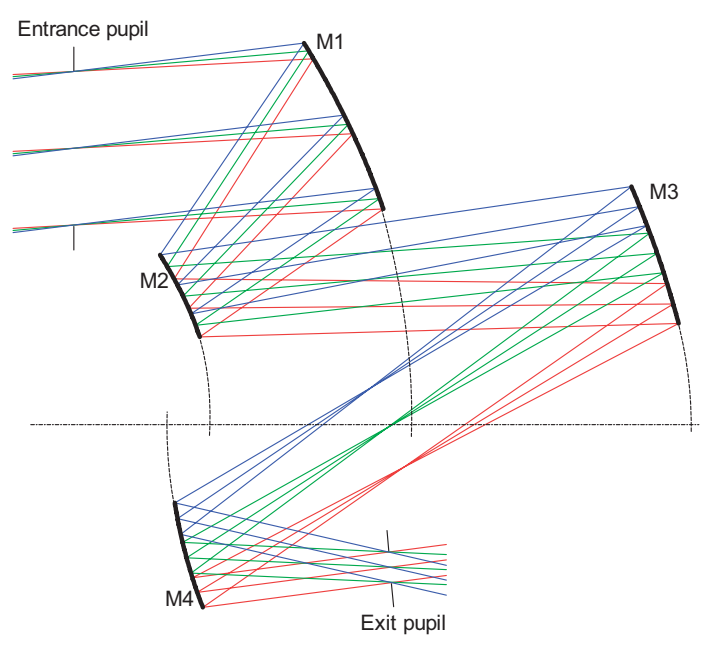
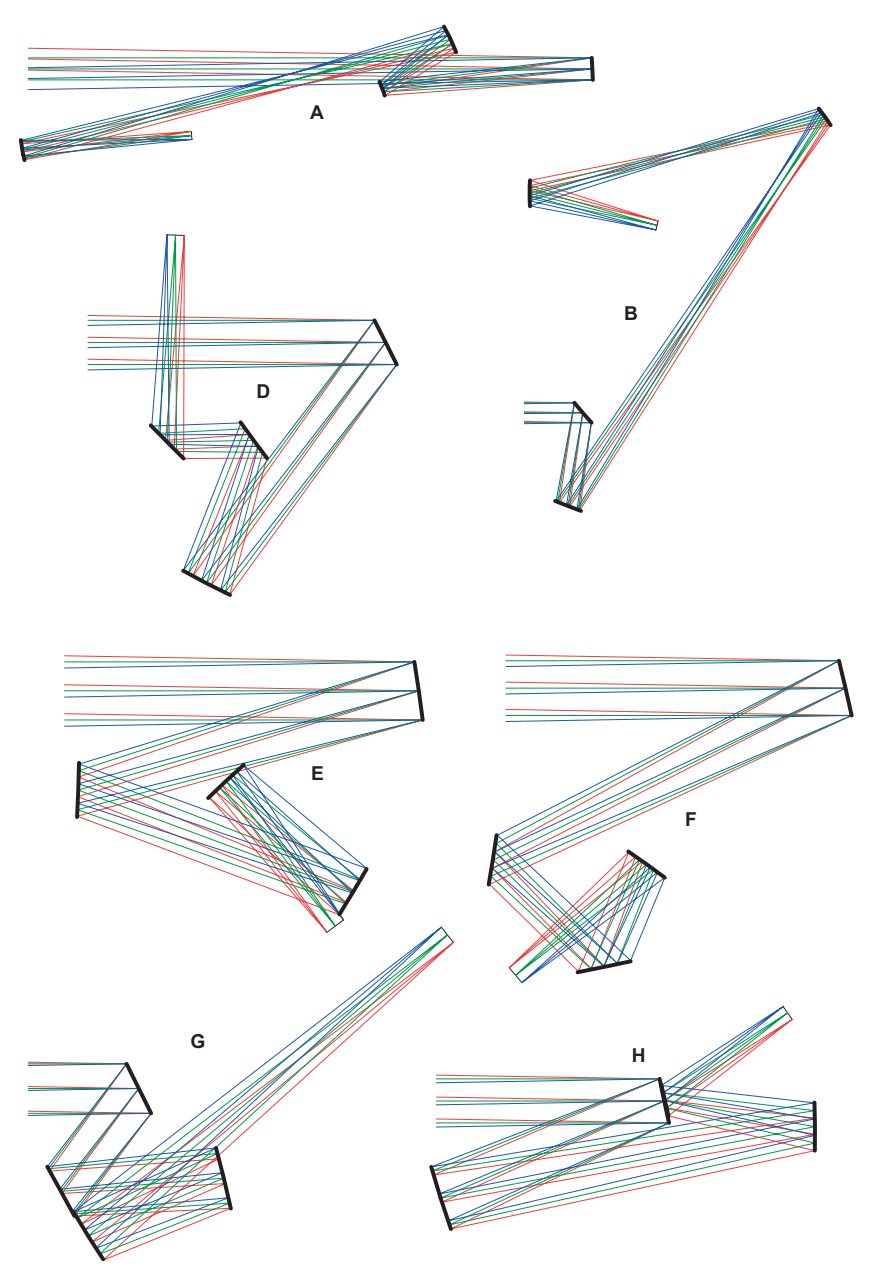


Figure 43-74: Afocal four-mirror telescope with angular magnification 4× after Kebo [43-32].

# 43.10.4 General Solutions for Four-mirror Schiefspiegler Telescopes

Howard and Stone [43-29] proposed four mirror oblique telescopes using only spherical surfaces from the ground, i.e., without resorting to previous centered design forms and then use it off-axis for removal of obstructions, or by incrementally modifying existing centered designs and forcing out obstruction in small steps.

The configurations found by Howard and Stone for four-mirror plane-symmetric telescopes are shown in figure 43-75 and in table 43-3. Also note the three-mirror solutions by Howard and Stone in section 43.9.6.



**Figure 43-75:** Four-mirror telescopes using only spherical mirrors [43-28].

**Table 43-3:** Construction parameters for the systems illustrated in figure 43-75. Construction data are given for 100 mm focal length and focal ratio F/10. Notice the sign conventions for radii, thicknesses and tilt angles given in section 43.17.

Parameter	Α	В	D	E	F	G	Н
$\theta_1$ (°)	2.690	40.512	26.711	8.166	13.107	26.411	11.880
$\theta_2(°)$	15.427	-12.151	9.176	-18.360	-35.143	-24.102	-6.402
$\theta_3$ (°)	-10.808	-21.051	-35.294	-10.393	-34.221	9.244	-10.501
$\theta_4(°)$	-4.853	-14.423	43.244	-5.973	-13.498	8.433	22.955
$\theta_{\scriptscriptstyle im}(°)$	-1.249	0.0159	0.0181	0.038	0.1265	-1.4797	-1.0268
$d_1$ (mm)	-95.112	-36.318	-60.639	-60.100	-69.308	-23.313	-53.580
$d_2$ (mm)	37.889	179.167	30.437	49.679	27.187	29.541	83.589
$d_3$ (mm)	-199.826	-116.825	-17.424	-28.644	-19.639	-26.666	-33.393
$d_4$ (mm)	76.6795	50.306	41.894	30.867	30.443	84.773	33.205
$R_1$ (mm)	-275.785	1053.408	-1975.50	-336.022	-282.966	-974.659	395.100
$R_2$ (mm)	-64.935	225.989	161.212	-494.805	-319.387	-441.112	218.103
$R_3$ (mm)	-99.990	-98.039	225.581	-384.025	-618.429	-234.742	-287.026
R <sub>4</sub> (mm)	96.339	84.246	378.931	148.104	125.976	473.037	-413.052

## 43.11 Three-mirror Off-axis Anastigmats (TMA)

The so-called three-mirror off-axis anastigmats (TMA) presented in this section are basically also "Schiefspiegler" telescopes as they avoid any aperture obscuration. If this is the only property considered they are likely to be grouped in one of the previous sections about three-mirror Schiefspieglers. However, there are other properties which separate TMA telescopes from the "conventional" Schiefspiegler telescopes:

- TMA telescopes provide a much larger field of view which can be up to 20° or even 30°.
- They provide an easily accessible exit pupil which allows effective stray light control or, placement of a so-called "cold-stop" in infrared (thermal) imaging applications.
- Unlike Schiefspieglers, the mirror surfaces are preferably aligned along a common axis but are used at off-axis sections for unobscured light paths.
- Surfaces are generally steep aspheres with higher-order terms a clear manufacturing disadvantage but which is accepted for the sake of image performance over a wide field of view.

Many TMA designs have been proposed and patented by Cook [43-9]–[43-12], but Korsch [43-37] has also contributed to this development in proposing this configuration for a collimator. TMA telescopes exist in reimaging and non-reimaging forms. A performance comparison of various TMA configurations was recently given by Marsh [43-50].

#### 43.11.1

### **Re-imaging TMA**

Figures 43-76 and 43-77 show relayed image-forming telescopes proposed by Cook [43-9], [43-10]. The mirrors are all hyperbolic sections and they are used off-axis in both aperture and field angle. The systems are well corrected for relatively fast aperture ratios (F/2.5 - F/5) and covering a large strip field of  $5^{\circ} \times 10^{\circ}$ . The larger field extension is typically perpendicular to the drawing plane.

The systems can be well shielded by a field stop at the intermediate image and by a second aperture stop at the real exit pupil. The latter is quite often a mandatory feature in Infrared imaging to block unwanted thermal radiation ("cold stop").

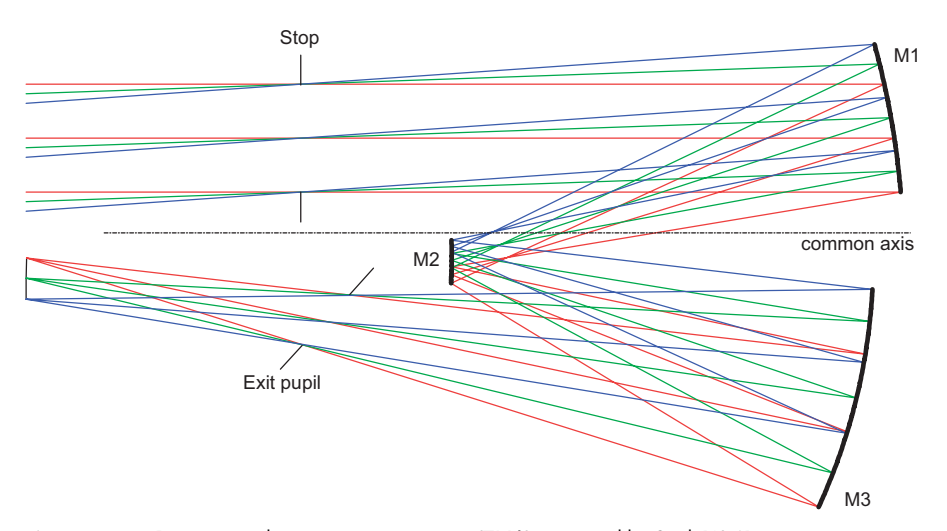


Figure 43-76: Re-imaging three-mirror anastigmat (TMA) proposed by Cook [43-9].

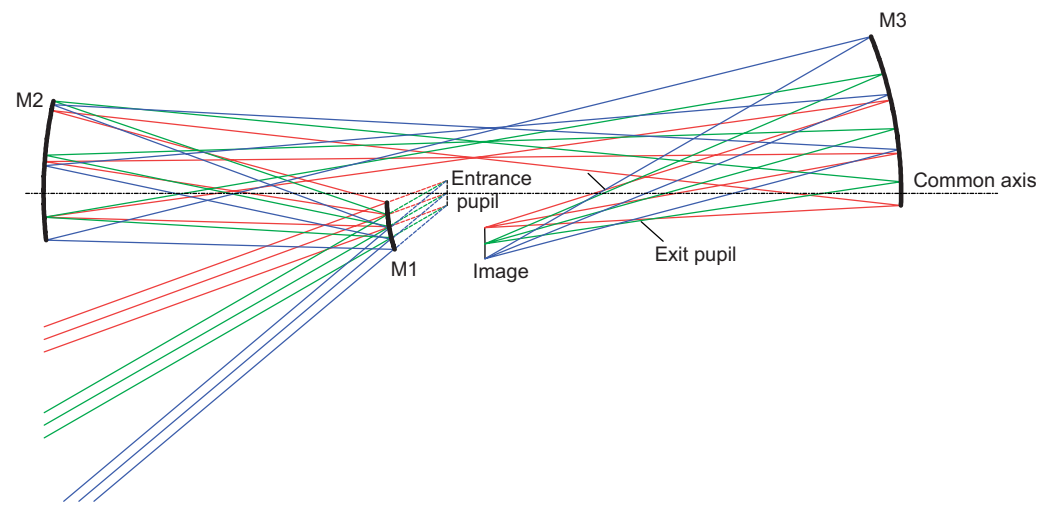


Figure 43-77: Wide field of view three-mirror anastigmat (TMA) proposed by Cook [43-10].

# 43.11.2 Non-re-imaging TMA

Non-re-imaging TMA designs are often seen as the reflecting equivalent of the classical triplet lens objective because of the (+ - +) power distribution. Figure 43-78 shows an example by Cook. The mirrors are all hyperbolic sections and they are used off-axis in both aperture and field angle. In addition, the secondary and tertiary mirror can be slightly decentered and tilted to improve performance and/or widen the field.

Other modifications of Cook's initial TMA design have been presented. One example is a solution by Sinclair where the base surface of the primary and tertiary mirror are at the same axial location and the off-axis segments of M1 and M3 can then be manufactured from a single solid master [43-76]. This would greatly simplify the manufacturing process.

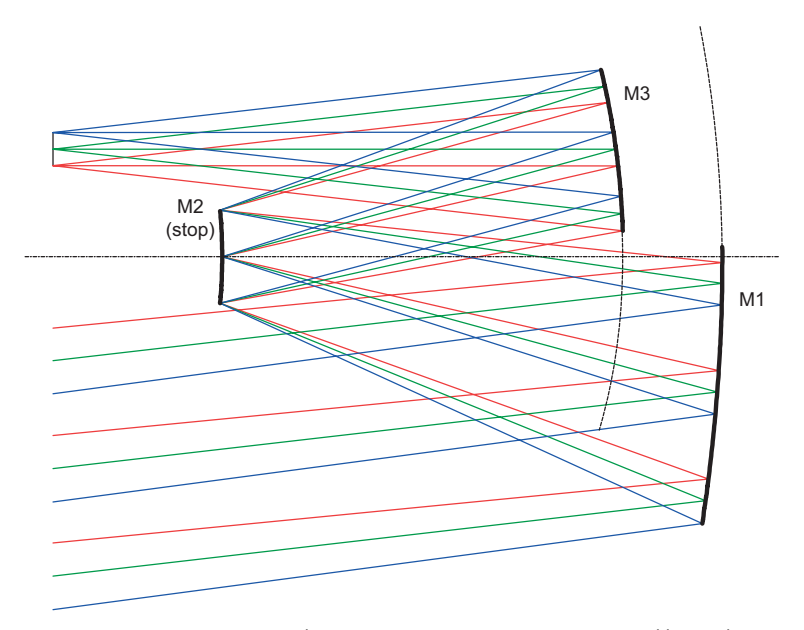


Figure 43-78: Non-re-imaging three-mirror anastigmat (TMA) proposed by Cook [43-9].

### 43.11.3 **Walrus**

The three-mirror all-reflective telescope proposed by Hallam [43-22], also known as 'Hughes Walrus' [43-94], can be considered as an inverse Baker system. The first two mirrors form an afocal system in front of a semi-Schmidt system (M3). The inverse Baker configuration alows reduction of the field angle at the tertiary mirror, however, at the expense of size. The overall length is about 3.4 times the focal length which was probably the reason to call it a 'walrus'.

The system provides a large rectangular field of view (20° along *Y*-axis, 30° along *X*-axis). The Schmidt aspherization is accomplished at the secondary mirror. Higher-order correction can be achieved if all mirrors are generalized aspheres.

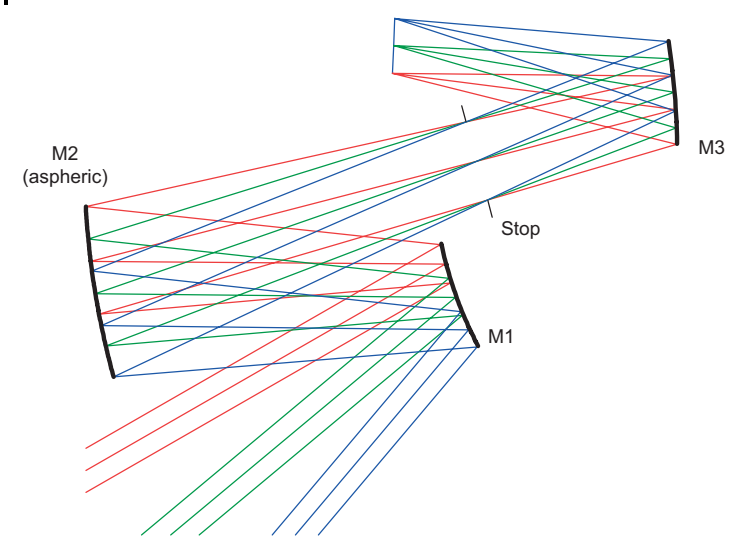


Figure 43-79: Ultra wide-angle three-mirror anastigmat ("Walrus") due to Hallam [43-22].

## 43.12 Two-axis Telescopes

#### 43.12.1

## Korsch Three-mirror, Two-axis Telescope

The flat-field design by Korsch (figure 43-80) covers a field-of-view of 1.5° at a diffraction limited performance. A 45° mirror (M4) located at the exit pupil folds the light beams and thus gives an accessible focal plane. This mirror also totally obstructs the center of the field-of-view (FOV). A distinct advantage, as pointed out by Korsch, is that this telescope configuration is totally free of stray light at the focal plane, without using extensive baffles. All three mirrors are hyperbolical, which complicates fabrication of the surfaces.

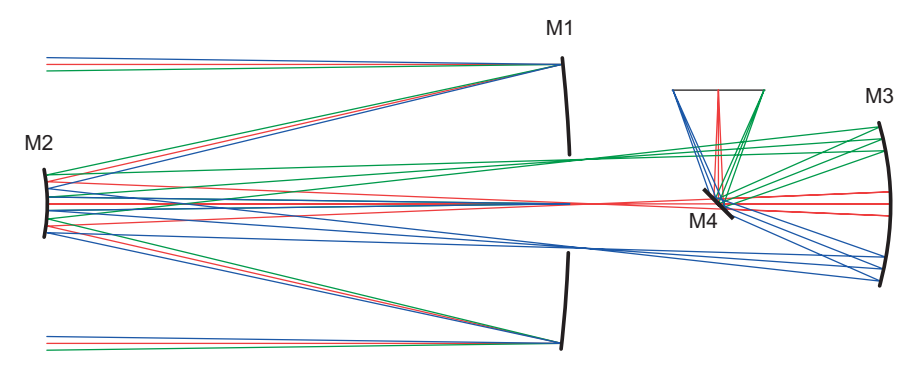


Figure 43-80: Three-mirror Korsch telescope with folding flat mirror [43-40].

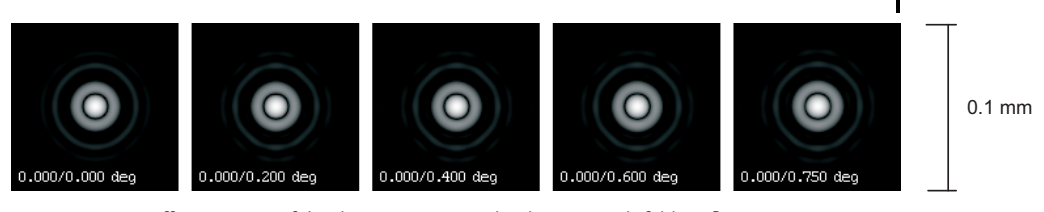


Figure 43-81: Diffraction PSF of the three-mirror Korsch telescope with folding flat mirror.

#### 43.12.2

## Two-axis Telescopes Derived from the Mersenne and Schmidt Principle

The geometry of new three-mirror and four-mirror telescopes can be derived from the solutions developed by Paul, Baker and Willstrop, which in turn are based on the properties of the Mersenne afocal telescope and the Schmidt telescope. On this basis, Wilson describes several four-mirror telescope configurations using a two-axis geometry to minimize central obstruction and to gain an accessible focus position [43-84], [43-96].

Two examples are discussed here. In the first solution (figure 43-82), the system consists of a Mersenne afocal telescope (M1, M2) with a spherical primary and a parabolic secondary mirror. M3 is essentially a Schmidt-type mirror with the center of curvature close to M2 (exactly at the exit pupil of the afocal telescope). M3 re-images this exit pupil on itself, so that this location would not be accessible for a fourth mirror. In a folded (two-axis) configuration, however, this is possible with a small flat mirror at the focus of M3. The fourth mirror then images the intermediate image (at the fold nirror) with magnification 2.

The system gives excellent image performance at F/7 over a field of 0.5°. According to Wilson, even the secondary mirror could be made spherical with a slightly reduced image quality.

In Wilson's second two-axis solution (figure 43-83), a real image is formed after the secondary mirror. The tertiary mirror M3 is again concentric to the exit pupil of the feeder telescope M1-M2. A real, accessible, image of the exit pupil is created at M4.

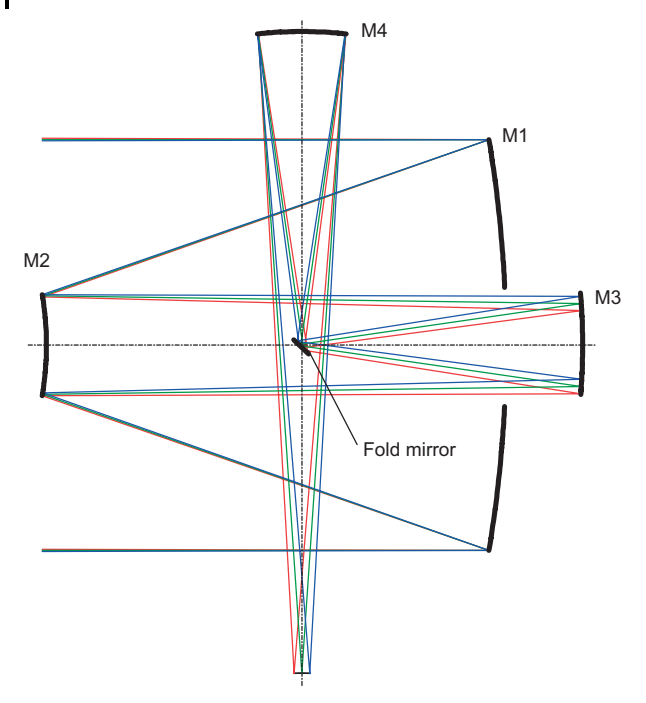


Figure 43-82: Two-axis system using four mirrors as proposed by Wilson and Delabre [43-84], [43-96].

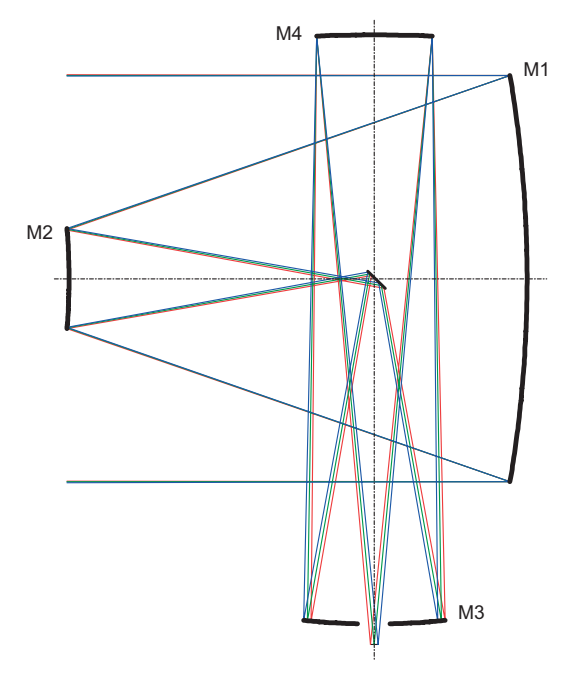


Figure 43-83: Second solution of a two-axis system using four mirrors, after Wilson and Delabre [43-84].

## 43.13 Catadioptric Telescopes

Optical systems that involve both lenses and mirrors are called *catadioptric* systems. In contrast, optical systems using only refraction (by lenses) are said to be "dioptric" telescopes.

#### 43.13.1

### Mangin Telescope

The simplest form of a catadioptric telescope is a negative meniscus with a reflecting back surface. The system was proposed by Mangin who used this configuration in searchlights as a replacement for the parabolic mirror. The refraction at the front surface of the Mangin telescope (or Mangin mirror) reduces the spherical aberration of a spherical mirror.

The Mangin telescope suffers from axial chromatic aberration in a similar way to the meniscus corrector in a Bouwers–Maksutov telescope. Increasing the thickness of the meniscus allows a reduction of the chromatic aberration, but not its elimination. Chromatic aberrations can be corrected with two different kinds of glasses, similar to an achromatic refractor telescope.

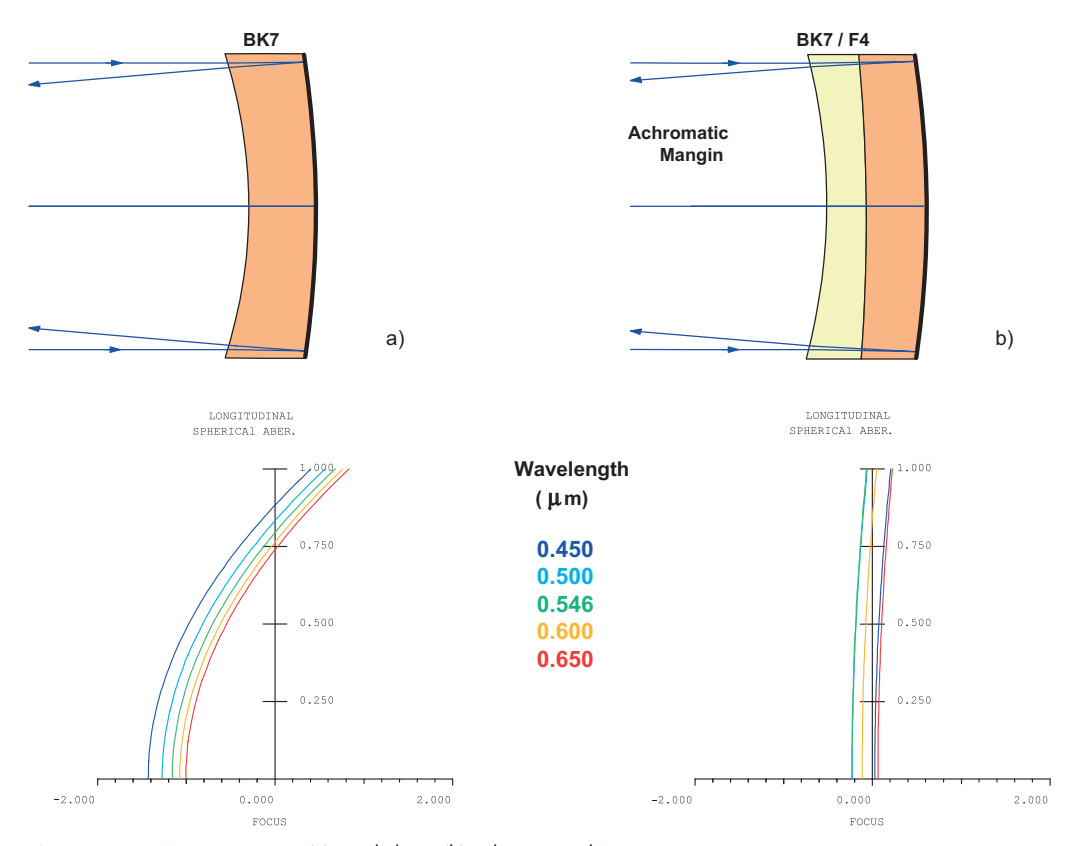


Figure 43-84: Mangin mirrors: (a) single lens; (b) achromatized Mangin mirror.

43.13.2

#### Schmidt Telescope

An advance in telescope design was made by the German Schmidt who moved the stop to the center of curvature of a spherical primary mirror. However, he was probably not the first to do this, because Kellner devised and patented this optical system in 1910 as a high-quality collimator [43-34]. However, it has since become known as the Schmidt system.

To compensate for the inevitable spherical aberration of a spherical mirror, Schmidt (Kellner) introduced an aspherical refracting corrector plate in the plane of the stop. The corrector plate corrects third-order spherical aberration and, due to its symmetric design, also third-order field coma and astigmatism. This is easily understood by the fact that a unique optical axis no longer exists and also off-axis beams are symmetrical to the chief ray. The image lies on a sphere which is concentric with the primary mirror, its radius being exactly half of the radius of curvature of the primary. See figure 43-85.

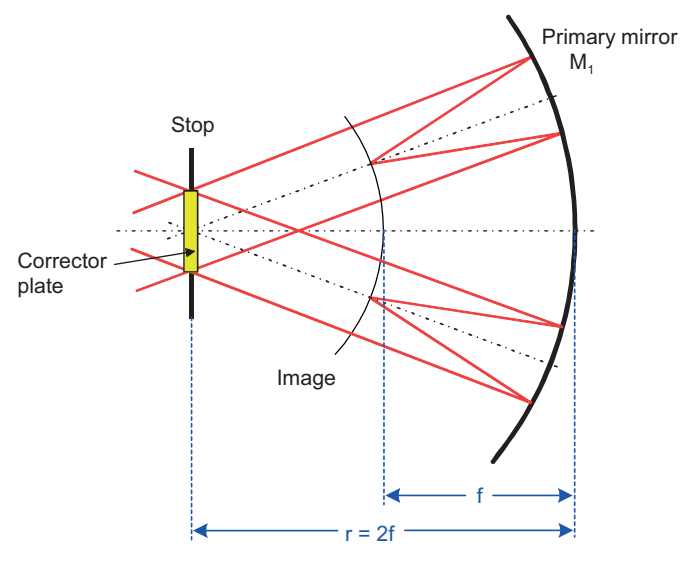


Figure 43-85: Design principle of the Schmidt telescope indicating the symmetry about the stop.

The price paid for the Schmidt design is its length. It has twice the focal length and is about three times the length of a Cassegrain telescope.

The corrector plate is aspherical and fully corrects spherical aberration. The profile of a corrector surface is usually defined by the polynomial series

$$z = Ar^4 + Br^6 + Cr^8 + Dr^{10} + \dots, (43-68)$$

where z is the axial deformation of the surface and r is the radial distance from the optical axis. A corrector profile with only a fourth power term ( $Ar^4$ ) corrects spheri-

cal aberration to third order, which would give (monochromatically) the same correction as the Bouwers telescope. Since the aspherical form is totally free, third-order and higher-order terms of the spherical aberration can be compensated. Even very steep primaries can be corrected by the corrector, if the latter can be fabricated to the required accuracy.

Since the corrector plate is a refracting element, it also introduces chromatic aberrations. The corrector profile, however, can only be optimized for one particular wavelength. At other wavelengths, spherical aberrations are under or overcorrected. This effect, called *spherochromatism*, is illustrated in figure 43-87 for a typical Schmidt plate. From figure 43-87 it is also evident that spherochromatism is the most significant residual error in a Schmidt telescope. Depending on the resolution requirement, this effect may significantly narrow the usable spectral range for a given telescope.

Spherochromatism in a single plate Schmidt corrector can be effectively reduced by a double plate corrector. The principle is identical to achromatizing a doublet refractor objective. In contrast to a doublet objective, which corrects *primary* axial chromatic aberrations, the achromatic Schmidt corrector corrects *third-order* chromatic effects. Figure 43-87 compares the spherochromatism of single- and double-plate Schmidt correctors.

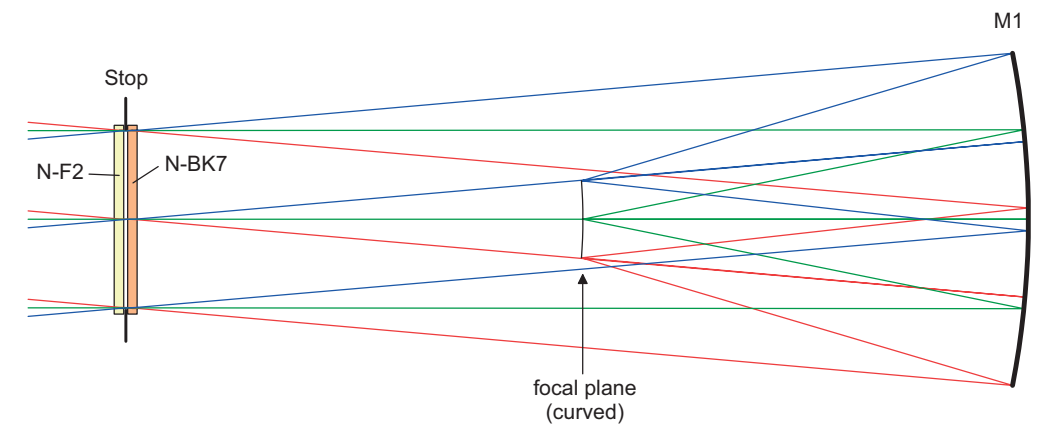


Figure 43-86: Schmidt telescope with achromatic corrector plate.

Because Schmidt correctors are essentially thin plates, they are highly susceptible to "ghost" effects, that is, spurious images due to double reflection of light at the (near) parallel air–glass interfaces of the corrector plate(s). Ghost images can be a serious problem in Schmidt telescopes (and all the Schmidt derivates discussed in the following sections) if the corrector surfaces are left uncoated. Figure 43-88 gives an example of this effect.

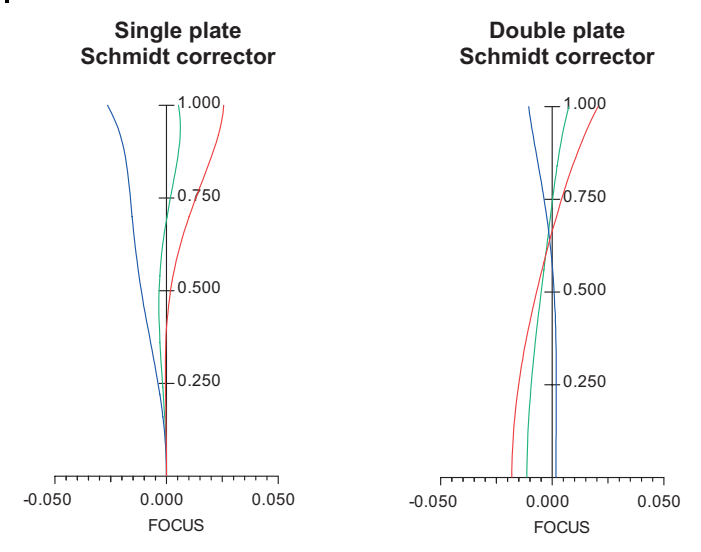


Figure 43-87: Longitudinal spherochromatism in single-plate and double-plate (achromatized) Schmidt correctors.

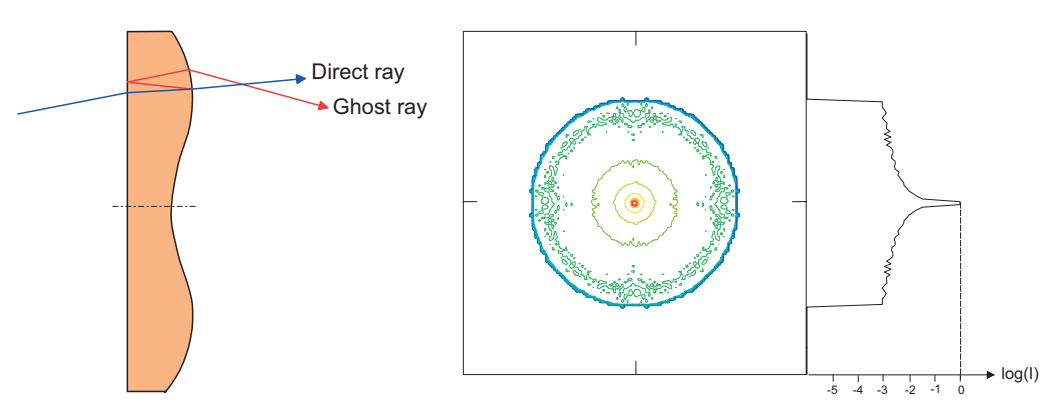


Figure 43-88: Ghost effects caused by residual reflections in a Schmidt corrector. Ray geometry not to scale. The plot to the right shows the intensity distribution of direct image and ghost blur on a logarithmic scale assuming an uncoated corrector plate.

### 43.13.3

### Wright-Väisälä Telescope

Soon after Schmidt's invention, solutions for overcoming the major weakness of the Schmidt telescope (its excessive length) were sought. Wright and Väisälä proposed a short form by placing the correcting plate at the focus (figure 43-89) and thus halving the length of the classical Schmidt telescope. If the first two Seidel aberrations (spherical aberration and field coma) are corrected, the corrector plate can be at any position. This, however, requires an aspherical (elliptical) primary mirror. Astigmatism cannot be corrected in this approach, which is the price to be paid for the short form.

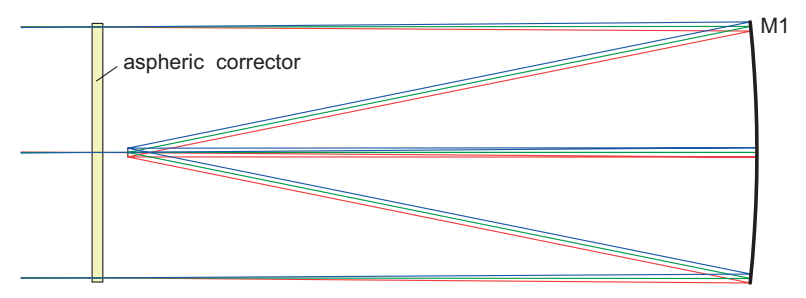
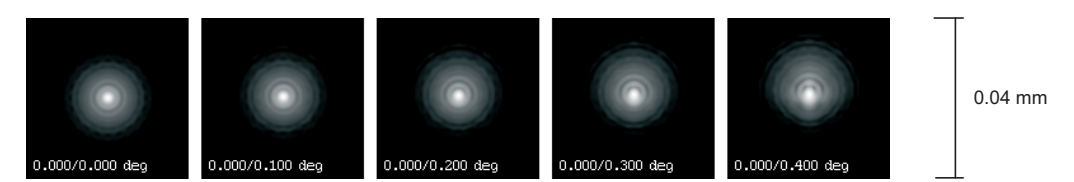


Figure 43-89: Wright–Väisälä telescope with corrector plate at the focus.



**Figure 43-90:** Diffraction PSF of a F2.5/500 mm Wright–Väisälä telescope on a flat field, FOV =  $\pm 0.4^{\circ}$ 

# 43.13.4

### Baker-Super-Schmidt Telescope

A Schmidt telescope with very fast relative aperture F/0.8 was patented by Baker [43-4]. The system consists of an aspherical achromatized corrector and two nearly concentric meniscus lenses as shown in figure 43-91.

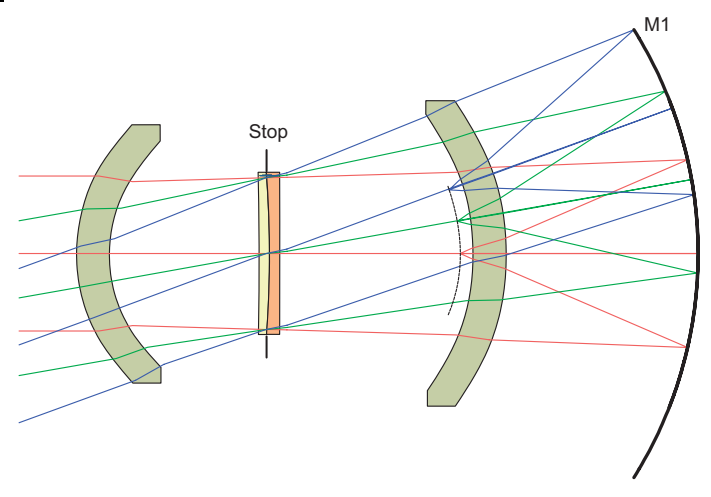


Figure 43-91: Baker-Super-Schmidt telescope

### 43.13.5

### Baker-Nunn Camera

The Baker–Nunn camera is essentially a modified Schmidt with the Schmidt plate replaced by a symmetrical lens triplet in the pupil. It is used to photograph earth-orbiting satellites. The effective focal ratio of the system is very fast at F/1 at a focal length of 510 mm giving an almost undistorted strip field of view of  $5^{\circ} \times 30^{\circ}$  on the curved film plane.

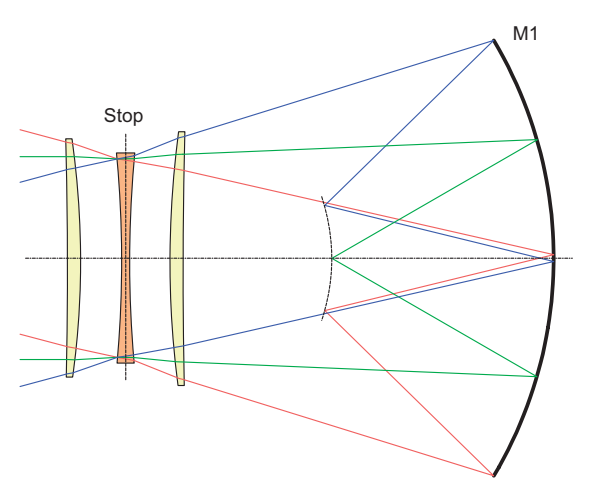


Figure 43-92: Baker-Nunn camera

The corrector is strictly symmetrical where the inner four surfaces of the corrector are aspherical. The corrector may be considered as two halves about the symmetry axis defined by the stop. Each half then resembles a single achromatic corrector, similar to the achromatic Schmidt plate.

The Baker–Nunn camera is clearly related to the Houghton telescope, which is discussed in section 43.13.10.

### 43.13.6

### Wynne Telescope

Shortly after Maksutov's work, Wynne proposed a system with two more-or-less concentric correctors. Wynne also split the front-side corrector into two lenses, as shown in figure 43-93. Due to the double or triple meniscus configuration, the system can be used at higher relative apertures than a classical Bouwers–Maksutov system

The corrector lenses are all made of the same glass type. The surfaces are not perfectly concentric about the stop, but are slightly re-optimized which gives a nearly self-achromatic behavior on-axis. As in the Bouwers–Maksutov corrector, there is higher-order chromatism, which can be partly corrected by adjusting the thicknesses of the corrector lenses. See section 43.13.14 for a more detailed description of the correction of spherochromatism in meniscus lenses.

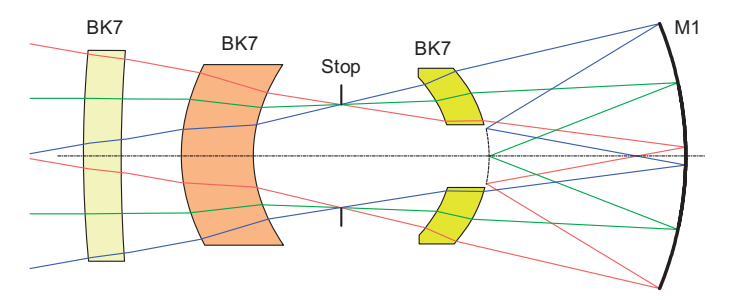


Figure 43-93: Meniscus system due to Wynne.

### 43.13.7

# Schmidt-Cassegrain Telescope

A natural extension of the Schmidt principle is the replacement of the spherical mirror of the Schmidt telescope by a two-mirror system of Cassegrain type. This combination is commonly called a Schmidt–Cassegrain telescope.

Because three aspherical surfaces are utilized, spherical aberration, coma and astigmatism can always be corrected for any geometry of the optical system [43-84]. The asphericities, however, depend on separations and power distribution. Baker [43-3] was the first to analyze various possibilities systematically. One of his solutions, shown in figure 43-94, option D, allowed a spherical secondary mirror. How-

ever, it required an image position in front of the primary mirror to limit the obstruction ratio to about 0.5 and maintain the flat-field condition ( $R_1 = R_2$ ).

The layouts of some Schmidt–Cassegrain configurations are shown in figure 43-94. Logical extensions to the Schmidt–Cassegrain configuration involve achromatizing the Schmidt plate (as discussed in section 43.13.2) and introducing a field flattener (see section 43.15.1).

Rutten and van Venrooji [43-65] also discuss the general differences between Schmidt–Cassegrain telescopes for visual use and for astrophotography. Visual Schmidt–Cassegrains usually have a curved field because the central obstruction ratio should be as small as possible. This implies a large secondary magnification and, thus, inability to fulfil the flat-field condition. Schmidt–Cassegrain telescopes for astrophotography are generally designed for larger fields of view and a flat field to accommodate a flat film or CCD. The large obstruction ratio is something which has to be accepted.

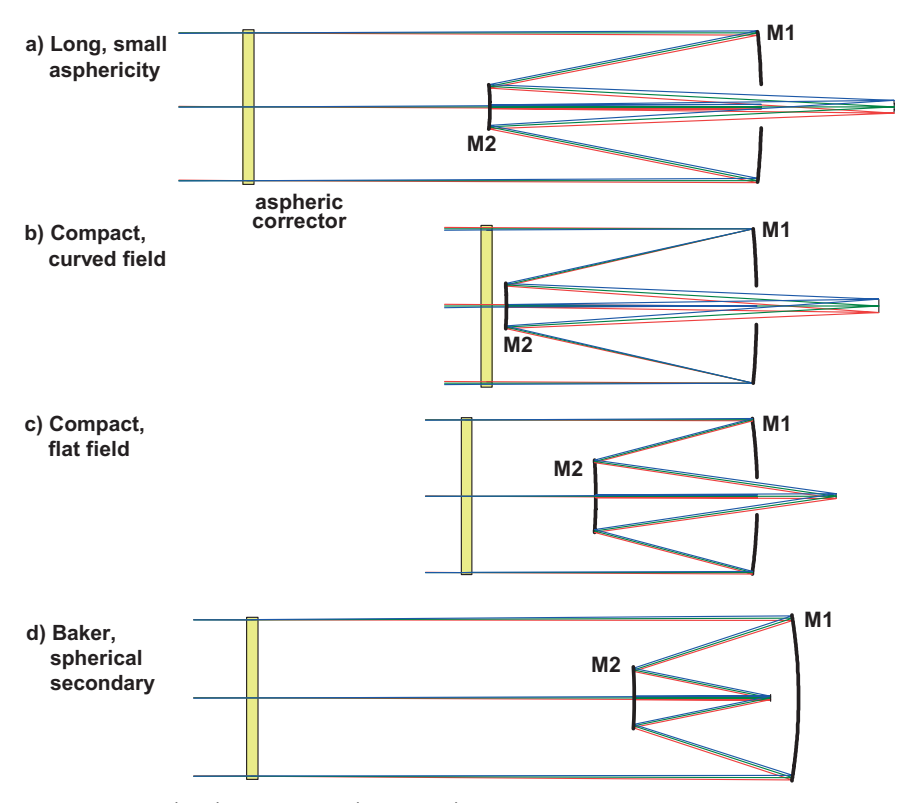


**Figure 43-94:** Schmidt–Cassegrain telescopes. The pictures a) to d) show several possible versions of this setup.

### Schmidt-Gregorian Telescope

The Schmidt–Gregorian telescope is a logical combination of the design principles derived from the Gregorian telescope and the Schmidt telescope. Correction of spherical aberration is accomplished by means of the aspherical Schmidt corrector plate and therefore the primary and secondary mirror can eventually be made spherical. In fast Schmidt–Gregory systems, however, aspherizing one or both mirrors helps to improve off-axis aberrations.

The general properties of the Schmidt–Gregorian telescope are similar to the classical Gregorian form as described in section 43.5.5.

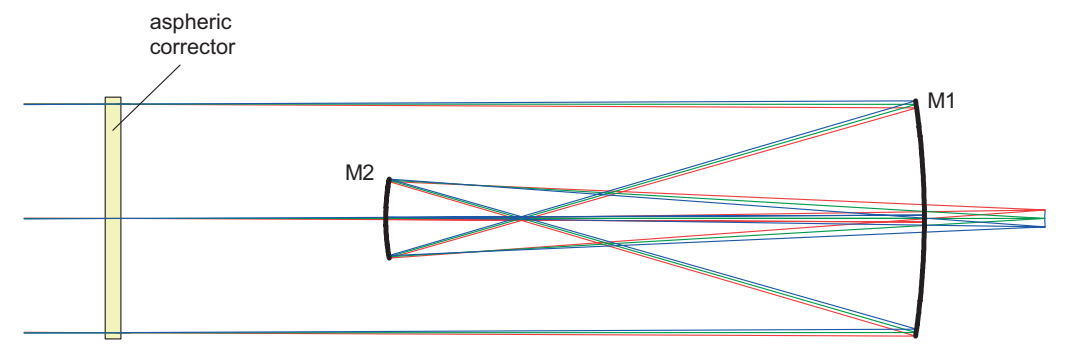


Figure 43-95: Schmidt-Gregorian telescope.

### 43.13.9

### Sigler Telescope

In order to avoid the manufacturing problems with full-aperture correctors, Sigler proposed an all-spherical catadioptric telescope using only small corrector lenses [43-75]. The design is based on previous works by Buchroeder and Dilworth [43-14]. Axial color correction is achieved by application of the dialyte principle described in conjuction with the Schupmann telescope (see section 43.14.9). The major difference from the Schupmann is that the objective lens is replaced by a mirror.

The telescope has some desirable features such as a small central obscuration (about 21% in diameter), an erect image, when used in conjunction with an eyepiece, and good stray light suppression due to the intermediate image (Lyot stop). Only one glass type (BK7) is used for all lenses.

Even though axial and lateral color can be well corrected, the Sigler design suffers from strong coma. This limits the usable field of view to about  $0.1^{\circ}$ – $0.2^{\circ}$ .

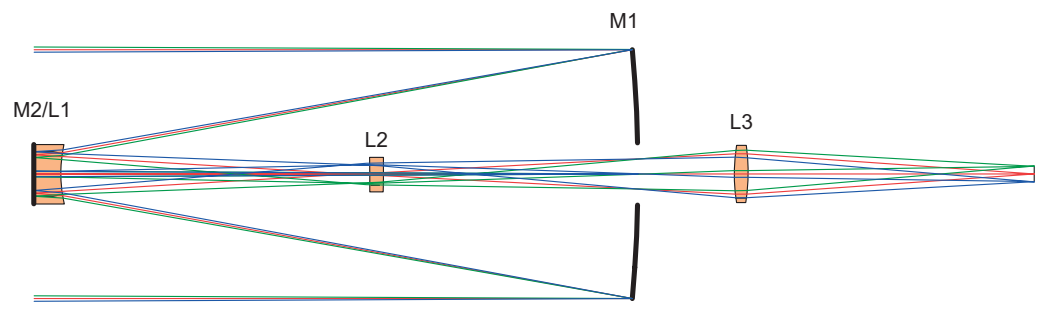


Figure 43-96: Sigler all-spherical catadioptric telescope [43-75].

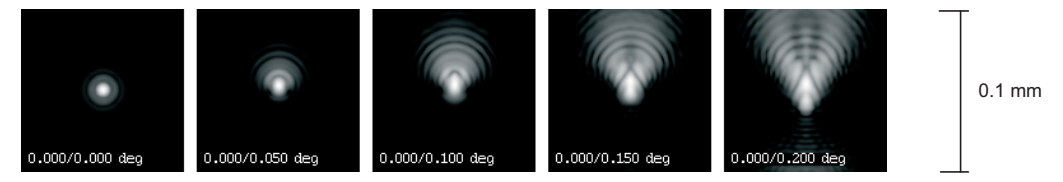


Figure 43-97: Diffraction PSF of a F7/1000 mm Sigler telescope over a FOV of ±0.2° indicating strong coma.

### 43.13.10

### **Houghton Telescope**

Based on the design principles of the Schmidt telescope (section 43.13.2) and the Newton telescope, Lurie, Houghton, Wright and Wäisälä published a number of intermediate forms by adding single or multiple lens refracting correctors [43-26], [43-47].

This family comprises a class of telescopes with refracting correctors covering the full aperture of the telescope. They are combined with a single primary mirror being either of spherical or conic section. The Houghton system utilizes a spherical primary mirror while the Wright, Lurie and Wäisälä systems use conical primary mirrors. Lurie also developed solutions with a spherical primary [43-47].

The primary intention of using a full aperture corrector system was to avoid the difficulties in making a Schmidt corrector. Although such systems are usually called Houghton-type systems, Houghton was probably not the first in his 1944 patent [43-26]. The first such system was developed and published in 1936 by Sonnefeld, who presented a similar solution with a spherical Mangin mirror of F-number 0.5, another was published in 1941 by Richter and Slevogt [43-61], [43-36].

The correcting system is preferably located at the center of curvature of the mirror. It is to be understood, however, that the correcting lens system can be placed at any position in the incident light beam. For these cases, the corrector provides enough degrees of freedom to balance the coma of the primary mirror. The corrector is of almost zero optical power and therefore will not introduce astigmatism, color, field curvature or distortion. Since the optical power only comes from the spherical primary mirror, the image is on a curved field. The Houghton designs are capable of large relative apertures (F-numbers) by using quite shallow curvatures for the correcting lenses.

Houghton showed that a corrector for an anastigmatic design can be made for a spherical primary mirror using three refractive elements, all of which use the same glass type. Furthermore, a spherical-mirror anastigmat with only two elements in the corrector requires glasses of different refractive indices. The glasses have identical primary dispersion to preserve chromatic correction. A small amount of secondary spectrum remains from the different partial dispersions of the glasses. However, the residual chromatic aberration introduced by the corrector is very small and it is typically below the Airy diameter for a given application.

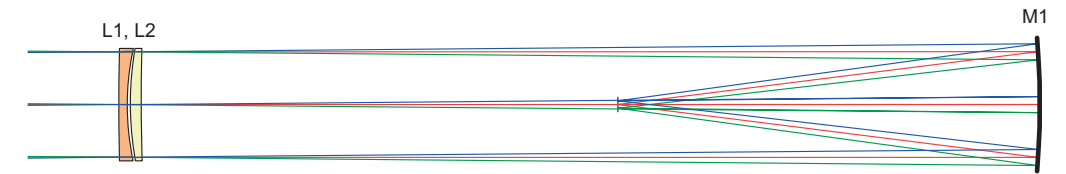


Figure 43-98: Telescope after Houghton [43-26].

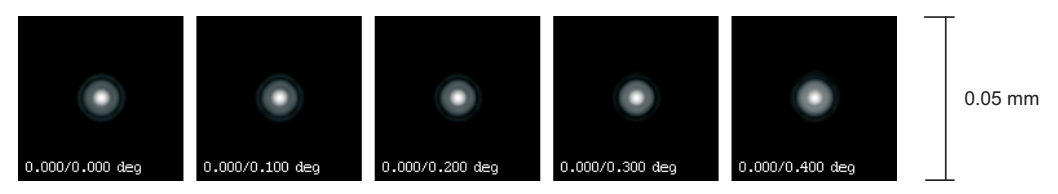


Figure 43-99: Diffraction PSF of a F4/800 mm Houghton telescope.

### 43.13.11

### **Buchroeder-Houghton Telescope**

Buchroeder used a three-lens corrector instead of two lenses in Houghton's design. This allows a slightly better correction of spherical aberration and shallower radii of curvature of the corrector lenses. With three lenses, more degrees of freedom are available and the choice of refractive indices is no longer restricted (as in the Houghton design) to correct for astigmatism. All corrector lenses can therefore be made of one inexpensive glass type (for example BK7).

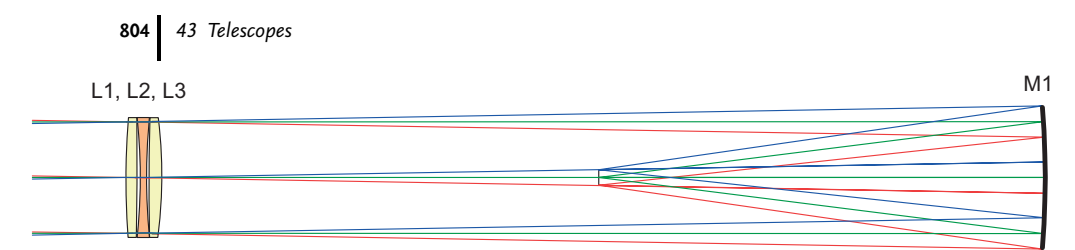


Figure 43-100: Buchroeder telescope.

### 43.13.12

# Houghton-Cassegrain Telescope

The design roots of the Houghton–Cassegrain are found in the Schmidt–Cassegrain telescope (section 43.13.7). The similarity to the Baker–Nunn camera is evident. The noticeable exception is the fact that only spherical surfaces are utilized. In addition, the corrector (plate) has been moved closer to the secondary mirror. As in the Houghton telescope, the aspherical Schmidt plate is replaced by a spherical two-lens corrector of zero optical power, and the primary and secondary mirrors are spherical. The corrector removes the spherical aberration of the telescope, but does not introduce chromatic aberrations by virtue of its zero optical power. A distinct advantage is the option to attach the secondary to the rear surface of the corrector lens so that spiders can be avoided (figure 43-102). The design is anastigmatic and coma-free; the only remaining primary aberration is the field curvature.



Figure 43-101: Houghton-Cassegrain telescope, flat field, F5/1000 mm.

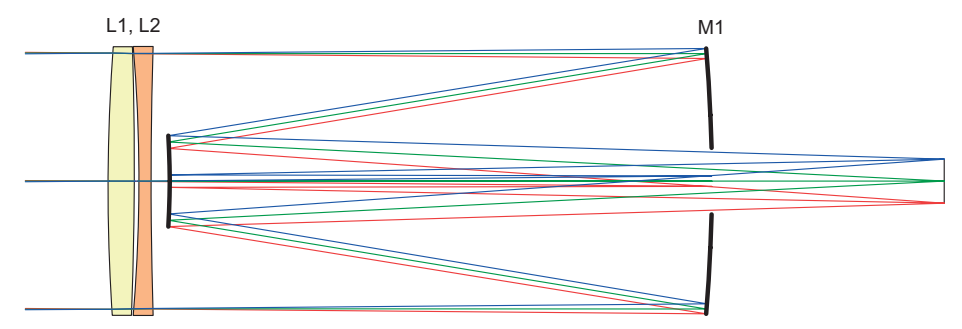


Figure 43-102: Houghton–Cassegrain telescope, short form, F10/2000 mm.

### Lurie-Houghton Telescope

The "Lurie-Houghton" telescope combines design elements from a proposal by Lurie [43-47] with elements of the Houghton telescope (spherical primary). Both modifications greatly simplify manufacture at the expense of astigmatism.

From a different viewpoint, the Lurie-Houghton may be considered as a generalized Schmidt telescope, since it adopts several principles from the Schmidt telescope. It utilizes a two-lens corrector (which also defines the stop) and a spherical primary mirror. In contrast to the classical Schmidt design, the corrector is moved away from the center of curvature of the primary mirror to achieve compactness. In this form, the corrector is now placed inside the focus of the primary mirror and the geometry is similar to a Wright-Wäisälä camera. The stop is now at a non-optimal position, which would introduce coma for a single-element corrector. However, the two-element corrector provides enough degrees of freedom to correct for spherical aberration and coma, but not astigmatism.

The corrector is overcorrected for spherical aberration in order to compensate for that of the primary mirror. Since the corrector is powerless, both lenses have identical, but opposite, optical power. If both lenses are made from the same glass, some residual amount of spherochromatism proportional to the dispersion of the glass remains, but with standard crown glass (e.g., BK7) it is well below the Airy disk diameter and therefore negligible.

A distinct advantage of the Lurie-Houghton design is the improved correction of coma compared to the Schmidt-Newton. A disadvantage is the relatively large central obstruction by the 45° folding mirror if the image plane is placed outside the main beam (figure 43-103).

The analytical setup of the Luri-Houghton design form is easily accomplished by a few equations: The radii of the corrector are obtained by

$$r_1 = -r_3 = \frac{2L(n-1)}{(Q+1)\varphi}, \qquad r_2 = -r_4 = \frac{2L(n-1)}{(Q-1)\varphi}$$
 (43-69)

with the auxiliary variables

$$L = \frac{(D-2)(2A-B)}{C}, \qquad Q = \frac{(2-D)L^2}{2C},$$
 (43-70)

$$A = \frac{n-2}{n(n-1)^2}$$
,  $B = \frac{2(2n+1)}{(n-1)^2}$ ,  $C = \frac{2(n+1)}{n(n-1)}$ ,  $D = d \cdot \Phi$ , (43-71)

where  $\Phi$  is the optical power of the primary mirror (= 2/r) and d is the distance of the last corrector surface from the primary mirror.

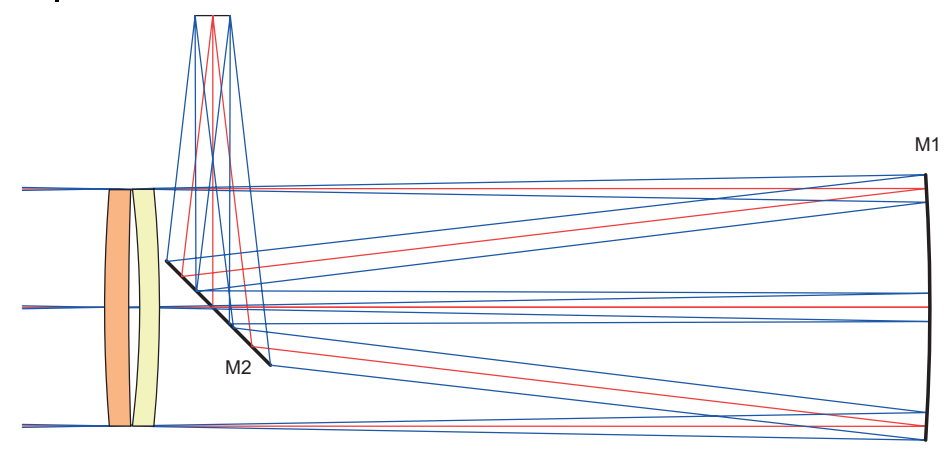


Figure 43-103: Luri-Houghton Telescope.

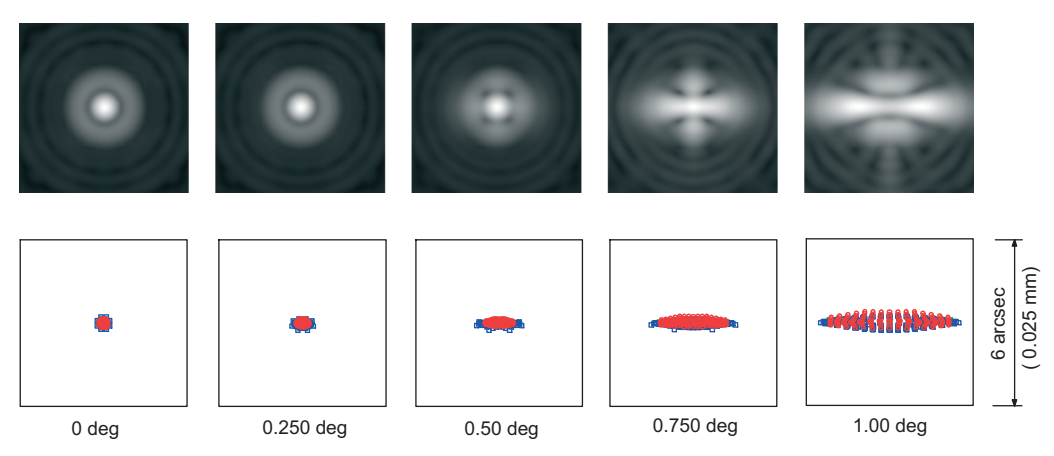


Figure 43-104: Diffraction PSF and spot diagram of the Luri–Houghton telescope.

# 43.13.14 **Bouwers–Maksutov Telescope**

The development of the Maksutov telescope was driven by the desire to replace the aspherical corrector plate of the Schmidt system with a more easily manufactured corrector. The solution, a meniscus corrector with spherical surfaces, was found almost independently by several researchers, namely Maksutov, Bouwers, Gabor and Penning [43-65]. Following the symmetry concept of the Schmidt telescope, in 1941, Bouwers proposed the concentric meniscus corrector. As with the Schmidt telescope, the stop is at the center of curvature of the spherical primary mirror M1 (see figure 43-105), as are the radii  $R_1$  and  $R_2$  of the corrector meniscus. This way the system has no unique axis and all off-axis aberrations are absent. The corrector

introduces spherical aberration of opposite sign to the primary mirror, thus effectively reducing the spherical aberration of the system. However, the relative aperture is limited to about F/4 caused by residual fifth-order spherical aberration.

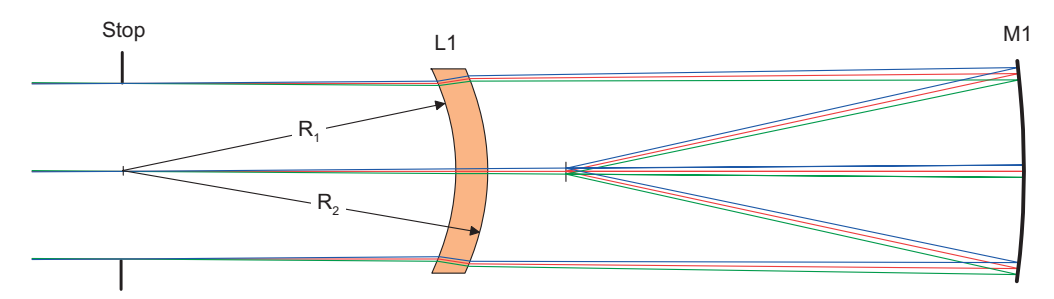


Figure 43-105: Bouwers telescope with concentric corrector.

Even though the concentric meniscus corrects for spherical aberration, longitudinal chromatic aberration remains uncorrected. This is a major disadvantage of Bouwer's design and therefore significantly limits the useful spectral bandwidth. Bouwers also suggested to achromatize the meniscus corrector by inserting a "ghost surface" such that the corrector is composed of two lenses cemented together where both glasses have nearly identical refractive index but different Abbe number [43-51], [43-65]. The secondary spectrum is achromatic. However, the most serious defect is then lateral color which increases linearly with the field angle. Figure 43-106 shows a typical achromatic corrector for a concentric Bouwers telescope.

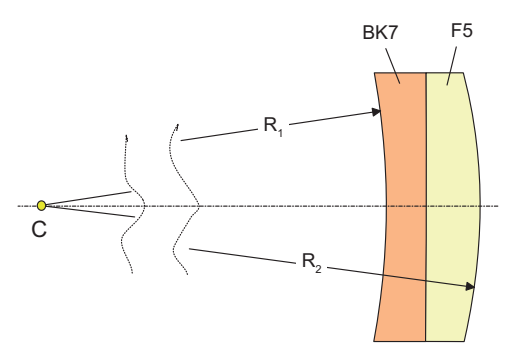


Figure 43-106: Achromatic full-aperture concentric corrector for a Bouwers telescope.

Maksutov showed in his 1955 paper [43-49] that the axial chromatic aberration in a meniscus lens can be minimized (but not corrected) if the axial thickness d of the corrector follows the condition

$$d = \frac{n^2}{n^2 - 1} \cdot (R_2 - R_1) . {(43-72)}$$

Since  $d = R_2 - R_1$ , this means that the corrector is no longer concentric. The centers of curvature of the meniscus surfaces are separated by

$$\Delta z = (R_2 - R_1) - d = -\frac{d}{n^2}. (43-73)$$

This affects the symmetry condition of the Schmidt principle, so coma, astigmatism and lateral color are re-introduced. As suggested by Maksutov, these aberrations can be partially eliminated by moving the corrector closer to the primary mirror and placing the stop at the corrector instead at the center of curvature of the primary mirror. This all leads to a very compact design compared to the Schmidt and Bouwers designs (figure 43-107). Since then, this telescope type is usually referred to as a "Maksutov".

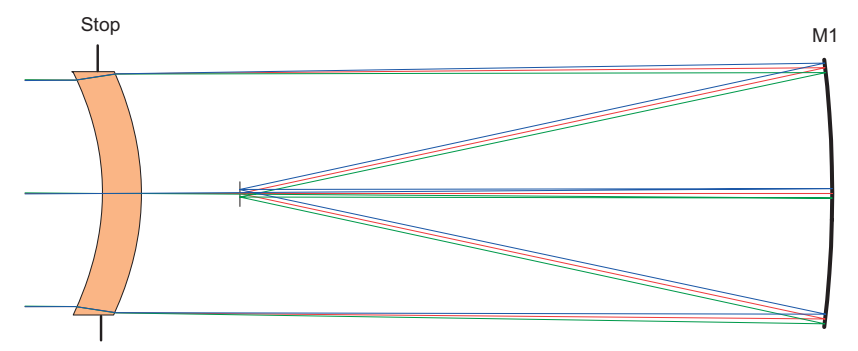


Figure 43-107: Maksutov telescope with non-concentric corrector.

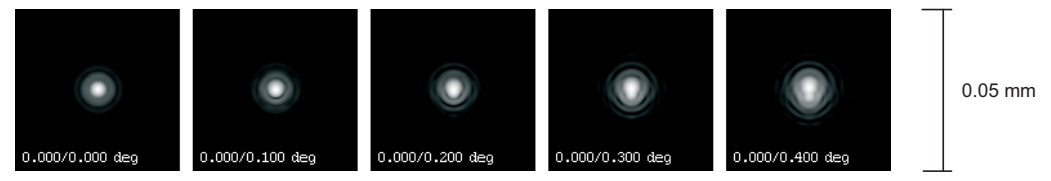
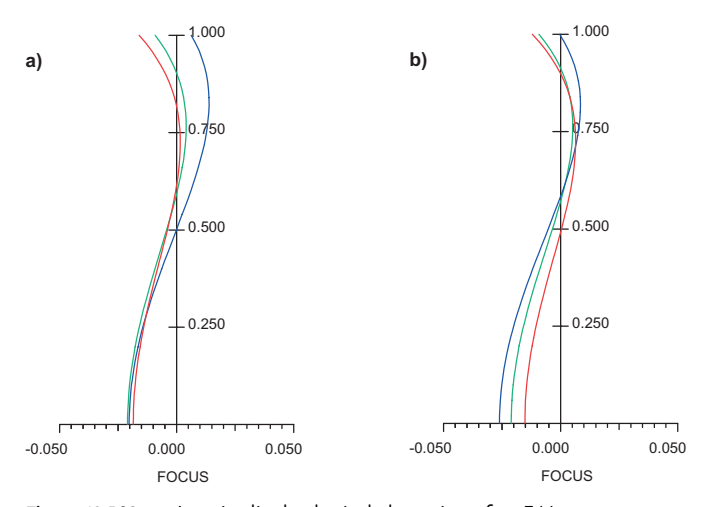


Figure 43-108: Diffraction PSF of an F4/800 mm Maksutov telescope.



Longitudinal spherical aberration of an F4/ 800 mm Maksutov telescope for different corrector thicknesses: a) corrected axial color; b) corrected zonal color.

Equation (43-72) indicates the optimum corrector thickness for correction of *paraxial* longitudinal color, however, for rays near the edge of the aperture longitudinal color aberration (spherochromatism) occurs. To minimize spherochromatism, the axial thickness and the curvatures are slightly varied such that a balance between axial and zonal color aberrations is achieved. Figure 43-109 indicates these conditions.

# 43.14 Catadioptric Maksutov-Cassegrain Telescopes

The basic principles of the Bouwers–Maksutov meniscus corrector can also be applied to the Schmidt–Cassegrain telescope by replacing the Schmidt plate with a meniscus-type element. Many variations of this approach have been published, and the most prominent ones are discussed in the following sections.

# 43.14.1 Maksutov-Gregory Telescope

The design proposed by Gregory combines the secondary mirror with the back surface of the meniscus corrector. The secondary mirror is then realized by evaporating a reflective coating onto the central area. Since the secondary mirror has to have the same radius as the back surface of the corrector, a design freedom is lost and the system suffers from strong coma, astigmatism and higher order spherical aberration. See figure 43-110 for the optical layout and figure 43-111 for the corresponding aberrations.

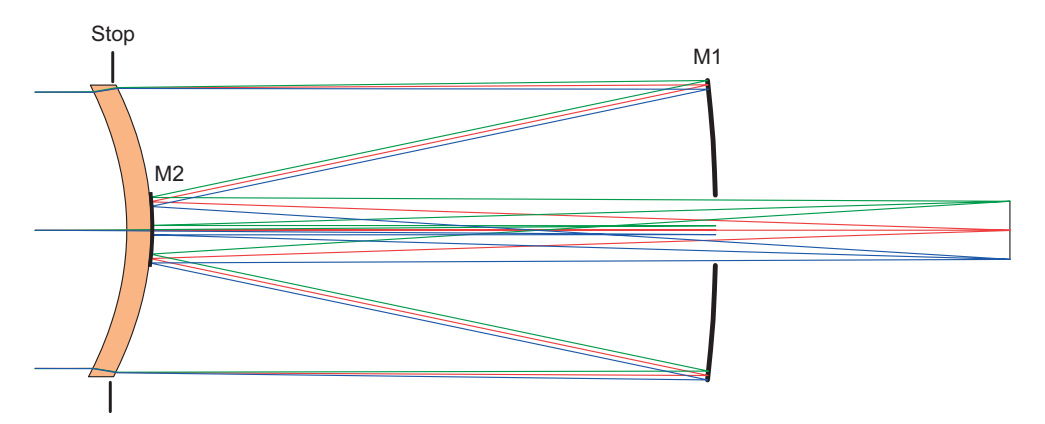


Figure 43-110: Maksutov-Gregory telescope.

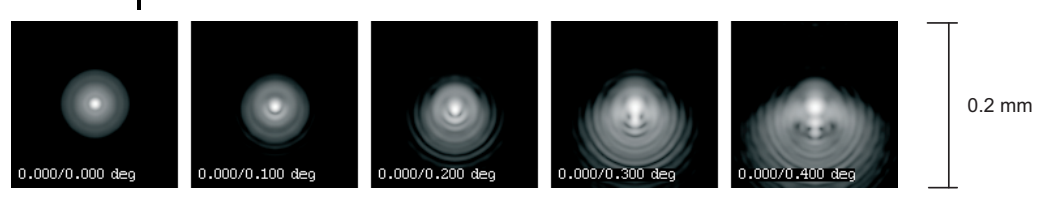


Figure 43-111: Diffraction PSF of a F15/3000 mm Maksutov–Gregory telescope.

# 43.14.2 Maksutov-Rumak Telescope

In the Maksutov–Rumak telescope [43-65] an additional degree of design freedom is introduced by separating the secondary mirror surface from the back surface of the meniscus corrector. The secondary mirror is no longer tied to the corrector's back surface as it is now a separate element and – being close to the corrector – it can be glued onto the corrector without requiring spider vanes for mounting.

This step decouples the curvature of the corrector and secondary mirror, which leads to a significant improvement in the overall performance, as shown in figure 43-113.

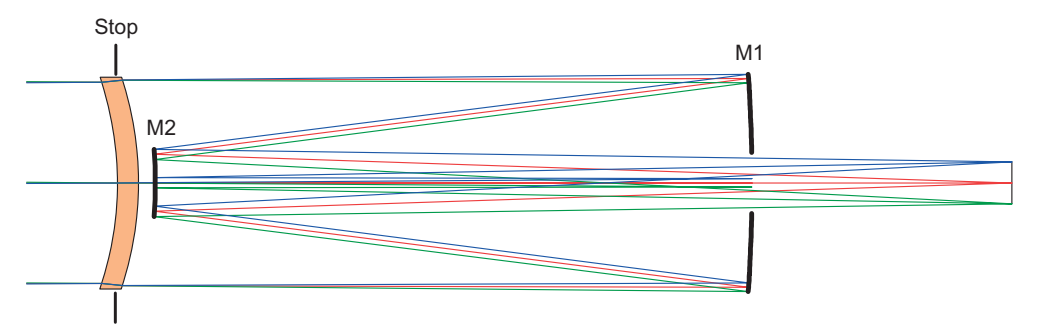


Figure 43-112: Maksutov-Rumak telescope.

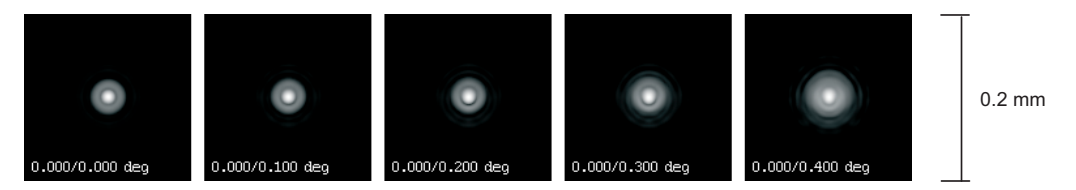


Figure 43-113: Diffraction PSF of an F15/3000 mm Maksutov–Rumak telescope.

### Aspherical Maksutov Telescope

It has been shown in the previous sections that the meniscus corrector in the all-spherical Bouwers–Maksutov telescopes cannot correct for higher-order (fifth-order) spherical aberration. This also limits the focal ratio of the Maksutov–Cassegrain variants to about F/4. Faster systems suffer from intolerable aberrations when only spherical surfaces are used.

The fifth-order spherical aberration of the Bouwers–Maksutov telescope can be corrected by an aspherical plate added to the meniscus lens, as proposed by Hawkins and Linfoot [43-84]. This system is sometimes also called a "Schmidt-meniscus Cassegrain" or "Super-Schmidt". The aspherization is very small and only needs to correct the residual higher-order spherical aberration. With the aspherical corrector, fast focal ratios as low as F/2 with practically diffraction-limited performance at the optical axis can be achieved.

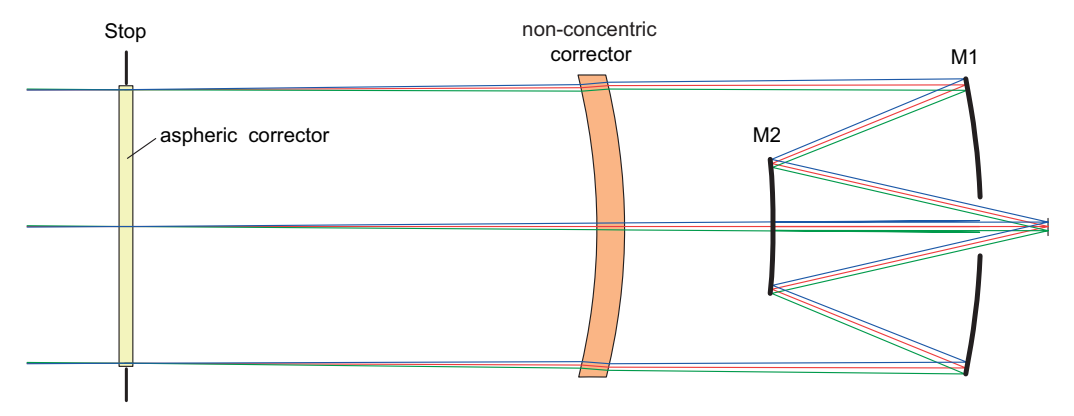
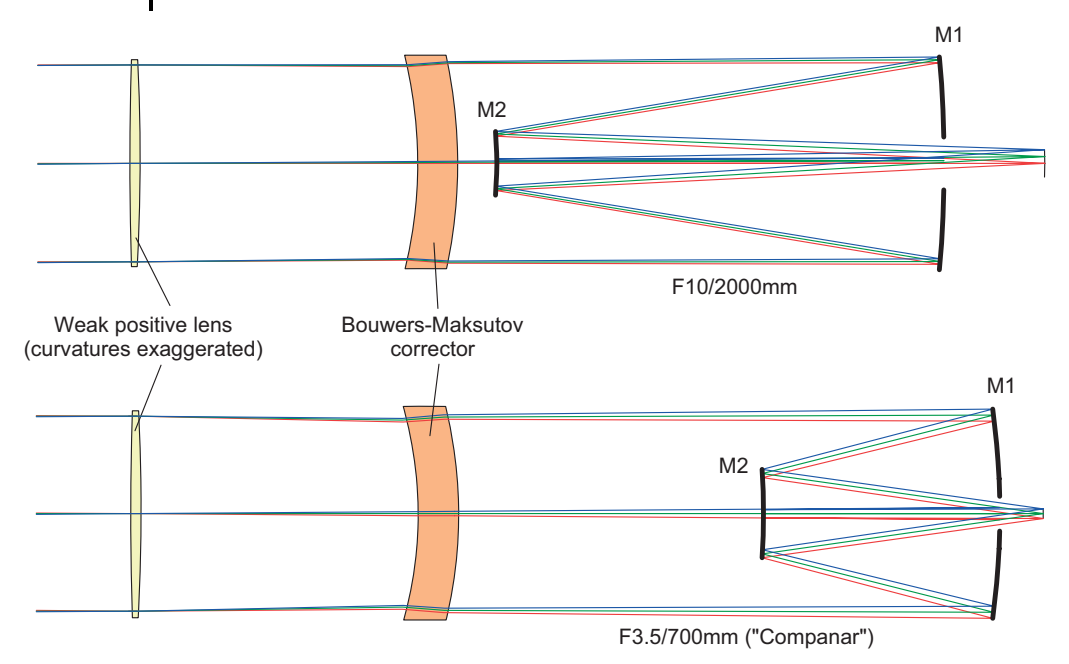


Figure 43-114: Maksutov-Cassegrain telescope with weak aspherical (Schmidt) corrector.

# 43.14.4 Bouwers-Cassegrain with Weak Corrector Lens

Another method of correcting the longitudinal chromatic aberration introduced by the concentric Bouwers meniscus corrector is given by Rutten and van Venrooji [43-65] where a weak positive lens in the concentric stop is added. Figure 43-115 shows an example in a Cassegrain configuration. The flat-field version is also denoted by Rutten and van Venrooji as "Companar".

The weak positive lens balances the axial chromatic aberrations of the concentric Bouwers meniscus. A single glass type can be used for both lens and meniscus. Because the concentric symmetry is preserved, all third-order aberrations, except the field curvature, can be corrected. Another advantage is that all surfaces are spherical which makes this telescope a useful solution for amateurs.



**Figure 43-115:** Bouwers–Cassegrain telescope with weak positive lens at the concentric stop. Designs are given with different Cassegrain configurations. (Top) F10/2000 mm system with curved field. (Bottom) F3.5/700 mm system with flat field ("Companar").

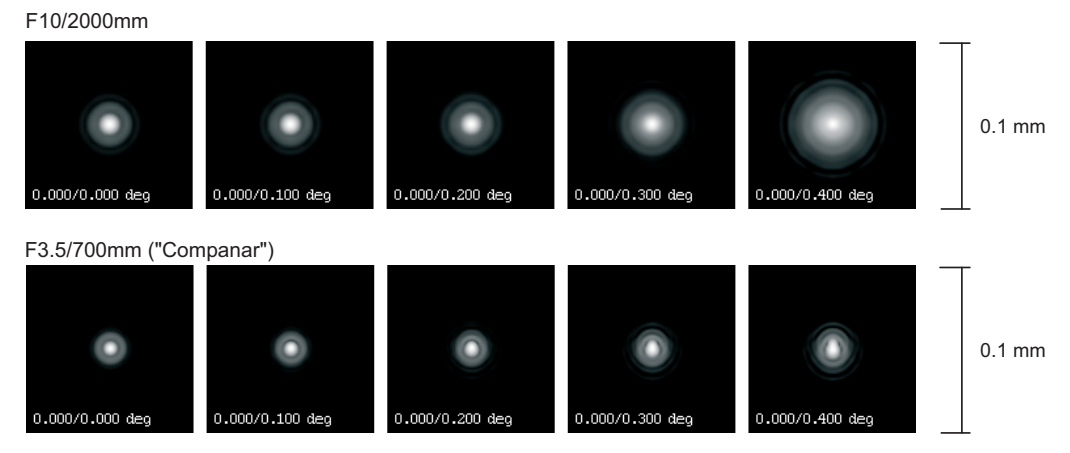


**Figure 43-116:** Diffraction PSF of the Bouwers–Cassegrain telescopes shown in figure 43-105. (Top) F10/2000 mm curvedimage system. (Bottom) F3.5/700 mm flat-image system. All PSF's are referred to a flat image surface.

### 43.14.5

# Schmidt-Bouwers Telescope

Similar to the Maksutov telescope, the concentric Bouwers telescope (see figure 43-105) can be enhanced with a corrector system to eliminate the residual higher-order spherical aberration. Hawkins and Linfoot proposed a weak achromat in the stop which corrects the longitudinal chromatic aberration of the Bouwers meniscus. An external surface of the achromatic corrector is aspherized to correct for higher-order spherical aberration. The achromatic corrector has no optical power but it is functionally identical to the achromatized meniscus corrector, as shown in figure 43-117.

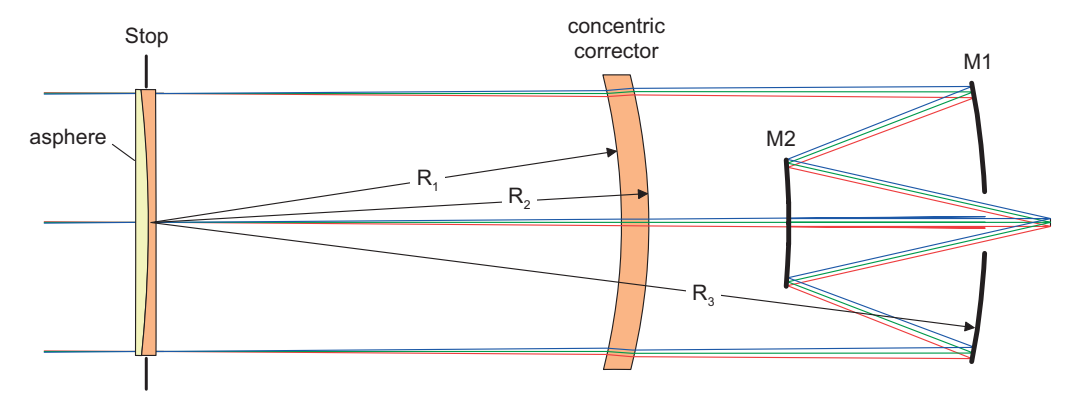


Figure 43-117: Bouwers-Cassegrain telescope with an achromatic corrector.

# 43.14.6 **Compact Maksutov Telescope**

The possibilities of reducing the length of a Maksutov telescope are limited, because this can only be achieved by increasing the optical power of the primary mirror which, in turn, increases higher order spherical aberration and requires much stronger curvature of the corrector meniscus. Dietzsch circumvented this problem on the basis of a Maksutov–Cassegrain type telescope by adding corrector lenses in the convergent beam [43-13]. The dioptric system increases the focal length of the system which then corresponds to a shortening of the tube length in relation to the final focal length. The overall length is approximately  $0.24 \times$  focal length. Axial and transverse color are corrected for a wide spectral range on a flat field. The image performance is limited by fifth-order spherical aberration.

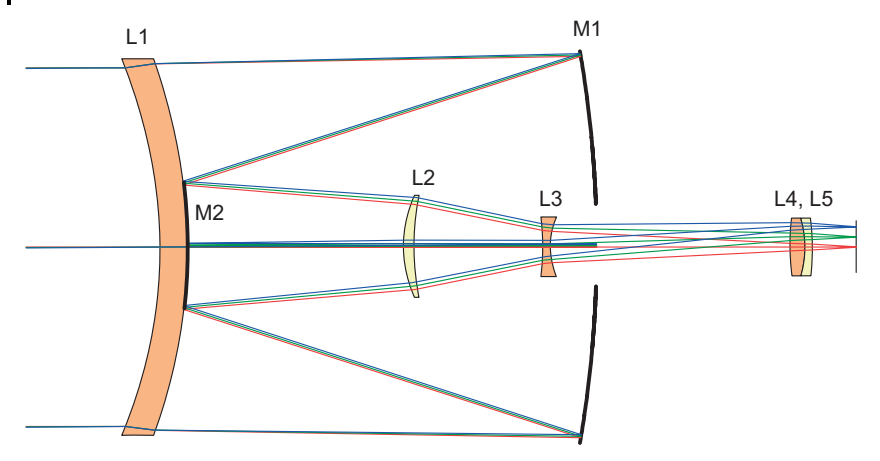


Figure 43-118: Compact Maksutov telescope F8/1000 mm [43-13].

# 43.14.7 **Klevtsov**

The Russian A. Klevtsov tried to avoid the manufacturing difficulties involved in making the large aspherical corrector in Schmidt–Cassegrain telescopes [43-35]. The system should be composed of only spherical surfaces, but still provide an image quality comparable to that of the Schmidt–Cassegrain. The system he proposed is shown in figure 43-119. The primary mirror is spherical and all corrections are performed by a thick quasi-afocal meniscus placed near the secondary mirror which itself is of the Mangin type. The corrector is used in a double path.

A notable deficiency of Klevtsov's design is the comparatively narrow operating spectral range (450–650 nm) due to the uncorrectable transverse color. This effect could possibly be reduced by a thinner meniscus (L2). However, a minimum thickness is required for control of spherochromatism.

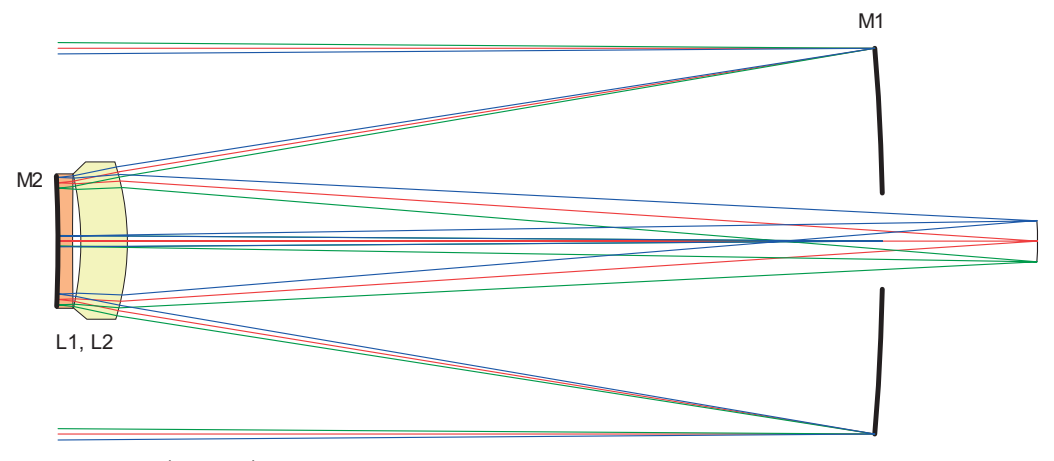
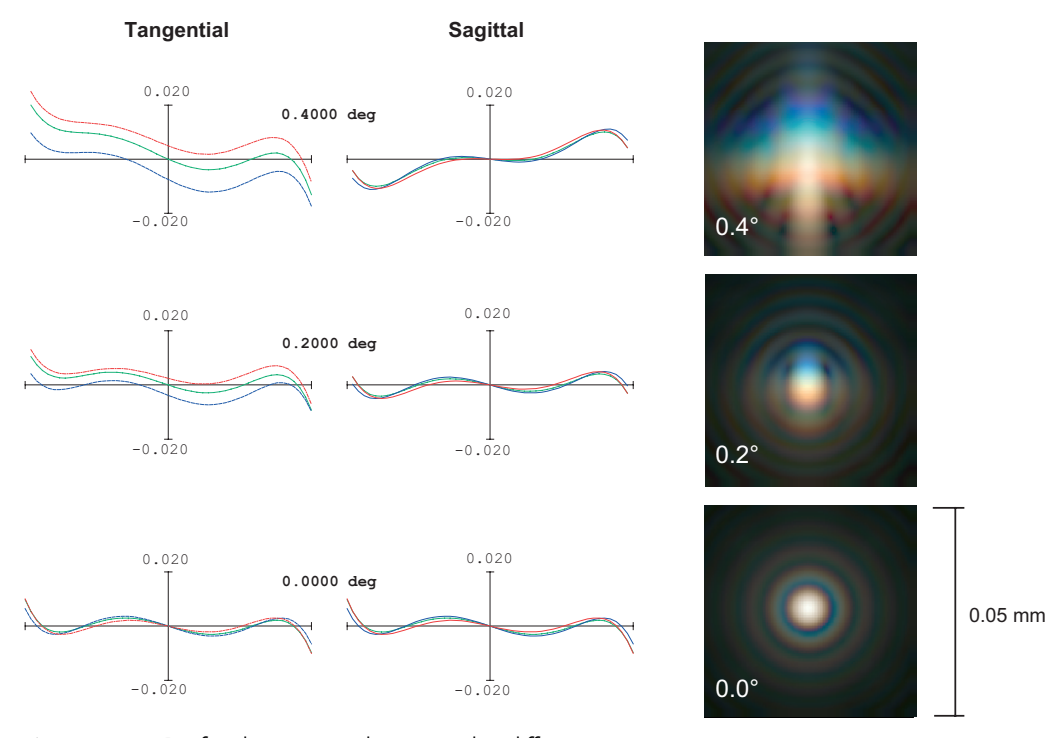


Figure 43-119: Klevtsov telescope [43-35].



**Figure 43-120:** Ray fan aberrations and corresponding diffraction PSF of the Klevtsov telescope indicating the residual lateral color.

43.14.8

### Other Forms of Catadioptric Telescopes

There are many possible forms of dioptric correctors for mirror telescopes of increasing complexity, far too many to be included within the scope of this book. Starting points are found in the books of Laikin [43-42], Smith [43-77] and papers from Powell [43-60], Lidwell [43-44], Tam [43-79], as well as others. Two examples are shown in figures 43-121 and 43-122. The design by Shenker uses both full-aperture and sub-aperture corrector lenses in a Cassegrain-type configuration, all of the lenses being made of the same glass type (BK7).

The system offers a very fast aperture ratio, F/1.2 over a relatively wide field of view of  $\pm 2.5^{\circ}$ . Axial and lateral chromatic aberrations are well corrected to third order. Only higher-order spherochromatism and residual fifth-order spherical aberration limit its performance. A clear disadvantage is also the large central obstruction.

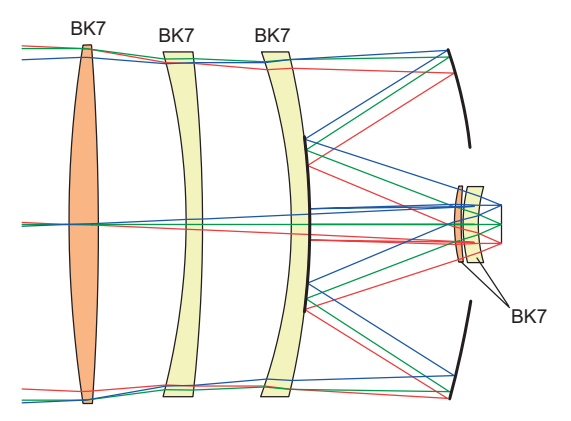


Figure 43-121: Catadioptric Cassegrain telescope after Shenker [43-90].

Another more complex catadioptric form is given by Iizuka as shown in figure 43-122. It is also based on the Cassegrain telescope, however, uses Mangin-type mirrors for control of spherical aberration. Also by decoupling the secondary mirror from the front lens more degrees of freedom are gained. This allows a very compact design with an overall length being only 28% of the focal length. For comparison, the Shenker design builds almost as long as the focal length, albeit at much higher speed.

Iizuka's designed this system primarily as a telephoto objective for SLR cameras, however, his design also nicely illustrates the migration from classical catadioptric telescopes by applying the same well-known design principles, but with increasing complexity.

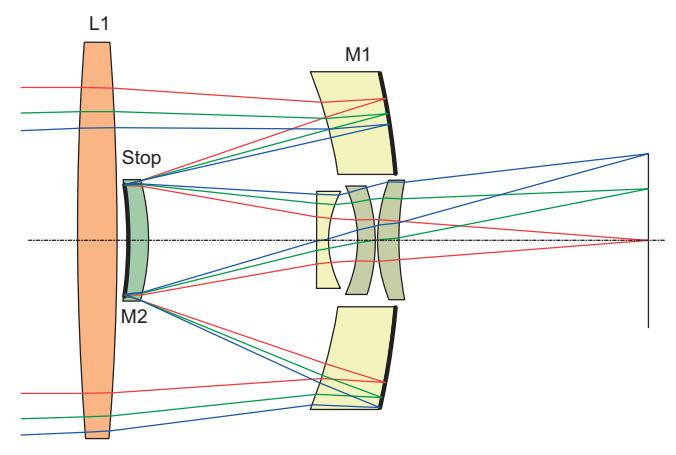


Figure 43-122: Telephoto lens by Iizuka [43-30].

### 43.14.9

### Schupmann Medial Telescope

The name "medial" is derived from the meaning "lying in the middle". The principle of Schupmann's telescope [43-69], [43-71] is based on the compensation of dispersion when using identical or near identical types of glass. The optical principle of the Medial is based on the *dialyte*, which consists in its simplest form of two lenses having a finite separation. To understand Schupmann's intention, we must consider the state of telescope manufacture in the 19<sup>th</sup> century. Although the achievement of Fraunhofer in constructing achromatic telescopes was outstanding at that time, the limitation induced by the secondary spectrum became increasingly apparent with increasing aperture diameter. Attempts to improve the two-lens achromats by threelens apochromats were extremely successful. However, their apertures were limited to approximately 10 inches due to the difficulties in producing glasses of anomalous dispersion of larger sizes.

Faced with this situation, the German Ludwig Schupmann (1851–1920) was the first to design truly apochromatic telescopes, and it is very interesting that he achieved this goal by employing only glasses with normal dispersion. Unfortunately, his invention attained little observance in the professional astronomical community and practical use was mainly limited to a few amateur telescopes.

We shall derive the conditions for which the cancelling of dispersion with one type of glass can be achieved. From the thick-lens formula, applied to two thin lenses separated by a distance d,

$$\Phi = \Phi_1 + \Phi_2 - d\Phi_1 \Phi_2 \tag{43-74}$$

and substituting the powers with

$$\Phi = (n-1)\left(\frac{1}{r_1} - \frac{1}{r_2}\right),\tag{43-75}$$

we obtain

$$\Phi = (n_1 - 1)R_1 + (n_2 - 1)R_2 - d(n_1 - 1)(n_2 - 1)R_1R_2, \tag{43-76}$$

where, for simplicity we write,  $R = \left(\frac{1}{r_1} - \frac{1}{r_2}\right)$ .

Since the two lenses are of the same glass, we set  $n_1 = n_2$ , so that

$$\Phi = (n-1)(R_1 + R_2) - d(n-1)^2 R_1 R_2. \tag{43-77}$$

If the combined power of the two lenses is to be independent of the variation of refractive index with color,  $d\Phi/dn$  must be zero, thus

$$\frac{\mathrm{d}\Phi}{\mathrm{d}n} = R_1 + R_2 - 2d(n-1)R_1R_2 = 0 \tag{43-78}$$

Replacing each (n-1)R term by  $\Phi$  and multiplying by (n-1) yields

$$\Phi_1 + \Phi_2 - 2d\Phi_1\Phi_2 = 0, (43-79)$$

$$d = \frac{\Phi_1 + \Phi_2}{2\Phi_1\Phi_2} = \frac{f_1 + f_2}{2} \ . \tag{43-80}$$

Secondary color vanishes, if two lenses made of the same glass are separated by half the sum of their focal lengths. In practise, the color correction is not perfect due to the chromatic variation of the ray heights at the second lens. The residual chromatic error also depends on the primary dispersion (Abbe number  $\nu$ ) of the glass; it is larger for more dispersive glasses. Nevertheless, the resulting system is still corrected at only two wavelengths, which corresponds to a simple achromat. However, the color residual can be as much as 100 times smaller than a conventional BK7-F2 achromat. In this case, the distinction between an apochromat or even a superachromat is academic.

The combined power of the dialyte

$$\Phi = \frac{\Phi_1 + \Phi_2}{2} \tag{43-81}$$

is always negative for a combination of a positive and a negative lens in a dialyte. In order to achieve a positive net power, Schupmann introduced a mirror to convert the virtual image to a real one.

A combination of two positive lenses gives zero transverse color, but large axial color. This dialyte form is applied, for example, in Huygen's eyepiece as shown in section 37.5.1.

Equality of glass types is an important, but not a necessarily sufficient, condition as large amounts of transverse chromatic aberration are introduced. The decisive factor lies in the field lens. From figure 45-123 we see that the field lens (i.e., the first convex surface of the deflecting prism) re-images the objective lens (point E) onto the corrector (point E'), i.e., the objective lens and the corrector are at conjugate points. With appropriate adjustment of the curvature of the prism surface (i.e., the optical power of the prism/field lens), transverse chromatic aberrations can be made vanishingly small.

If all optical elements were perfectly aligned along the optical axis, the compensation of the longitudinal and transverse chromatic aberration would be perfect. However, then the image plane would not be at an accessible position because it would coincide with the deflecting prism. Hence, a tilt of the corrector is required to separate the beams, but introduces astigmatism and, to a much greater extent, lateral color. The astigmatism is compensated by a small tilt of the objective lens, whereas the lateral color can be perfectly compensated by an appropriate tilt of the deflecting prism.

Since the corrector is used at unit magnification, the system is theoretically free from coma. However, the condition of 1:1 magnification can only be maintained for the principal wavelength, while for other wavelengths a deviation from unit magnification can be observed. This effect is solely caused by the large longitudinal chromatic error of the corrector, which is needed to compensate for the equally large axial chromatism of the objective lens. Hence, different magnifications for varying wavelengths create chromatism of the coma. Schupmann developed methods to compensate this effect down to a negligible quantity, at least for the center of the field. In addition to the nominal tilt of the whole compensation, the front lens must be tilted and laterally displaced.

Thus, there are four tilted components (objective lens, field lens, whole compensator and lenses within the compensator) and a lateral shift involved, which makes final tuning for optimum performance a tedious task.

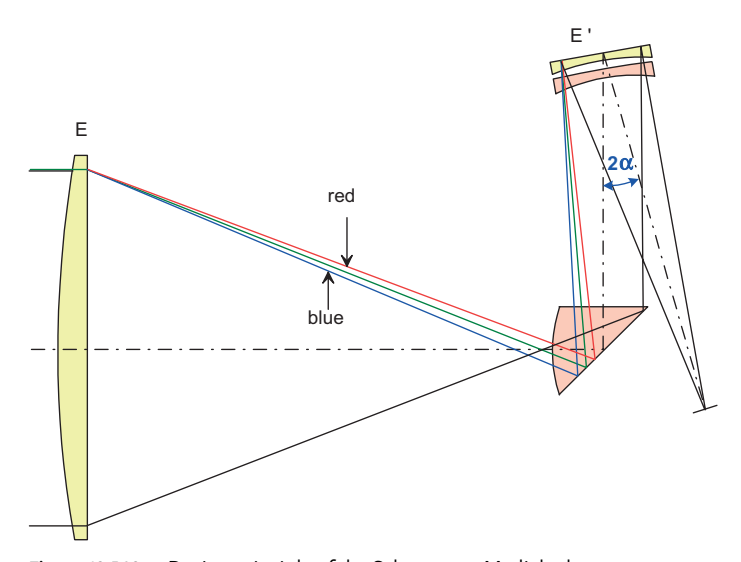
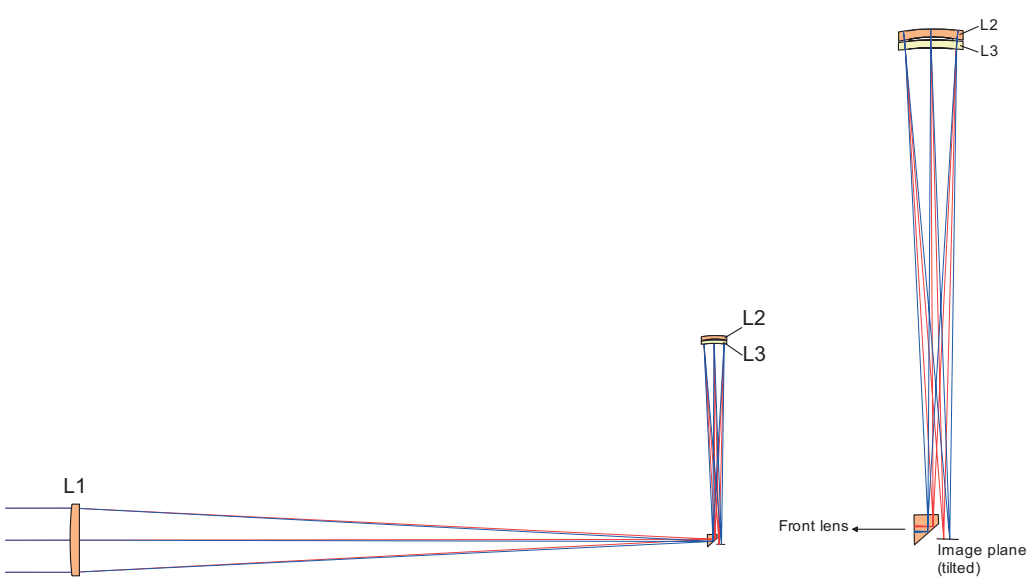


Figure 43-123: Design principle of the Schupmann Medial telescope.

There are several notable disadvantages of the Schupmann telescope.

- The usable field of view is rather small and is limited by the fact that the beams in the relay system must be separated.
- Typical F-numbers of the Schupmann telescope are F/15 F/20 which are definitely too large for deep sky or star field observation. On the other hand, the Schupmann telescope is almost ideally suited for moon or planetary observation.
- Due to the many tilts, the image plane is no longer perpendicular to the main optical axis. Although this effect is small (< 5°), it is noticeable and the image plane tilt increases if larger field extents are required.



**Figure 43-124:** Practical example of the Schupmann telescope. An enlarged view of the relay optics is given to the right of the figure.

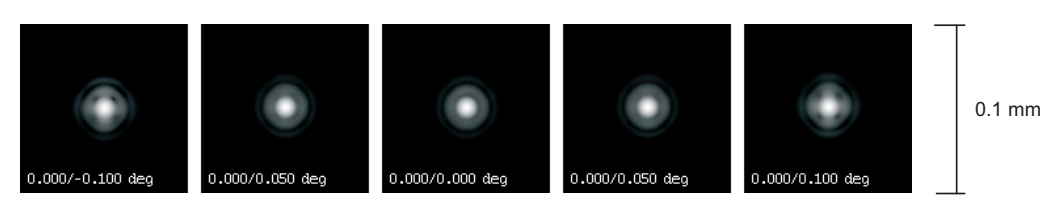


**Figure 43-125:** Diffraction PSF of the Schupmann telescope over a total field of view of 0.2° for an F/15 system.

A variant of the Schupmann principle is shown in figure 43-126 where the prism at the intermediate focus has been replaced by a shallow concave mirror. The curvature of this mirror (M1) is set to perform the necessary pupil imaging, that is, the pupil of the front lens onto the corrector.

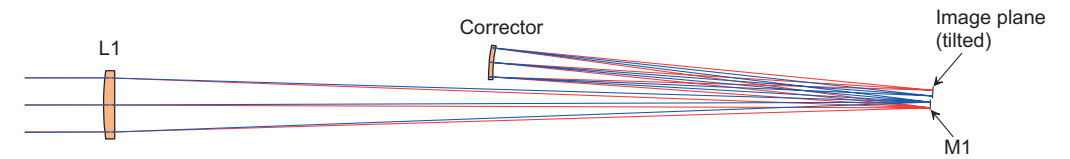


Figure 43-126: Variant of the Schupmann telescope using a mirror (M1) instead of a prism.

### 43.14.10

### Schupmann Brachymedial

Another telescope utilizing the dialyte principle is the Schupmann Brachymedial which was already proposed by Hamilton in 1814. Here the singlet objective is compensated by a concave mirror of the Mangin type. Schupmann improved Hamilton's design by introducing an air space between the compensating lens and the mirror, thus gaining more degrees of freedom for the correction of spherical aberration.

Even though the secondary spectrum is well corrected, a notable disadvantage of the Brachymedial is the large transverse color aberration which cannot be corrected with this design. This narrows the usable field to about 0.1° to 0.2°.

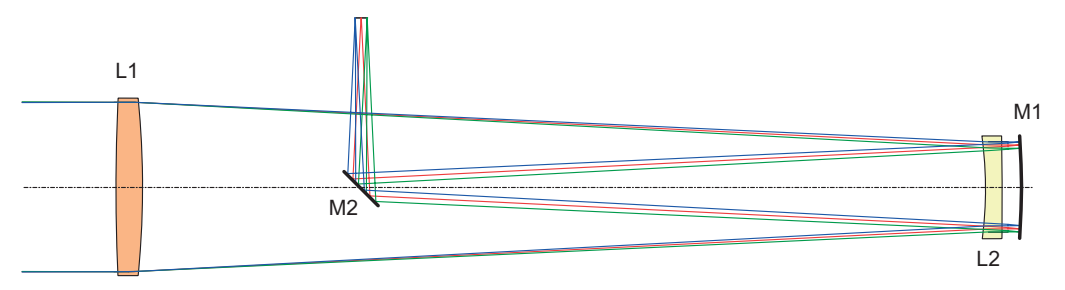


Figure 43-127: Brachymedial according to Schupmann.

# 43.15 Telescopes with Field Correctors

Field correctors are lenses placed in the convergent beam of a telescope in order to reduce or even fully correct residual aberrations in the telescope. The most prominent aberrations in telescopes are field curvature, coma and astigmatism. Because these aberrations depend on the field, and typically increase with the field coordi-

nate, they are commonly called the field corrector. If only field curvature is to be corrected, these components are also called "field flatteners".

Field correctors are typically placed close to the image in order to keep dimensions of the optical components small.

### 43.15.1

# Field-flattening Lens

Many telescopes have a curved focal surface, which is suitable for visual observation (with an eyepiece) due to the ability of the eye to accommodate when viewing offaxis fields. In photographic applications, however, a flat field is required.

The simplest way to flatten a curved image surface is to use a single lens close to the focal surface as shown in figure 43-128. The optical power of the field-flattening lens is negative in Newton or Cassegrain telescopes, whereas a positive power is required in a Schmidt telescope.

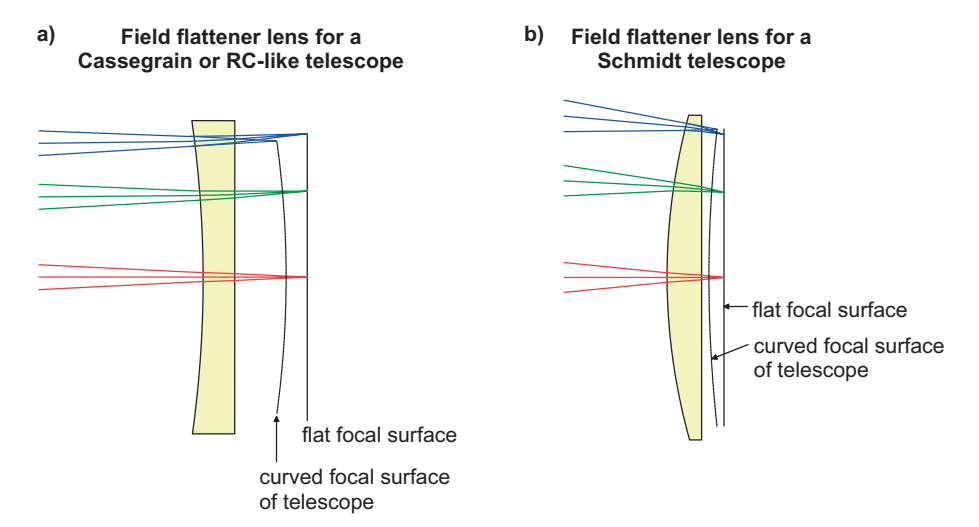


Figure 43-128: Field-flattening lens for a Cassegrain/RC telescope (a) and a Schmidt telescope (b).

Assuming a lens where one surface is flat ( $R_1 = \infty$ ), the radius of the other surface  $R_2$  can be determined by [43-84], [43-65]

$$R_2 = \frac{n-1}{n} \cdot R_{\rm P} \,, \tag{43-82}$$

where  $R_P$  is the radius of the curved field surface (the Petzval radius). Equation (43-82) is an approximation which is only valid in the absence of astigmatism and if the field-flattening lens is closely attached to the focal surface. The latter condition also imposes some practical problems, because mechanical mounting of the lens inside an SLR,  $6 \times 6$  or C-mount camera body would be very difficult. Also because the lens

is very close to the film or CCD plane, any surface irregularities such as scratches or dust become visible.

The field flattening lenses can also be made achromatic, mainly to correct transverse color introduced by single-lens correctors. Examples are given by Laux [43-43].

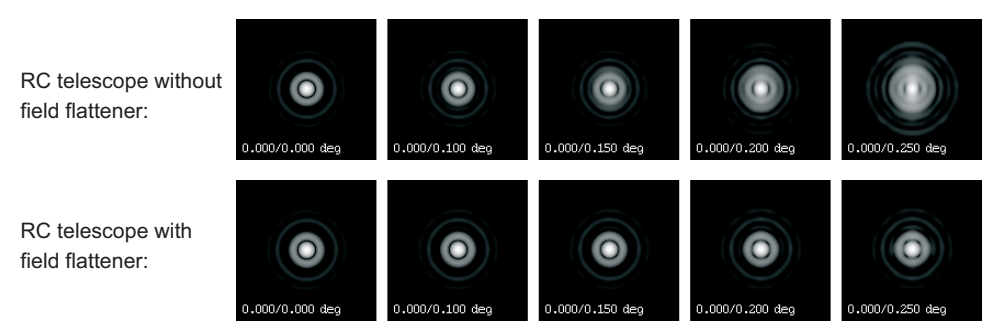


**Figure 43-129:** Diffraction PSF of a F10/2000 mm Ritchey—Chretien (RC) telescope without (top) and with (bottom) field-flattening lens.

# 43.15.2 Correctors for a Parabolic Mirror (Newton Telescope)

There are many different designs of corrector for a parabolic mirror (Newton telescope). The major aberrations in a Newtonian telescope, which need to be corrected, are coma and field curvature. Two designs are discussed. The most widely known corrector is that designed by Ross in 1935 [43-63].

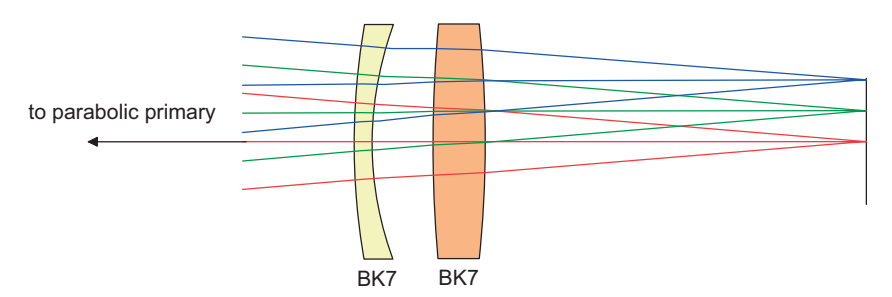


**Figure 43-130:** Ross corrector for an F12/2400 mm parabolic primary mirror (Newton telescope). Design data after Rutten and van Venrooji [43-65].

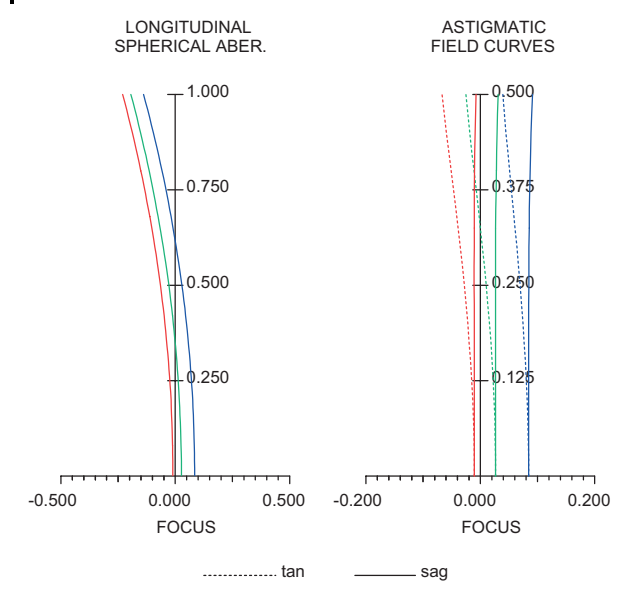


**Figure 43-131:** Field aberrations of the Ross corrector shown in figure 43-130. The corrector is used in combination with an F6/1200 mm parabolic mirror.

The two-lens Ross corrector as shown in figure 43-130 effectively eliminates coma, but introduces significant amounts of spherical aberration and axial chromatic aberration, into the system. The resulting spot sizes are significantly larger than the Airy disc which makes this system less favorable for visual observation. In photographic applications, however, the Ross corrector gives satisfactory results.

More advanced correctors for the parabolic mirror, as shown in figure 43-132, not only correct coma but also allow a much better control of sthe pherical aberration and axial chromatic color. An example is given in figure 43-133.

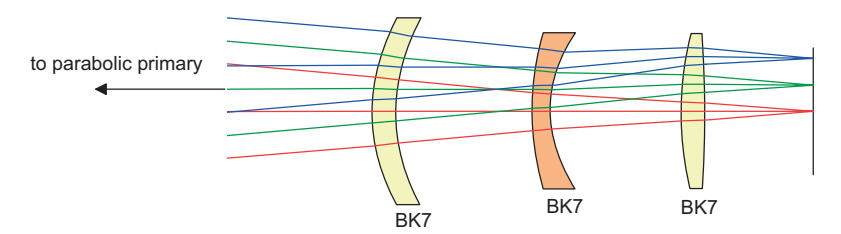


Figure 43-132: More advanced corrector for a parabolic primary mirror (Newton telescope).

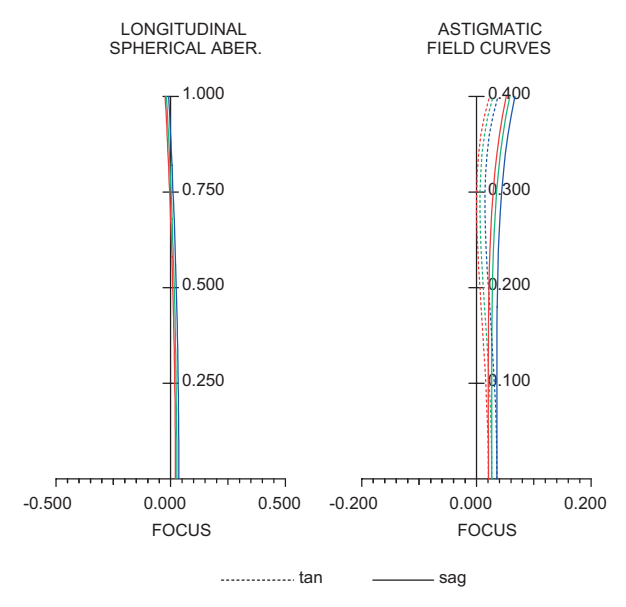


Figure 43-133: Field aberrations of the three-lens corrector shown in figure 43-132.

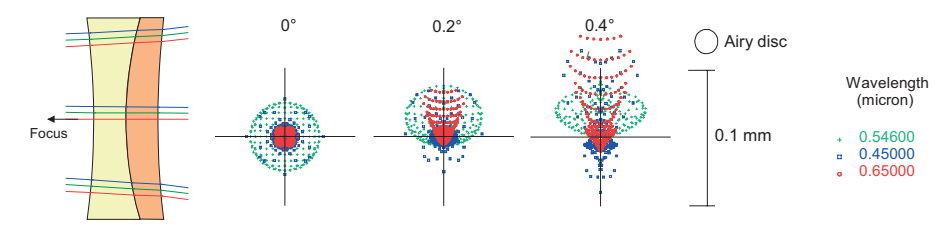
# 43.15.3 Correctors for a Spherical Mirror

Systems using a spherical primary mirror are becoming increasingly important because they exhibit a significant cost advantage over systems that employ an aspherical primary mirror. Despite of this fact, only very little work has been devoted to develop sub-aperture correctors for spherical primaries.

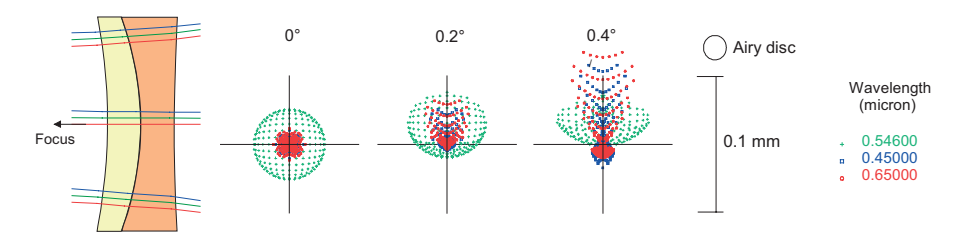
Rutten and van Venrooji give some classical examples as shown in figure 43-134. The achievable optical performance is limited, because it is impossible to correct spherical aberration, coma and color with a two-lens configuration simultaneously.

More advanced correctors have been proposed in order to overcome this limitation, for example a four-lens corrector in two groups by Jones and James [43-93].

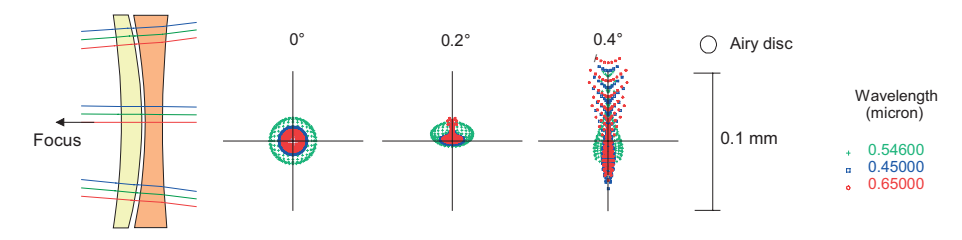
## a) Jones



# b) Brixner



# c) Jones-Bird



# d) Jones-James

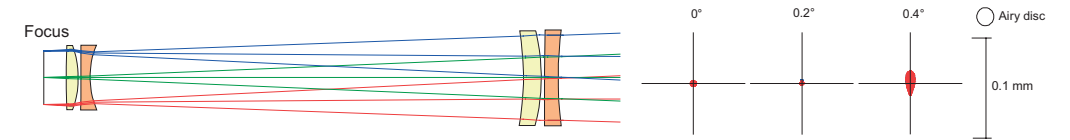


**Figure 43-134:** Corrector systems for a F4/800 mm spherical primary mirror. All two-lens designs are after Rutten and van Venrooji [43-65], the four-lens design is from Jones and James [43-93].

### 43.15.4

# **Corrector for Cassegrain and RC Telescopes**

A two-lens corrector for Cassegrain and Ritchey–Chretien telescopes is shown in figure 43-135. The form is similar to a design by Wynne [43-84]. Other corrector forms

for Cassegrain telescopes are given by Wilson [43-88] and Terebizh [43-91]. The corrector removes astigmatism and field curvature. Curvatures and separations must be individually optimized for the Cassegrain and RC forms. Gascoigne and Wilson also give examples of aspherical plate correctors, however, they cannot correct field curvature [43-84], [43-92].

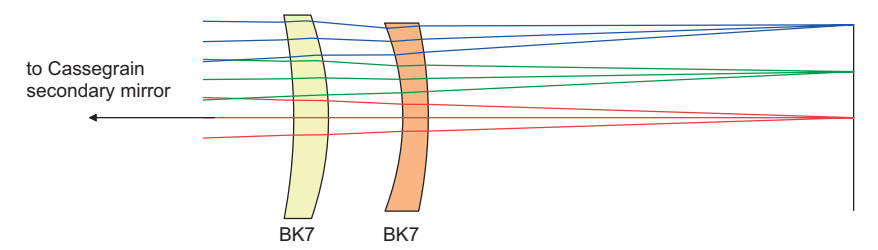


Figure 43-135: Field corrector for a Cassegrain telescope.

### 43.15.5

### **Focal Reducers**

A focal reducer is a system of lenses with positive power, which is placed in front of the image in a telescope. The purpose is to reduce the focal length of the telescope and increase its "speed". Enabling shorter exposure times to be achieved in astrophotography. Such lenses are sometimes called 'Shapley lenses'.

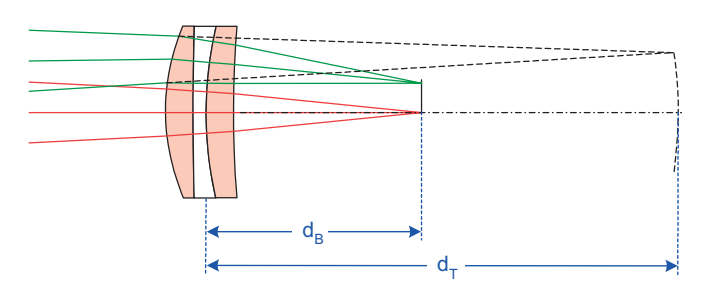


Figure 43-136: Shapley focal reducer lens on an F10/2000 mm RC telescope. Reduction ratio  $m_R = 0.5$ .

The focal length of the combined system and the reduction ratio are determined by [43-65]

$$f_{\text{comb}} = \frac{f_{\text{T}} \cdot f_{\text{R}}}{f_{\text{R}} + d_{\text{R}}}, \tag{43-83}$$

$$m_{\rm R} = \frac{f_{\rm comb}}{f_{\rm T}} \,, \tag{43-84}$$

where  $f_T$  is the telescope focal length,  $f_R$  is the reducer focal length and  $d_R$  is the distance of the reducer lens in front of the telescope focus. The thickness of the reducer is ignored in these equations.

The new focal distance  $d_{\rm B}$  is then obtained by

$$d_{\rm R} = m_{\rm R} \cdot d_{\rm T} \,. \tag{43-85}$$

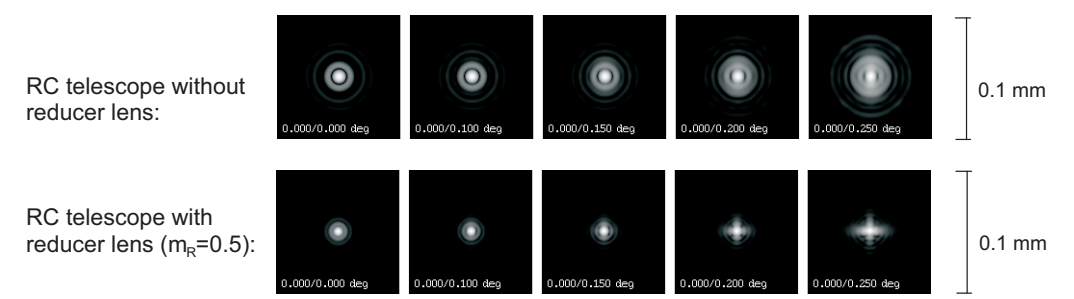


**Figure 43-137:** Diffraction PSFs for an F10/2000 mm Ritchey–Chretien (RC) telescope (top) and with  $m_{\rm R}=0.5$  focal reducer (bottom) resulting in a F5/1000 mm system. Note that the image height is halved with the reducer lens.

### 43.15.6

# **Focal Extenders**

A focal extender is a system of lenses with negative power, which is placed in front of the image produced by a telescope. The purpose is to increase the focal length of the telescope and therefore – when used in conjunction with an eyepiece – to increase the telescope's magnification. These lenses are commonly known as Barlow lenses.

The focal length of the combined system and the extension ratio are determined by [43-65]

$$f_{\text{comb}} = \frac{f_{\text{T}} \cdot f_{\text{R}}}{f_{\text{R}} - d_{\text{R}}}, \tag{43-86}$$

$$m_{\rm R} = \frac{f_{\rm comb}}{f_{\rm T}} \,, \tag{43-87}$$

where  $f_T$  is the telescope focal length,  $f_R$  is the reducer focal length and  $d_R$  is the distance of the reducer lens in front of the telescope focus. The thickness of the reducer is ignored in these equations.

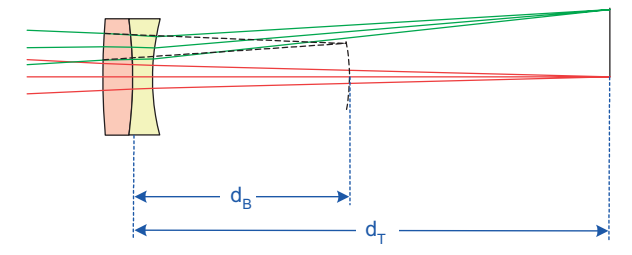


**Figure 43-138:** Barlow focal extender on an F10/2000 mm RC telescope. Extension ratio  $m_R = 2.0$ .

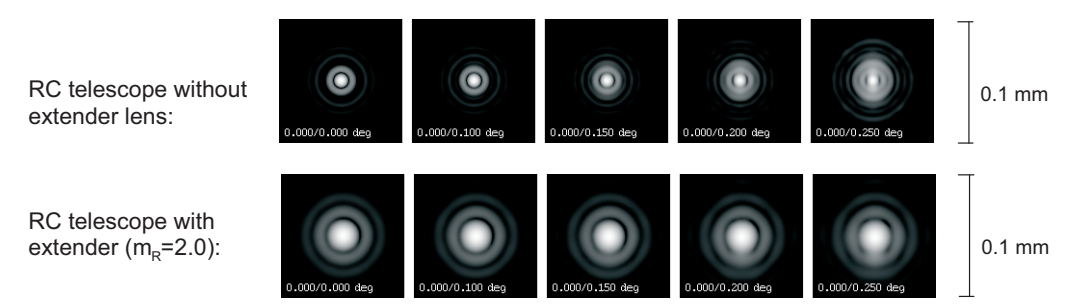


**Figure 43-139:** Diffraction PSFs for an F10/2000 mm Ritchey—Chretien (RC) telescope (top) and with an  $m_{\rm R}=2.0$  focal extender (bottom) resulting in an F20/4000 mm system. Note that the image height is doubled with the extender lens.

# 43.16 The Effects of Aperture Obscuration

There has been extensive literature produced and endless debate about the detrimental influence of aperture obscuration. In particular, obstructions caused by the secondary mirror and also the spider vanes holding the secondary, which are of primary interest in astronomical telescopes. Also, internal baffles and undersized lenses lead to a loss of light at the edge of the field (commonly described as "vignetting") which is another form of obscuration.

The three major effects of obscuration are as follows.

- It reduces the amount of light received by the instrument. The decrease of light corresponds to the area of obscuration.
- The diffraction pattern of an object is modified. Energy is moved from the central Airy disk to the outer rings.
- The contrast is lowered for low spatial frequencies but exceeds the contrast of unobscured systems at very high spatial frequencies.

These aspects are covered in the following sections on the basis of diffraction theory. An instrument without any obscuration is better than one which has it and the smaller the obscuration the better. But it would be absurd to minimize the obscuration to the detriment of the complete design. In the worst case, rigorous attempts at reducing obscuration to the ultimate limit may lead to a highly stressed design and the additional risk of other optical problems.

A typical effect will be an increased alignment sensitivity, because the powers of the lenses or mirrors would also increase. Another mistake, where a telescope's performance is sacrificed for minimum central obscuration, is making the secondary mirror of a Cassegrain or the folding diagonal of a Newton as small as possible, so that only the axial beam passes without vignetting. This mistake produces field-angle-dependent vignetting (because the undersized secondary or folding mirror cuts out portions of the off-axis beams), but mirrors (and lenses) generally have a tendency towards steeper surface-form errors near to the edge ("turned edge" or roll-off). This results ultimately in a poorer quality telescope.

It is therefore important not to reduce the central obscuration by excluding every other optical consideration. For completeness, we summarize other important factors which may affect a telescope's resolution to a much higher degree than obscuration alone.

- Optical limitations due to surface-form errors of mirrors and lenses (turned down edge), residual design aberrations (spherical aberration, coma, astigmatism, field curvature).
- Mechanical limitations: misalignment of optical components caused by improper adjustment or due to thermal deformation of the instrument.
- Observational constraints such as atmosphere, thermal equilibrium of the telescope and the resulting tube currents

#### 43.16.1

### Central Obstruction

One of the most obvious kind of obstruction is caused by a centrally placed secondary mirror (e.g., Cassegrain, Maksutov, etc.) or a folding diagonal mirror in Newtonian systems. Central obstruction is most commonly expressed as a percentage of the aperture diameter. We denote it as *linear* obstruction in contrast to the *area* obstruction which is a percentage of the collecting aperture area. A 20% linear obstruction results in a 4% loss of the light received and even a 40% linear obstruction gives only 16% loss of light received. It is therefore evident that, even with large obstructions, the loss of light is moderate.

The effects of central obscurations (i.e., forming annular apertures) have been studied by many writers. Already Airy [43-1] had calculated, in 1841, the intensity in the diffraction rings of annular apertures with a remarkably high accuracy and Tschunko [43-80] gave results for the whole range of central obscuration ratios.

The normalized intensity of the diffraction pattern of an annular aperture is given after Born–Wolf [43-7] by

$$I(x,\varepsilon) = \frac{1}{\left(1 - \varepsilon^2\right)^2} \left[ \left( \frac{2J_1(x)}{x} \right) - \varepsilon^2 \left( \frac{2J_1(\varepsilon x)}{\varepsilon x} \right) \right]^2, \tag{43-88}$$

where  $\varepsilon$  is the obscuration ratio, which is a positive number between 0 and 1. The central Airy disc of the diffraction pattern becomes smaller with increasing central obstruction, as shown in figures 43-140 and 43-141. This improvement in resolution, however, is accompanied by more pronounced secondary maxima, i.e., the energy moves from the central disc to the outer rings. This effect becomes even more visible by comparing the encircled energy for various obscurations as shown in figure 43-143. From eq. (43-88), the energy integral is given by

$$L(x,\varepsilon) = \frac{1}{1-\varepsilon^2} \left[ I(x,\varepsilon=0) + \varepsilon^2 I(x,\varepsilon) - 4\varepsilon \int_0^x \left( \frac{J_1(x) \cdot J_1(\varepsilon x)}{x} \right) dx \right]. \tag{43-89}$$

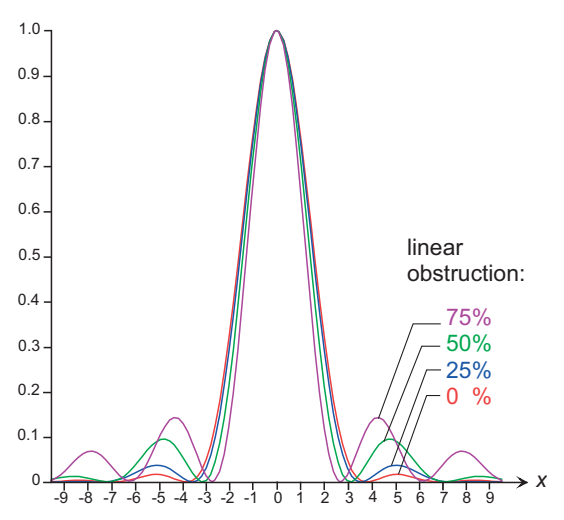
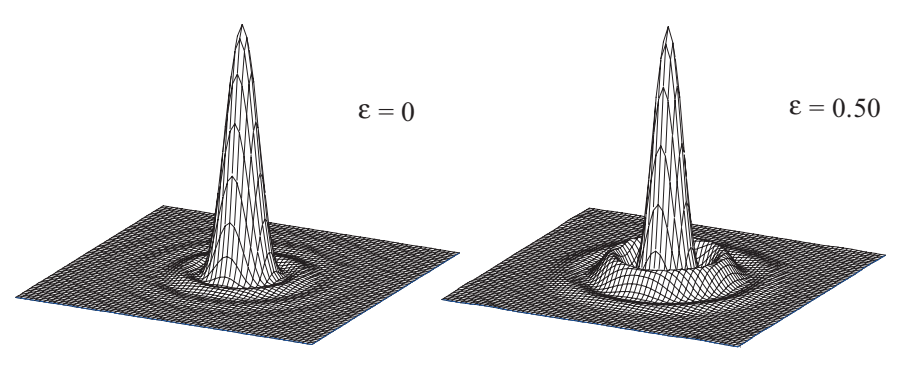
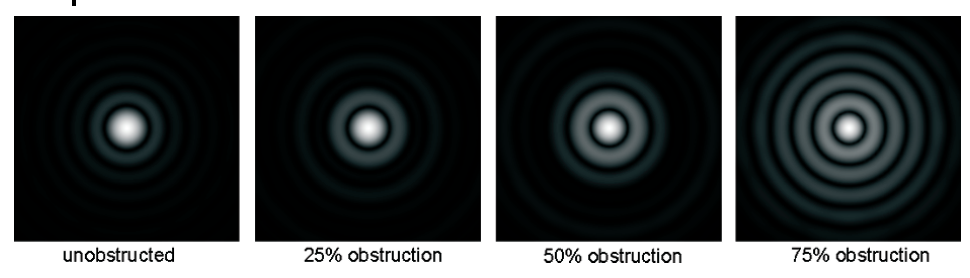


Figure 43-140: Diffraction point spread function (PSF) for various amounts of linear aperture obscuration.



**Figure 43-141:** Diffraction point spread function (PSF) of an aberration-free optical system shown for two obstruction ratios  $\varepsilon$ .



**Figure 43-142:** Diffraction patterns resulting from central obscuration. Note the decreasing diameter of the central Airy disc with increasing obstruction.

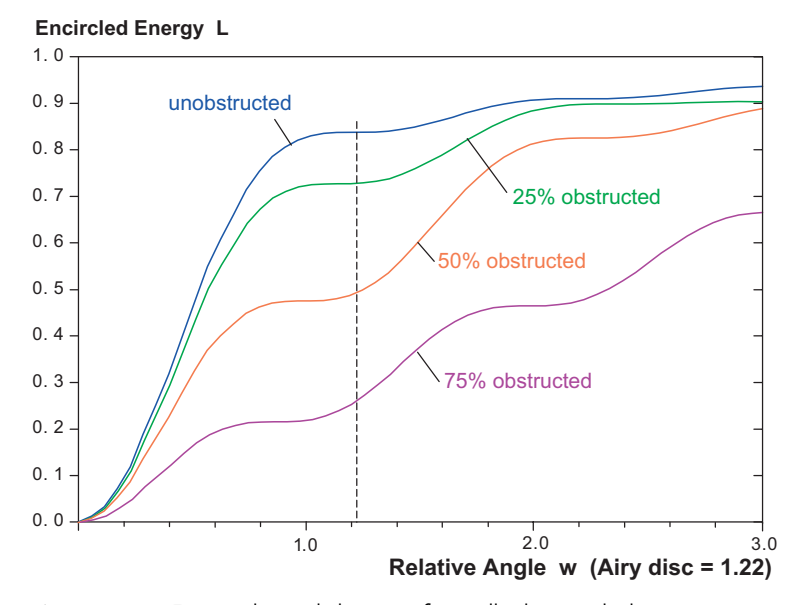


Figure 43-143: Fractional encircled energy of centrally obstructed telescopes.

Not only is the brightness of the image reduced (proportional to the area of obstruction), but the contrast is also considerably reduced. Figure 43-144 shows the contrast transfer (MTF) at various levels of the central obstruction. Depending on the obstruction ratio, the contrast will be considerably reduced at low and medium spatial frequencies. This effect is due to the increased intensity of the diffraction rings, as shown in figures 43-140 and 43-142. High frequencies near to the limit frequency, however, exhibit a higher contrast, which slightly exceeds the contrast of an unobstructed aperture. This effect can be explained by the reduced diameter of the central disc with increasing obstruction ratio.

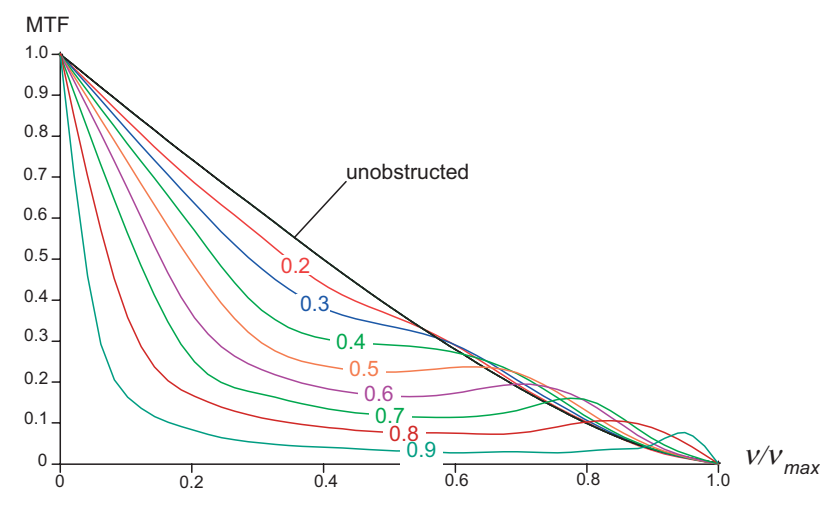


Figure 43-144: Modulation transfer function (MTF) for obstructed apertures.

From the plots in figures 43-140 to 43-144 we can draw a number of conclusions.

- At low and medium spatial frequencies, an obstructed system provides the same contrast as an unobstructed system of correspondingly smaller aperture, or, conversely, an obstructed system behaves no better at low/medium frequencies than one with a correspondingly smaller aperture.
- The contrast transfer of an obstructed system for low-contrast objects (planetary details, nebulae) is lower compared to an unobstructed system with the same aperture.
- The limit frequency of obstructed telescopes is not altered. In fact, its contrast response is even slightly higher compared with an unobstructed telescope of the same aperture. This effect is especially advantageous for high-contrast objects (stars, edges of planets, etc.).

No agreement is given in the literature as to which level of obstruction may be tolerated. Kutter, an advocate of unobstructed telescopes, considered that a central obscuration of ratio 0.1 was tolerable, while Linfoot and Wolf [43-45] thought a value of  $\varepsilon=0.25$  was appropriate, which corresponds to the greatest central obstruction regarded as tolerable by users of visual telescopes. On the other hand, the central obstruction of the Kitt Peak 84-in.(213 cm) telescope is 0.37 of the full aperture; and Ritchey–Chretien systems covering a wider field require still larger central obstructions. Thus, for modern telescopes, typically about 0.4 of the diameter is obstructed.

We must distinguish between visual observation, photographic/photometric observation and the inherent contrast of an object. A comparison of the point spread functions in figure 43-140 for  $\varepsilon=0$  and  $\varepsilon=0.25$  shows how small the difference is of the relative intensities in different parts of the image. In particular, the size of the bright central disc is almost unaffected. Now taking into consideration the influence of the atmosphere ("seeing") it seems to be unlikely that there will be any practical

difference. This assumption is supported by MTF considerations, because the worst-case MTF degradation for  $\varepsilon=0.25$  is only in the order of 10% as indicated in figure 43-144.

### 43.16.2

### **Spider Obstruction**

Besides the central obstruction, the most common obstruction is the "spider" which holds the secondary mirror in axial reflecting systems (e.g., Cassegrain-type telescopes). Like any aperture obstruction, spider vanes cause light diffraction which extends and smears the image. For linear spider vanes, each vane produces diffraction spikes at right angles to the direction of the vane. For photographic applications, this effect can be very problematic for bright stars, when the image of the star is greatly overexposed.

In figure 43-145, a collection of the effects of various forms of spiders are shown compared to apertures without a spider. A logarithmic scale has been chosen to better reveal the subtle details of the diffraction peaks, and to simulate the effects seen with overexposed bright stars.

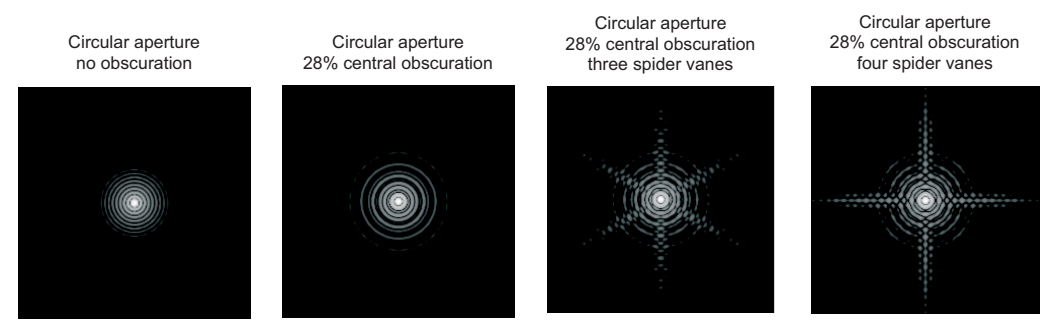


**Figure 43-145:** Images of a perfect telescope, but with different spider obstructions of the entrance aperture. The images are for monochromatic light and are given on a logarithmic scale for better representation of the low-intensity diffraction effects.

Various attempts have been made to suppress the diffraction spikes caused by a conventional (straight) spider. Using curved vanes and masking the aperture with round or elliptical holes were two propositions. An excellent account of the effect of various forms of spider vanes and of sub-apertures is given by Everhart and Kantorsky [43-17]. However, these attempts constitute a fundamental misunderstanding, because diffraction will *always* occur at spider vanes, independent of their shape. Other forms of vanes or apertures will modify the appearance of the spikes so that they are less annoying, but the diffracted energy is still there and spread into other angular regimes. Thus, the energy of the central maximum and the contrast are still lowered by the same amount.

The most important factor in spider diffraction is the *fraction* of the aperture which is covered by the vanes. Only when the width of the spider vanes becomes small compared with the wavelength of light, will spider diffraction become undetectable.

# 43.17 Telescope Design Prescriptions

This section summarizes the prescription data of all telescopes presented in this chapter. Where appropriate, all prescription data are referred to an entrance pupil of 200 mm in order to allow the best comparison of telescope performance.

Since many of the references to classical telescopes are very old and date back to the 19<sup>th</sup> century, all glasses presented in the design prescriptions have been replaced by modern types from Schott and Ohara.

Prescription data are given in tabular form with columns headed: radius, distance and glass name. The sign conventions for curvatures and thicknesses (separations) are determined according to the following rules:

- The radius of curvature of a surface is positive if the center of curvature lies
  to the right of the surface, otherwise it is negative. This rule is independent
  of the direction of the light, i.e., whether the light travels from left to right
  (the default condition) or whether it travels from right to left (after reflection
  from a mirror).
- The thickness (separation) of two consecutive surfaces is positive if (in the axial direction) the next surface lies to the right of the current surface. If it lies to the left, it is negative.
- In the case of tilted and decentered surfaces, the sign conventions apply to the local coordinate system of the current surface.
- Surface tilt angles are always given in degrees. A positive tilt means a rotation in the counter-clockwise direction, a negative tilt is in the clockwise direction.

Aspherical surfaces are described by a standard polynomial of the form

$$z = \frac{c \cdot r^2}{1 + \sqrt{1 - (k+1)c^2r^2}} + Ar^4 + Br^6 + Cr^8 + Dr^{10} + \dots,$$
(43-90)

where *c* is the curvature, *k* the conic constant,  $r = \sqrt{x^2 + y^2}$  the radial height, and *A*, *B*, *C*, *D* are aspherical coefficients. The conic constant *k* yields:

k < -1 hyperbola k = -1 parabola -1 < k < 0 ellipse at major axis (prolate ellipse) k > 0 ellipse at minor axis (oblate ellipse) k = 0 sphere.

Special attention should be paid to tilted and/or decentered surfaces. Three tilt moduli are possible, which are defined by the following abbreviations:

- decenter and return, the surface is decentered but does not alter the opti-DAR cal axis.
- NAX surface normal defines the new (optical) axis for all subsequent surfaces,
- bend, i.e., the axis follows the law of reflection on that surface. BEN

All telescope designs presented in this chapter are also provided in electronic form. They may be freely downloaded from http://www.optenso.com in the OpTaliX® format. Because OpTaliX neatly interfaces with other commercial optical design packages, i.e., it provides comprehensive import and export filters, designs may be easily converted to Zemax, Code V, Oslo, ASAP and other packages.

### Cassegrain Telescope F/10: Sect. 43.5.1

```
# TYPE RADIUS DISTANCE GLASS INDEX
3J S Infinity 0.10000E+21 1.000000
TO>AM -1200.0000 -426.92308 -1.000000
2 AM -494.5055 576.92308 1.000000
                                                                 APE-Y
OBJ S
                                                                    0.00
STO>AM
                                                    -1.000000
                                                                100.00
                                                                 30.79
8.76
 2 AM -494.5055
MG S Infinity
                            576.92308
                                                      1.000000
IMG S
                                                     1.000000
ASPHERES:
  # Type
  1 EVEN -1.000000000 0.0000000E+00 0.0000000E+00 0.0000000E+00
  2 EVEN -3.4489795920 0.00000000E+00 0.0000000E+00 0.0000000E+00
PARAXIAL DATA AT INFINITE CONJUGATES:
                                              SH1 (Princ.Plane 1) -3453.33333
                             2000.00000
                                              SH2 (Princ.Plane 2) -1423.07692
   FNO
                               10.00000
   EPD (Entr.Pup.Dia.)
                              200.00000
```

# Ritchey-Chretien Telescope F/10: Sect. 43.5.2 RADIUS

# TYPE

```
Infinity 0.10000E+21
OBJT S
                                            1 000000
                                                       0 00
         -1200.0000 -426.92308
                                           -1.000000 100.00
STO>AM
  2 AM
          -494.5055
Infinity
                                           1.000000
                                                     30.79
                      576.92308
TMG S
                                                       8.76
ASPHERES.
  # Type
          -1.0696266930 0.00000000E+00 0.0000000E+00 0.0000000E+00
  2 EVEN -4.1566206430 0.00000000E+00 0.0000000E+00 0.0000000E+00
PARAXIAL DATA AT INFINITE CONJUGATES:
               2000.00000
                                       SH1 (Princ.Plane 1)
                                                            -3453.33333
                                      SH2 (Princ.Plane 2) -1423.07692
                         10.00000
   EPD (Entr.Pup.Dia.)
                         200.00000
```

APE-Y

INDEX

DISTANCE GLASS

#### Dall-Kirkham Telescope F/10: Sect. 43.5.3

# TYPE	RADIUS	DISTANCE	GLASS	INDEX	APE-Y	
OBJ S	Infinity	0.10000E+21		1.000000	0.00	
STO>AM	-1200.0000	-426.92308		-1.000000	100.00	
2 SM	-494.5055	576.88346		1.000000	30.79	
IMG S	Infinity			1.000000	8.76	
ASPHERES:						
# Type	K		A	В		C
1 EVEN	-0.6571468416	0.00000000	E+00	0.0000000E+00	0.0000000	00E+00
PARAXIAL D	ATA AT INFINIT	E CONJUGATES	:			
EFL		2000.0000	0	SH1 (Princ.Pla	ane 1)	-3453.33333
FNO		10.0000		SH2 (Princ.Pla	ane 2)	-1423.07692
EPD (En	tr.Pup.Dia.)	200.0000	0			

#### Pressman-Camichel Telescope F/10: Sect. 43.5.4

# TYPE	RADIUS	DISTANCE	GLASS	INDEX	APE-Y	
OBJ S	Infinity	0.10000E+21		1.000000	0.00	
STO>SM	-1200.0000	-426.92308		-1.000000	100.00	
2 AM	-494.5055	576.42587		1.000000	30.79	
IMG S	Infinity			1.000000	8.76	
ASPHERES:						
# Type	F	ζ	A	В		C
2 EVEN	6.3603351090	0.00000000	E+00	0.0000000E+00	0.000000	00E+00
PARAXIAL D	ATA AT INFINIT	E CONJUGATES	:			
EFL		2000.0000	0	SH1 (Princ.Pla	ane 1)	-3453.33333
FNO		10.0000	0	SH2 (Princ.Pla	ane 2)	-1423.07692
EPD (En	tr.Pup.Dia.)	200.0000	0			

### Gregorian Telescope: Sect. 43.5.5

# TYPE

OBJ	S	Infinity 0	.10000E+21	1.000000	0.00
STO:	>AM	-1200.0000	-820.23813	-1.000000	100.00
2	AM	358.9881	820.23813	1.000000	30.79
3	S	Infinity	150.00000	1.000000	30.79
IMG	S	Infinity		1.000000	8.76
ASPHI	ERES:				
#	Type	K	A	В	C
1	EVEN	-1.0000000000	0.0000000E+00	0.0000000E+00	0.0000000E+00
2	EVEN	-0.3968999571	0.0000000E+00	0.0000000E+00	0.0000000E+00

PARAXIAL DATA AT INFINITE CONJUGATES: EFL -2643.24294 -13.21621 SH1 (Princ.Plane 1) -12078.88729 SH2 (Princ.Plane 2) 2793.24294 FNO EPD (Entr.Pup.Dia.) 200.00000

RADIUS DISTANCE GLASS INDEX APE-Y

### Gregorian Telescope, Aplanatic: Sect. 43.5.5

#	TYPE	RADIUS	DISTANCE	GLASS	S INDEX	APE-Y	
OBJ	S	Infinity	0.10000E+21		1.000000	0.00	
STO:	>AM	-1200.0000	-820.23813		-1.000000	100.00	
2	AM	358.9820	820.23813		1.000000	42.40	
3	S	Infinity	150.25919		1.000000	20.40	
IMG	S	Infinity			1.000000	18.48	
ASPHI	ERES:						
#	Type	K		A	В		C
1	EVEN	-0.9764378586	0.00000000	E+00	0.0000000E+00	0.000000	00E+00
2	EVEN	-0.4325300269	0.00000000	E+00	0.0000000E+00	0.000000	00E+00
PARA	AXIAL	DATA AT INFINIT	E CONJUGATES	5:			
1	EFL		-2643.0000	0	SH1 (Princ.Pla	ane 1)	-12077.98249
]	FNO		-13.2150	0	SH2 (Princ.Pla	ane 2)	2792.91082
1	EPD (E	ntr.Pup.Dia.)	200.0000	0			

### Schwarzschild Telescope: Sect. 43.5.6

#	TYPE	RADIUS	DISTANCE	GLASS		INDEX	APE-Y	
OBJ	S	Infinity	0.10000E+21			1.000000	0.00	
1>	S.	Infinity	1300.00000			1.000000	145.75	
STO	SM	500.0000	-1000.00000			-1.000000	100.00	
3	SM	1500.0000	1875.00000			1.000000	527.72	
IMG	S	Infinity				1.000000	13.42	
PARA	AXIAL	DATA AT INFINI	TE CONJUGATES	:				
E	EFL		375.0000	0	SH1	(Princ.Plan	ne 1)	1800.00000
E	NO		1.8750	0	SH2	(Princ.Plan	ne 2)	1500.00000
E	EPD (E	Entr.Pup.Dia.)	200.0000	0				

# Schwarzschild Aplanatic Telescope: Sect. 43.5.6

#	TYPE	RADIUS	DISTANCE	GLASS	INDEX	APE-Y		
OBJ	S	Infinity	0.10000E+21		1.000000	0.00		
STO	>AM	-3000.0000	-750.00000		-1.000000	100.00		
2	SM	1000.0000	300.00000		1.000000	63.51		
IMG	S	Infinity			1.000000	10.53		
ASPI	HERES:							
#	Type		K	A	В		C	
1	EVEN -	0.10010211E+0	2 0.00000000	E+00	0.0000000E+00	0.0000000	0E+00	
PAR	AXIAL D	ATA AT INFINI	TE CONJUGATES	::				
]	EFL		600.0000	0	SH1 (Princ.Pl	ane 1)	900.00000	
1	FNO		3.0000	0	SH2 (Princ.Pl	ane 2)	-300.00000	
1	EPD (En	tr.Pup.Dia.)	200.0000	0				

```
Couder Anastigmatic Telescope:
                              Sect. 43.5.7
  # TYPE
                                                        APE-Y AP
               RADTUS
                         DISTANCE GLASS
                                                 INDEX
            Infinity 0.10000E+21
                                             1.000000
OBJ S
                                                          0.00
STO>AM
           -3900.0000 -1200.00000
                                             -1.000000
                                                        100.00
 2 SM
          666.6666
569.9113
                       230.78936
                                             1.000000
                                                         59.72
IMG S
                                             1.000000
ASPHERES:
  # Type
  1 EVEN -0.17534618E+02 0.00000000E+00 0.0000000E+00 0.0000000E+00
 PARAXIAL DATA AT INFINITE CONJUGATES:
                                         SH1 (Princ.Plane 1)
                                                               2160.00007
-369.23074
                          599.99996
                            3.00000
                                         SH2 (Princ.Plane 2)
   EPD (Entr.Pup.Dia.)
                          200.00000
Loveday Telescope:
                      Sect. 43.5.8
  # TYPE
             RADIUS DISTANCE GLASS
                                                        APE-Y
                                                INDEX
            Infinity 0.10000E+21
                                             1.000000
OBJ S
                                                          0.00
         -2400.0000 -900.00000
-600.0000 900.00000
                                                        100.00
STO>AM
                                             -1.000000
 2 AM
                                              1.000000
                                                         39.78
           -2400.0000 -1000.00000
                                             -1.000000
  3 AM
                                                          49.28
           Infinity
  4 SMD
                       200.00000
                                              1.000000
                                                         49.28
                                                         4.54
TMG S
            Infinity
                                              1.000000
ASPHERES:
  # Type
                                                   В
  DECENTER / TILTS :
                        YDE
                                  ZDE
              XDE YDE ZDE ADE BDE CDE TLM TSEQ
0.0000 0.0000 0.0000 -45.0000 0.0000 0.0000 BEN XYZABC
  #
PARAXIAL DATA AT INFINITE CONJUGATES:
                         4800.00000
                                         SH1 (Princ.Plane 1)
SH2 (Princ.Plane 2)
                                                                3600.00000
   FNO
                           24.00000
                                                               -4600.00000
   EPD (Entr.Pup.Dia.)
                          200.00000
Paul-Baker Telescope:
                             Sect. 43.6.1
  # TYPE
              RADIUS DISTANCE GLASS
                                                INDEX
                                                        APE-Y
             Infinity 0.10000E+21
OBJ S
                                              1.000000
                                                          0.00
                                                        111.02
                       -160.00000
  1 > AM
            -440.0000
                                             -1.000000
                       118.42930
-59.99516
STO AM
           -120.0000
-120.0000
                                              1.000000
                                                          27.25
                                             -1.000000
  3 SM
                                                          36.06
TMG S
            -175.3368
                                             -1.000000
                                                          3.93
ASPHERES.
  # Type
         -1.000000000 0.0000000E+00 0.0000000E+00 0.0000000E+00 1.4755426010 0.10737905E-06 0.24471861E-11 0.00000000E+00
  1 EVEN
  2 EVEN
 PARAXIAL DATA AT INFINITE CONJUGATES:
                         220.00000
                                        SH1 (Princ.Plane 1) 1592.21613
   FNO
                            1.10000
                                         SH2 (Princ.Plane 2)
                                                               160.00000
```

EPD (Entr.Pup.Dia.)

200.00000

### Sect. 43.6.2 Willstrop Mersenne-Schmidt Telescope:

# TY OBJ S STO>AM 2 AM 3 AM IMG S	Infinity -640.0000 -243.2392	DISTANCE 0.10000E+21 -198.36000 395.54176 -197.83808	GLASS	INDEX 1.000000 -1.000000 1.000000 -1.000000	APE-Y 0.00 100.00 39.78 49.28 4.54	
ASPHER # Ty 1 EV 2 EV 3 EV	pe F EN -0.9987205698 EN -0.7489331935	0.0000000 5 0.0000000 6 0.0000000	E+00 0 E+00 0	B 0.0000000E+00 0.0000000E+00 0.0000000E+00	0.0000000	00E+00
FNO EPD	(Entr.Pup.Dia.)	2.6006	8	SH1 (Princ.Pla	. ,	322.31189

### Korsch Three-mirror, Single-axis Telescope: Sect. 43.6.3

#	TYPE	RADIUS	DISTANCE	GLASS	INDEX	APE-Y
OBJ	S	Infinity	0.10000E+21		1.000000	0.00
STO	AM	-1200.0000	-450.00000		-1.000000	100.00
2	AM	-333.3333	192.30743		1.000000	29.82
3	AM	-461.5389	-196.15429		-1.000000	33.96
4	S	Infinity	0.00114		-1.000000	9.43
IMG	S	Infinity			-1.000000	9.43
ASPI	HERES	:				
#	Type	K		A	В	C
1	EVEN	-1.2629390000	0.00000000	E+00	0.0000000E+00	0.0000000E+00
2	EVEN	-2.8432160000	0.00000000	E+00	0.0000000E+00	0.0000000E+00
3	EVEN	-1.4014770000	0.00000000	E+00	0.0000000E+00	0.0000000E+00
PAR	AXIAL	DATA AT INFINIT	E CONJUGATES	:		
1	EFL		900.0005	1		
1	FNO		4.5000	0		
1	EPD (1	Entr.Pup.Dia.)	200.000	0		

# Robb Three-mirror Telescope: Sect. 43.6.4

#	TYPE	RADIUS	DISTANCE	GLASS	IN	DEX	APE-Y			
OBJ	S	Infinity	0.10000E+21		1.000	000	0.00			
STO	AM	-774.0933	-243.21667		-1.000	000	100.00			
2	AM	-356.6867	413.21667		1.000	000	41.62			
3	AM	-660.0000	-165.00000		-1.000	000	37.73			
4	S	Infinity	0.00133		-1.000	000	17.49			
IMG	S	Infinity			-1.000	000	17.49			
ASPI	HERES:									
#	Type	K	1	4	В			C	D	
1	EVEN	-1.1290400	0.0000000E+0	0.243759	38E-17	0.472	208445E-	-23	0.28425020E-25	
2	EVEN	-2.8278000	0.20765025E-12	0.668022	19E-15	0.115	85974E-	-17	0.0000000E+00	
3	EVEN	-5.0850300	0.0000000E+0	0.000000	00E+00	0.000	00000E+	+00	0.0000000E+00	
PARA	AXIAL I	DATA AT INFIN	ITE CONJUGATES							
1	EFL		999.9972	SH1	. (Princ	.Plane	1)	23	33.08593	
]	FNO		4.99999	SH2	(Princ	.Plane	2)	9	99.99550	
1	EPD (Er	ntr.Pup.Dia.)	200.000	)						

```
Beach Four-mirror Space Telescope: Sect. 43.7
  # TYPE
                RADTUS
                           DISTANCE GLASS
                                                    INDEX
                                                            APE-Y
             Infinity 0.10000E+21
                                                 1.000000
 OBJ S
                                                              0.00
           -2380.5600
-1176.3590 628.46400
-2380.5600 -598.83900
20008.9490 482.49916
            -2380.5600 -628.61880
 STO>AM
                                                -1.000000 500.00
  2 AM
                                                 1.000000
                                                             241.48
                                                -1.000000
  3 AM
                                                            235.97
         3823808.9490
                                                 1.000000
   4 AM
                                                            111.40
                                                 1.000000
             Infinity
 ASPHERES:
  # Type
                    K
                                                    В
                                    A
  1 EVEN
          -1.3909000 -0.24220117E-13  0.28780933E-19 -0.37822110E-24
  2 EVEN
           -1.9035000 -0.51697705E-12 -0.56413484E-16 -0.18484100E-21
          -1.9035000 -0.5169//056-12 -0.504301905E-16 -0.96952614E-22 0.25539613E-29
  3 EVEN
  4 EVEN
           0.0000000 -0.20760183E-09 -0.15853658E-15 -0.52690010E-20 -0.41144256E-25
 PARAXIAL DATA AT INFINITE CONJUGATES:
                                           SH1 (Princ.Plane 1)
                                                                   1333 95275
   EFT.
                           2413 00000
                              2.41300
                                            SH2 (Princ.Plane 2) -1930.49930
    EPD (Entr.Pup.Dia.)
                            1000.0000
Kutter Two-mirror Schiefspiegler Telescope:
                                            Sect. 43.8.1
                                                            APE-Y
  # TYPE
                RADIUS
                           DISTANCE GLASS
                                                    INDEX
              Infinity 0.10000E+21
 OBJ S
                                                 1.000000
                                                              0.00
 STO>DSM
            -6477.0000 -1828.80000
-6528.7751 2480.71469
                                                -1.000000
                                                            100.00
  2 DSM
                                                 1 000000
                                                             50 18
 TMG SD
             Infinity
                                                 1 000000
                                                            20 11
 DECENTER / TILTS :
                           YDE
                                     ZDE
                XDE
                                                 ADE
                                                            BDE
                                                                        CDE TLM TSEQ
  #
                        0.0000 0.0000 2.4900 0.0000 0.0000 BEN XYZABC
0.0000 0.0000 -5.8714 0.0000 0.0000 BEN XYZABC
0.0000 0.0000 -3.9085 -0.0001 0.0000 NAX XYZABC
                                                                   0.0000 BEN XYZABC
   1
              0.0000
   2
              0.0000
                       0.0000
              0.0000
 PARAXIAL DATA AT INFINITE CONJUGATES:
   EFL
                           5700.00000
                                            SH1 (Princ.Plane 1)
                                                                   -3193.29730
                                           SH2 (Princ.Plane 2) -3218.82353
                             28.50000
   EPD (Entr.Pup.Dia.)
                             200.0000
Herrig Two-mirror Schiefspiegler Telescope:
                                            Sect. 43.8.2
  # TYPE
               RADIUS DISTANCE GLASS
                                                   INDEX
                                                            APE-Y
             Infinity 0.10000E+21
                                                 1.000000
                                                              0.00
 STO>SDM
          16200.0000 -1043.00000
5140.0000 1043.00000
                                                           100.00
                                                -1.000000
  2 SDM
                                                 1.000000
                                                             117.38
            16200.0000 -1043.00000
  3 SDM
                                                -1.000000
          5140.0000 1190.28787
                                                           140.63
  4 SDM
                                                 1.000000
 IMG SD
              Infinity
                                                 1.000000
 DECENTER / TILTS :
              #
                                                             BDE
                                                                        CDE TLM TSEQ
                                                        0.0000
                                                                    0.0000 DAR XYZABC
                                                          0.0000
                                                                    0.0000 DAR XYZABC
                                                          0.0000
                                                                     0.0000 DAR XYZABC
  3
                                                          0.0000
                                                                    0.0000 DAR XYZABC
0.0000 NAX XYZABC
   4
                                                         0.0000
   5
 PARAXIAL DATA AT INFINITE CONJUGATES:
                                                                   2663.38715
                                            SH1 (Princ.Plane 1)
   EFT.
                         2272.56532
    FNO
                             11.36283
                                            SH2 (Princ.Plane 2)
                                                                    -970.27746
    EPD (Entr.Pup.Dia.)
                             200.0000
```

# Herrig Three-mirror Schiefspiegler Telescope, Variant 1: Sect. 43.8.2, figure 43-57

#	TYPE	RADI	US DIST	ANCE GLASS		INDEX APE	E – Y	
OBJ	S	Infini	ty 0.10000	E+21	1.0	00000 0.	.00	
STO:	>SDM	36923.07	69 -843.2	7692	-1.0	00000 100.	.00	
2	SDM	5692.30	77 862.8	7692	1.0	00000 108.	.09	
3	SDM	36923.07	69 -915.3	2308	-1.0	00000 81.	64	
4	SDM	7230.76	92 1128.9	2308	1.0	00000 59.	31	
IMG	SD	Infini	ty		1.0	00000 8.	.56	
DECE	ENTER	/ TILTS :						
#		XDE	YDE	ZDE	AD	E BDE	CDE	TLM TSEQ
1		0.0000	0.0000	0.0000	12.000	0.0000	0.0000	DAR XYZABC
2		0.0000	-375.4462	0.0000	21.100	0.0000	0.0000	DAR XYZABC
3		0.0000	-91.6815	0.0000	12.145	0.0000	0.0000	DAR XYZABC
4		0.0000	-189.2769	0.0000	14.967	0.0000	0.0000	DAR XYZABC
5		0.0000	309.7538	0.0000	20.355	0.0000	0.0000	NAX XYZABC
PARA	AXIAL	DATA AT INF	INITE CONJU	GATES:				
E	EFL		2397	.88149	SH1 (Pri	nc.Plane 1)	1959.00	347
E	NO		11	.98941	SH2 (Pri	nc.Plane 2)	-1133.88	686
E	EPD (E	Entr.Pup.Dia	.) 20	0.0000				

# Herrig Three-mirror Schiefspiegler Telescope, Variant 2: Sect. 43.8.2, figure 43-57

# TYPE OBJ S STO>SDM 2 SDM 3 SDM 4 SDM IMG SD	RADIUS Infinity 90823.6364 6661.8182 90823.6364 11030.9091 Infinity	0.10000E+2 -970.0000 957.4727 -1005.0727 1243.0000	1 0 3 3	1.00000 -1.00000 -1.00000 -1.00000 -1.00000 1.00000	0 0.00 100.00 0 105.71 0 80.75 0 54.64		
DECENTER # 1 2 3 4 5	0.0000	YDE 0.0000 -278.1455 89.4000 179.3473 -212.8727	ZDE 0.0000 0.0000 0.0000 0.0000	ADE 8.0000 18.5000 7.9430 -11.3140 -15.0000	BDE 0.0000 0.0000 0.0000 0.0000 0.0000	CDE TLM 0.0000 DAR 0.0000 DAR 0.0000 DAR 0.0000 DAR 0.0000 NAX	XYZABC XYZABC XYZABC XYZABC
EFL FNO	DATA AT INFIN	2816.62 14.08 200.0	580 313	SH1 (Princ.P. SH2 (Princ.P.	lane 1) lane 2)	1942.34107 -1466.41112	

# Herrig Three-mirror Schiefspiegler Telescope, Variant 3: Sect. 43.8.2, figure 43-57

# TYPE OBJ S STO>SDM 2 SDM 3 SDM 4 SDM IMG SD	18100.0000 18100.0000	0.10000E+21 -1521.70000 1568.66000 -1549.14000 2316.60048	GLASS	INDEX 1.000000 -1.000000 1.000000 -1.000000 1.000000	0.00 100.00 211.42 161.51	
PICKUPS :						
2 PIK	CUY 1 C	0.000				
2 PIK	ASP 1					
4 PIK	CUY 1 C	0.000				
4 PIK	ASP 1					
DECENTER	,					
#	XDE	YDE	ZDE	ADE	BDE	CDE TLM TSEQ
1	0.0000	0.0000	0.0000	8.0000	0.0000	0.0000 DAR XYZABC
2	0.0000	-494.4200	0.0000	10.4000	0.0000	0.0000 DAR XYZABC
3	0.0000	-379.2400	0.0000	6.0190	0.0000	0.0000 DAR XYZABC
4	0.0000	-592.4800	0.0000	11.4170	0.0000	0.0000 DAR XYZABC
5	0.0000	28.0000	0.0000	13.7560	0.0000	0.0000 NAX XYZABC
PARAXIAL	DATA AT INFIN	NITE CONJUGATES	3:			
EFL		3117.9002	25	SH1 (Princ.Pl	ane 1)	3330.72598
FNO		15.5895	0	SH2 (Princ.Pl	ane 2)	-702.25577
EPD (E	ntr.Pup.Dia.)	200.000	0.0			

### Yolo Telescope: Sect. 43.8.3

# TYP	E RADIUS	DISTANCE	GLASS	INDEX	APE-
OBJ S	Infinity	0.10000E+21		1.000000	0.00
STO>ADM	-8584.0000	-1320.00000		-1.000000	100.00
2 ADM	8292.4107	1724.73498		1.000000	80.50
	8148.6940				
IMG SD	Infinity			1.000000	16.00

### ASPHERES:

#	Type	K	A	В	C
1	EVEN	-8.6241439170	-0.77173823E-12	0.0000000E+00	0.0000000E+00
2	דאים עים	0 100006665.03	_0 20244222E-10	0 0000000000000000000000000000000000000	0 0000000000000000000000000000000000000

# DECENTER / TILTS :

#	XDE	YDE	ZDE	ADE	BDE	CDE TLM TSEQ
1	0.0000	0.0000	0.0000	4.7000	0.0000	0.0000 BEN XYZABC
2	0.0000	0.0000	0.0000	3.5838	0.0000	0.0000 BEN XYZABC
3	0.0000	0.0000	0.0000	-1.4146	0.0000	0.0000 NAX XYZABC

### PARAXIAL DATA AT INFINITE CONJUGATES:

EFL	2500.00000	SH1	(Princ.Plane 1	795.90848
FNO	12.50000	SH2	(Princ.Plane 2	768.87232
EPD (Entr.Pup.Dia.)	200.0000			

Kutter Tri-Schiefspiegler Telescope	: Sect. 43.9.1

# TYPE OBJ S STO>SDM 2 SDM 3 SDM IMG SD	RADIUS Infinity -4130.0400 -6025.1340 -33268.9200 Infinity	DISTANCE 0.10000E+21 -1028.70000 664.21000 -866.73104		INDE: 1.000000 -1.000000 1.000000 -1.000000	0.00 100.00 56.44 0 45.13		
DECENTER	/ TILTS :						
#	XDE	YDE	ZDE	ADE	BDE	CDE T	TLM TSEQ
1	0.0000	0.0000	0.0000	5.1600	0.0000	0.0000 E	BEN XYZABC
2	0.0000	0.0000	0.0000	-15.2000	0.0000	0.0000 E	BEN XYZABC
3	0.0000	0.0000	0.0000	-34.9400	0.0000	0.0000 E	BEN XYZABC
4	0.0000	0.0000	0.0000	8.7407	0.0000	0.0000 N	IAX XYZABC
EFL FNO	DATA AT INFINI ntr.Pup.Dia.)	TE CONJUGATE 2983.673 14.918 200.00	17 37	SH1 (Princ.P. SH2 (Princ.P.		-674.4996 2115.8913	

Buchroeder Tri-Schiefspiegler Telescope:				Sect. 43.9.1	
# TYPE	RADIUS	DISTANCE	GLASS	INDEX	APE-Y

OBJ S	Infinity	0.10000E+21		1.000000	0.00		
STO>SDM	-4762.5000	-1357.31250		-1.000000	100.00		
2 SDM	-4762.5000	1062.13687		1.000000	48.38		
3 SDM	-33281.2500	-701.80165		-1.000000	36.65		
IMG SD	Infinity			-1.000000	14.08		
DECENTER	/ TILTS :						
#	XDE	YDE	ZDE	ADE	BDE	CDE T	LM TSEQ
1	0.0000	0.0000	0.0000	3.1500	0.0000	0.0000 B	EN XYZABC
2	0.0000	0.0000	0.0000	-9.6000	0.0000	0.0000 B	EN XYZABC
3	0.0000	0.0000	0.0000	-38.5500	0.0000	0.0000 B	EN XYZABC
4	0.0000	0.0000	0.0000	9.0195	0.0000	0.0000 N	AX XYZABC
PARAXIAL	DATA AT INFINI	TE CONJUGATE	S:				
EFL		4001.089	03	SH1 (Princ.P)	lane 1)	-1553.3185	1
FNO EPD (E	ntr.Pup.Dia.)	20.005		SH2 (Princ.Pl	lane 2)	3297.8727	7
(2		200.00					

Brunn Four-mirror Schiefspiegler Telescope:	Sect. 43.9.2

# TYPE	RADIUS	DISTANCE	GLASS	INDEX	APE-Y		
OBJ S STO>SDM 2 SDM 3 SDM 4 SDM IMG SD	Infinity -5600.0000 -5200.0000 -5200.0000 Infinity Infinity	1440.00000 -480.00000		1.000000 -1.000000 1.000000 -1.000000 1.000000	53.92 37.23 30.10		
DECENTER / # 1 2 3 4 5	XDE 0.0000 0.0000 0.0000 0.0000 0.0000	0.0000 0.0000 0.0000	ZDE 0.0000 0.0000 0.0000 0.0000	ADE -3.2500 7.2700 6.8200 34.0000 7.7384	BDE 0.0000 0.0000 0.0000 0.0000 0.0000	CDE TLM 0.0000 BEN 0.0000 BEN 0.0000 BEN 0.0000 BEN 0.0000 NAX	XYZABC XYZABC XYZABC XYZABC
EFL FNO	DATA AT INFINI	TE CONJUGATES 3805.0820 19.0254 200.000	2	SH1 (Princ.Pl SH2 (Princ.Pl		3274.62206 -3370.18977	

Stevi	ck–Pa	ul Four-mirror S	chiefspiegler 1	Telesco	pe: Sect. 4	3.9.2			
OBJ STO: 2 3 4	SDM AD SDM SDM SDM	RADIUS Infinity -5015.1268 -2499.2572 Infinity -2187.7779 Infinity Infinity	-1432.56000 1200.00000 710.00000 -730.25000	GLASS	1.00000 -1.00000 1.00000 1.00000 -1.00000 1.00000	0.00 100.00 45.73 200.00 62.48 30.28			
#	HERES: Type EVEN		K	A	B 0.00000000E+00	0.000000	C		
	EVEN	0.00000000			0.0000000E+00	0.000000			
DEC	ENTER	/ TILTS :							
#		XDE	YDE	ZDE	ADE	BDE	CDE	TLM	TSEQ
1		0.0000	0.0000	0.0000	-3.0400	0.0000	0.0000	BEN	XYZABC
2		0.0000	0.0000	0.0000	5.5369	0.0000	0.0000	BEN	XYZABC
3		0.0000	-50.0000	0.0000	0.0000	0.0000	0.0000	DAR	XYZABC
4		0.0000	0.0000	0.0000		0.0000	0.0000	BEN	XYZABC
5		0.0000	0.0000	0.0000		0.0000	0.0000	BEN	XYZABC
6		0.0000	0.0000	0.0000	9.0001	0.0000	0.0000	NAX	XYZABC
	AXIAL EFL	DATA AT INFINI	TE CONJUGATE:		SH1 (Princ.Pl	ane 1)	11163.548	21Ω	
	FNO		14.272		SH2 (Princ.Pl		-2664.80		
		Entr.Pup.Dia.)	200.00		onz (rrine.rr	unc 2)	2004.00.	550	
Shafe	er Thro	ee-mirror Schiefs	sniegler Telesc	cone.	Sect. 4	394			
Julian	J. 11111	ocor ociliers	piogici icies	oope.	0001. 4	0.0.7			

Shafer Three-mirror Schiefspiegler Telescope:				Sect	. 43.9.4		
# TYPE	RADIUS	DISTANCE	GLASS	IND	EX APE-Y		
OBJ S	Infinity	0.10000E+21		1.0000	0.00		
STO>SDM	-4799.9999	-1599.99996		-1.0000	00 100.00		
2 SDM	-11847.6077	200.00000		1.0000	00 36.36		
3 SDM	-11821.9237	-645.48223		-1.0000	00 28.77		
IMG SD	Infinity			-1.0000	0.04		
DECENTER / # 1 2 3 4	XDE 0.0000 0.0000 0.0000 0.0000	YDE 0.0000 0.0000 0.0000 0.0000	ZDE 0.0000 0.0000 0.0000 0.0000	ADE 3.0000 -22.5000 -22.5000 7.5813	BDE 0.0000 0.0000 0.0000 -0.0004	CDE TLM 0.0000 BEN 0.0000 BEN 0.0000 BEN 0.0000 NAX	XYZABC XYZABC XYZABC
PARAXIAL I	ATA AT INFINI	TE CONJUGATES	5:				
EFL		2471.6089			Plane 1)	107.66597	
FNO		12.3580	04	SH2 (Princ.	Plane 2)	1825.89113	
EPD (Er	ntr.Pup.Dia.)	200.000	0.0				

Solano Three	-mirror Schief	sniegler Teles	cone.	Sect. 4	395		
			•				
# TYPE	RADIUS	DISTANCE	GLASS	INDEX 1.000000 -1.000000 1.000000 -1.000000	APE-Y		
OBJ S	Infinity	0.10000E+21		1.000000	0.00		
STO>SDM	-7180.0000	-1300.00000		-1.000000	100.00		
2 SDM	9844.2500	1262.50000		1.000000	68.44		
3 SDM	9844.2500	-320.32818		-1.000000	27.15		
IMG SD	Infinity			-1.000000	9.38		
DECENTER /	TILTS :						
#	XDE	YDE	ZDE	ADE 4.2000 3.2300 41.2200	BDE	CDE TLM	TSEQ
1	0.0000	0.0000	0.0000	4.2000	0.0000	0.0000 BEN	XYZABC
2	0.0000	0.0000	0.0000	3.2300	0.0000	0.0000 BEN	XYZABC
3	0.0000	0.0000	0.0000	41.2200	0.0000	0.0000 BEN	XYZABC
4	0.0000	0.0000	0.0000	6.6996	0.0000	0.0000 NAX	XYZABC
PARAXIAL DA	ATA AT INFINI	TE CONJUGATE	S:		- 1		
EFL		2609.337	43	SH1 (Princ.Pl	ane 1)	-492.51537	
FNO EPD (Ent	r Pun Dia )	13.046	69 00	SH1 (Princ.Pl	ane 2)	2289.43800	
Shafer Four-	mirror Schiefs	piegler Telesc	ope:	Sect. 4	3.10.2		
# TYPE	RADIUS	DISTANCE	GLASS	INDEX 1.000000	APE-Y		
OBJ S	Infinity	0.10000E+21		1.000000	0.00		
1>SMD	1502.6000	-676.78777		-1.000000 1.000000	112.81		
STO SMD	1775.3680	705.68027		1.000000	190.08		
3 SMD	3206.6872	-1058.75800		1.000000	149.10		
4 SMD	2272.4330	1153.80871					
IMG SD	1502.6000 1775.3680 3206.6872 2272.4330 Infinity			1.000000	29.53		
DECENTER /	TILTS :						
#	XDE	YDE	ZDE	ADE	BDE	CDE TLM	TSEQ
1	0.0000	0.0000	0.0000	-16.4400	0.0000	0.0000 BEN	XYZABC
2	0.0000	0.0000	0.0000	12.0000	0.0000	0.0000 BEN	XYZABC
3	0.0000	0.0000	0.0000	-15.9400	0.0000	0.0000 BEN	XYZABC
5	0.0000	0.0000	0.0000	ADE -16.4400 12.0000 -15.9400 6.0000 4.4187	0.0000	0.0000 BEN	XYZABC
				4.4107	0.0000	0.0000 WH	711 DADC
PARAXIAL DA	ATA AT INFINI	TE CONJUGATE	S:	SH1 (Princ.Pl	ano 1)	1447 35463	
ELT		4 270	22	CIIO (Princ.Pl	ane 1)	298.43777	
EPD (Ent	r.Pup.Dia.)	200.00	00	SH1 (Princ.Pl SH2 (Princ.Pl	ane 2)	230.43777	
				lay:		n 2	
						··-	
# TYPE	RADIUS	DISTANCE	GLASS	INDEX 1.000000 -1.000000	APE-Y		
OBJ S	1011111ty	1170 50000		1.000000	0.00		
1>SM 2 DSM	-2002.4129	-1170.58260 370.85590		1 000000	290.59		
	13695.3702	370.85590		1.000000			
3 SMD	422 0162	-234.66/53		-1.000000	36.32		
4 DSM STO DSM	422.0163	-234.66753 207.61599 -207.61599 401.68601		-1.000000 1.000000 -1.000000	137.28		
6 DSM	422 0163	401.61599		1.000000	127 00		
	Infinity	401.00001		1.000000	137.03		
				1.000000	13.21		
DECENTER /							
#	XDE	YDE	ZDE	ADE	BDE	CDE TLM	TSEQ
2	0.0000	0.0000	0.0000	-6.5000	0.0000	U.UUUOO DAR	XYZABC
3	0.0000 -	100 7420	0.0000	-9.5000	0.0000	0.0000 DAR	AYZABC
4 5	0.0000 -	198./439	0.0000	0.0000	0.0000	0.0000 DAR	AIZABC
6	0.0000 -	100 7/20	0.0000	0.0000	0.0000	0.0000 DAR	AIZABC
7	0.0000 -	275 0000	0.0000	ADE -6.5000 -9.5000 0.0000 0.0000 0.0000 -7.6781	0.0000	0.0000 DAR 0.0000 NAX	AIAABC
/	0.0000 -	2/3.0000	0.0000	-/.0/81	0.0000	U.UUUU NAX	AIZABC
	ATA AT INFINI						
EFL		-816.000	00	SH1 (Princ.Pl	ane 1)	-4406.33925	
FNO		-3.295		SH2 (Princ.Pl	ane 2)	1227.67681	
EPD (Ent	tr.Pup.Dia.)	200.00	UU				

Kebo Afocal Four-mirror Telescope: Sect. 43.10.3								
# TYPE	RADIUS	DISTANCE	GLASS	INDEX	APE-Y			
OBJ S		0.10000E+21	GLINDO	1.000000	0.00			
STO>SD	Infinity	2.25000		1.000000	0.50			
2 AM	-4.1056	-1.34369		-1.000000	0.20			
3 AMD	-1.5691	3.14859		1.000000	0.20			
4 AMD	-5.6910	-3.43660		-1.000000	0.20			
5 AMD	3.3216	1.80000		1.000000	0.20			
6 S	Infinity	999.52934		1.000000	0.20			
IMG SD	Infinity			1.000000	0.20			
ASPHERES:								
# Type	K		A	В		C		
2 EVEN	-0.9440738982			0.0000000E+00	0.000000			
3 EVEN	-1.2255146740			0.0000000E+00	0.000000			
4 EVEN	-2.1160937570			0.0000000E+00	0.000000			
5 EVEN	0.2309119409	0.0000000	DE+00	0.0000000E+00	0.000000	00E+00		
DECENTER	/ TILTS :							
#	XDE	YDE	ZDE	ADE	BDE	CDE TLM TSEQ		
1	0.0000	1.8000	0.0000		0.0000	0.0000 DAR XYZABC		
3	0.0000	0.0000	0.0000	-1.4900	0.0000	0.0000 DAR XYZABC		
4	0.0000	0.0000	0.0000		0.0000	0.0000 DAR XYZABC		
5	0.0000	0.0000	0.0000		0.0000	0.0000 DAR XYZABC		
7	0.0000	0.0000	0.0000	-0.7538	0.0000	0.0000 NAX XYZABC		
	DATA AT INFINIT	E CONJUGATES	5:					
MAG (1	Magnification)	-5.1260	9	SH1 (Princ.Pla	ane 1)	-1160.07995		
EPD (I	Entr.Pup.Dia.)	1.000	0.0	SH2 (Princ.Pla	ane 2)	225.83848		

Cook TMA Telescope, Variant 1: Sect. 43.11.1								
# TYPE		DISTANCE	GLASS					
OBJ S	Infinity			1.000000	0.00			
STO>SD	Infinity			1.000000				
2 AM		-750.00000		-1.000000				
3 AM		700.00000		1.000000				
4 AM	-995.1093	-1405.88321		-1.000000	410.94			
IMG SD	Infinity			-1.000000	68.21			
ASPHERES	:							
# Type		K	A	В		C		
2 EVEN								
3 EVEN	-0.42241045E+0	2 0.00000000	E+00	0.0000000E+00	0.000000	00E+00		
4 EVEN	-0.091265237	9 0.00000000	DE+00	0.0000000E+00	0.000000	00E+00		
	/							
DECENTER	,							
#	XDE	YDE	ZDE		BDE	CDE TLM TSEQ		
1		200.0000	0.0000		0.0000	0.0000 DAR XYZABC		
5	0.0000	0.0000	0.0000	-0.7538	0.0000	0.0000 NAX XYZABC		
PARAXIAL	DATA AT INFINI	TE CONJUGATES	3:					
EFL		-960.0720	)1	SH1 (Princ.Pla	ane 1)	-2657.04365		
FNO		-5.3337	73	SH2 (Princ.Pla		-2366.06829		
	Entr.Pup.Dia.)	180.000		. ,	,	<del></del>		
212 (		100.000						

### Cook TMA Telescope, Variant 2: Sect. 43.11.1 # TYPE RADTUS DISTANCE GLASS INDEX APE-Y RADIUS DISTANCE Infinity 0.10000E+21 1.000000 OBJ S 0.00 1.000000 50.00 Infinity -240.00000 921.7600 -1360.00000 STO>SD 3 AM 1738.8000 3400.00000 4 AM -1691.5387 -1650.65543 IMG SD Infinite 2 AM -1.000000 80.00 1.000000 80.00 -1.000000 80.00 -1.000000 80.00 ASPHERES: K 4 EVEN 0.9782004353 0.19063321E-10 0.14980268E-16 0.68497511E-24 DECENTER / TILTS : XDE YDE ZDE ADE BDE CDE TLM TSEQ 0.0000 0.0000 0.0000 0.0000 0.0000 DAR XYZABC 0.0000 0.0000 0.1465 0.0000 0.0000 NAX XYZABC XDE YDE ZDE ADE BDE CDE TIM TSEO # PARAXIAL DATA AT INFINITE CONJUGATES: -400.00000 SH1 (Princ.Plane 1) -601.52840 SH2 (Princ.Plane 2) -2049.11803 -601.52840 FNO -4.00000 EPD (Entr.Pup.Dia.) 100.0000 Hallam Non- re-imaging TMA Telescope: Sect. 43.11.3 INDEX APE-Y 1.000000 0.00 -1.000000 929.19 RADIUS DISTANCE GLASS # 11FB OBJ S Infinity 0.1000U6+21 1>SM 2024.3779 -1729.84305 2 AM 4048.7558 1954.77392 STO SD Infinity 997.99580 Infinity 0.10000E+21 1.000000 1076.41 1.000000 202.44 -1.000000 596.09 Infinity 997.99580 -4048.7558 -1412.46751 4 SM -1.000000 IMG SD Infinity -1.000000 254.64 ASPHERES: K В # Type K A B C 2 EVEN -0.7290570000 0.00000000E+00 0.00000000E+00 # Type DECENTER / TILTS : XDE YDE ZDE ADE BDE CDE TLM TSEQ 0.0000 0.0000 0.0000 15.0000 0.0000 0.0000 DAR XYZABC 0.0000 562.3272 0.0000 -2.4107 0.0000 0.0000 NAX XYZABC # 3 5 PARAXIAL DATA AT INFINITE CONJUGATES:

SH1 (Princ.Plane 1) 1631.51560 SH2 (Princ.Plane 2) -573.07890

849.20350

4.24602

200.0000

FNO

EPD (Entr.Pup.Dia.)

Korsch Three-mirror Two-axis Telescope: Sect. 43.12.1								
# TYPE	RADIUS	DISTANCE	GLASS	INDEX	APE-Y			
OBJ S	Infinity	0.10000E+21		1.000000	0.00			
STO>AM		-370.48000		-1.000000	100.00			
2 AM	-169.2660	598.92829		1.000000	20.72			
3 AM	-206.8570	-122.66686		-1.000000	55.39			
4 SMD	Infinity	81.50514		1.000000	10.00			
IMG S	Infinity			1.000000	33.00			
ASPHERES:								
# Type	K		A	В		C		
1 EVEN	-0.9703196781	0.0000000	DE+00 0	0.0000000E+00	0.0000000	0E+00		
2 EVEN	-1.7452723280	0.00000000	DE+00 0	.0000000E+00	0.0000000	0E+00		
3 EVEN	-0.5594873649	0.0000000	DE+00 0	0.0000000E+00	0.0000000	0E+00		
DECENTER	/ TILTS :							
#	XDE	YDE	ZDE	ADE	BDE	CDE TLM	1 TSEQ	
4	0.0000	0.0000	0.0000	45.0000	0.0000	0.0000 BEN	I XYZABC	
EFL FNO	DATA AT INFINIT	E CONJUGATES -2400.0000 -12.0000 200.000	00	SH1 (Princ.Pla SH2 (Princ.Pla		72826.02219 2481.50347		

Paul-Schm	idt Four-mirror T	wo-axis Teles	scope, V	ariant 1:	Sect. 43.1	2.2
# TYPE	RADIUS	DISTANCE	GLASS	II	NDEX APE-Y	
OBJ S	Infinity	0.10000E+21		1.000	0.00	
STO>AM	-600.0000	-225.00000		-1.000	0000 100.00	
2 AM	-300.0000	150.00000		1.000	0000 24.69	
3 XD	Infinity	0.00000		1.000	0.00	
4 SM	Infinity	0.00000		-1.000	0000 4.59	
5 XD	Infinity	-170.00000		-1.000	0.00	
6 AM	340.0000	290.00000		1.000	0000 34.73	
7 AM	-600.0000	-300.00214		-1.000	0000 28.43	
IMG S	Infinity			-1.000	0000 1.85	
ASPHERES:						
# Type		K	A	F	3	C D
1 EVEN	0.000000000			_	_	00 0.0000000E+00
2 EVEN						14 0.0000000E+00
6 EVEN						15 0.1699343E-18
						14 0.8626815E-18
	/ TILTS :					
#	XDE	YDE	ZDE	ADE	BDE	CDE TLM TSEQ
3	0.0000	0.0000	0.0000	45.0000	0.0000	0.0000 NAX XYZABC
5	0.0000	0.0000	0.0000	45.0000	0.0000	0.0000 NAX XYZABC
PARAXIAL	DATA AT INFINI	TE CONJUGATE	S:			
EFL		-1058.823		SH1 (Princ	c.Plane 1)	-4801.03806
FNO		-5.294			c.Plane 2)	-1358.82353
EPD (E	Entr.Pup.Dia.)	200.00	00	,	*	

Paul-Schmidt Four-mirror Two-axis Telescope, Variant 2: Sect. 43.12.2							
# TYPE RADIUS DISTANCE GLASS INDEX APE-Y OBJ S Infinity 0.10000E+21 1.000000 0.00 STO>AM -600.0000 -225.00000 -1.000000 100.00 2 AM -150.0000 262.50000 1.000000 24.56 3 AM -312.5000 -137.50000 -1.000000 22.53 4 SMD Infinity 152.67750 1.000000 3.32 5 AM -187.5000 -312.50650 -1.000000 21.72 6 S Infinity -0.00037 -1.000000 3.82 IMG S -240.0000 -3.00000 -1.000000 3.82							
ASPHERES: # Type							
DECENTER / TILTS : # XDE YDE ZDE ADE BDE CDE TLM TSEQ 4 0.0000 0.0000 0.0000 45.0000 0.0000 0.0000 BEN XYZABC							
PARAXIAL DATA AT INFINITE CONJUGATES:  EFL -1458.37222 SH1 (Princ.Plane 1) -8580.85371  FNO -7.29186 SH2 (Princ.Plane 2) -1458.37156  EPD (Entr.Pup.Dia.) 200.0000							
Schmidt Telescope with Achromatic Corrector Plate: Sect. 43.13.2							
# TYPE RADIUS DISTANCE GLASS INDEX APE-Y OBJ S Infinity 0.10000E+21 1.000000 0.00 1>A 91973.3680 10.00000 N-F2 1.624089 100.61 2 S Infinity 1.00000 1.000000 100.08 STO S Infinity 10.00000 N-BK7 1.518726 100.00 4 A 74394.0578 1000.00000 1.000000 100.57 5 SM -1000.0000 -500.03320 -1.000000 187.53 IMG S -495.5069							
ASPHERES: # Type K A B C 1 EVEN 0.0000000000 0.34289002E-10 -0.12429877E-14 -0.38378518E-19 4 EVEN 0.0000000000 0.51714223E-09 -0.42885572E-15 -0.57780336E-19							
PARAXIAL DATA AT INFINITE CONJUGATES:  EFL 500.00000 SH1 (Princ.Plane 1) 1013.78967  FNO 2.49988 SH2 (Princ.Plane 2) -0.04662  EPD (Entr.Pup.Dia.) 200.0000							
Wright-Wäisälä Telescope Sect. 43.13.3							
# TYPE RADIUS DISTANCE GLASS INDEX APE-Y OBJ S Infinity 0.10000E+21 1.000000 0.00 STO>S Infinity 11.67789 N-BK7 1.518726 100.00 2 A Infinity 520.00000 1.000000 100.02 3 AM -1000.0000 -499.98006 -1.000000 101.94 IMG S Infinity -1.000000 8.57							
ASPHERES: # Type							
PARAXIAL DATA AT INFINITE CONJUGATES:  EFL 500.00000 SH1 (Princ.Plane 1) 527.68927  FNO 2.50000 SH2 (Princ.Plane 2) 0.00000  EPD (Entr.Pup.Dia.) 200.0000							

#### Bouwers-Cassegrain with Weak Corrector Lens: Sect. 43.13.4

#	TYPE	RADIUS	DISTANCE	GLASS	INDEX	APE-Y
OBJ	S	Infinity	0.10000E+21		1.000000	0.00
STO	>S	10112.0427	10.16000	N-BK7	1.518726	100.00
2	S	-5328.8337	280.97000		1.000000	100.01
3	S	-393.4012	40.63700	N-BK7	1.518726	97.91
4	S	-469.7111	553.87550		1.000000	101.34
5	SM	-800.0000	-240.00000		-1.000000	107.24
6	SM	-773.4724	284.15143		1.000000	45.38
IMG	S	Infinity			1.000000	4.89

PARAXIAL DATA AT INFINITE CONJUGATES: 699.99920 EFL 3.50000 EPD (Entr.Pup.Dia.) 200.00000

Baker-Nunn Camera: Sect. 43.13.5

#	TYPE	RADIUS	DISTANCE	GLASS	INDEX	APE-Y
OBJ	S	Infinity	0.10000E+21		1.000000	0.00
1:	>S	-5277.3787	26.40498	LLF1	1.550985	285.01
2	A	-2269.2710	105.37081		1.000000	283.03
STO	A	-3270.7870	15.94263	SK3	1.611272	244.97
4	A	3270.7870	105.37081		1.000000	251.95
5	A	2269.2710	26.40498	LLF1	1.550985	297.21
6	S	5277.3787	915.95380		1.000000	299.16
7	SM	-1046.9823	-547.07488		-1.000000	536.04
TMG	S	-512.4247			-1.000000	129.61

ASPHERES:

K A B C C 0.0000000000 -0.40612765E-09 0.17596461E-15 0.00000000E+00 # Type 2 EVEN 3 EVEN 0.0000000000 -0.62710956E-09 -0.33236090E-15 -0.14307651E-20 4 EVEN 0.000000000 0.62710956E-09 0.33236090E-15 0.14307651E-20 5 EVEN 0.000000000 0.40612765E-09 -0.17596461E-15 0.00000000E+00

PARAXIAL DATA AT INFINITE CONJUGATES:

SH2 (Princ.Plane 1) 1126.32610 SH2 (Princ.Plane 2) -47 00070 500.00000 1.00000 EPD (Entr.Pup.Dia.) 500.00000

#### Wynne Camera: Sect. 43.13.6

#	TYPE	RADIUS	DISTANCE	GLASS	INDEX	APE-Y
OBJ	S	Infinity	0.10000E+21		1.000000	0.00
1:	>S	3181.3457	66.00000	BK7	1.518721	175.91
2	S	4461.8494	88.08000		1.000000	167.29
3	S	307.5855	123.84000	BK7	1.518721	144.74
4	S	215.5057	155.28000		1.000000	109.67
STO	S	Infinity	192.00000		1.000000	89.52
6	S	-188.2483	63.36000	BK7	1.518721	124.34
7	S	-221.2859	340.08000		1.000000	147.69
8	SM	-606.7200	-339.37872		-1.000000	229.87
IMG	S	-246.9984			-1.000000	47.75

PARAXIAL DATA AT INFINITE CONJUGATES:

275.00062 SH1 (Princ.Plane 1) 1001.00350 EFL 1.37500 SH2 (Princ.Plane 2) EPD (Entr.Pup.Dia.) 200.00000

EFL

FNO

EPD (Entr.Pup.Dia.)

#### Baker Super-Schmidt Telescope: Sect. 43.13.7 # TYPE RADTIIS DISTANCE GLASS INDEX APE-Y OBJ S Infinity 0.10000E+21 1 000000 0 00 418.01 365.47 250.42 108.71200 BK7 571.5000 485.9020 1>S 1.518721 2 S 1.000000 1.624078 501.65000 35.56000 F2 33.02000 SK2 STO A -299288.2000 -3441.7000 1.609935 256.83 4 S 5 S Infinity 607.56800 1.000000 607.56800 108.71200 BK7 6 S -744.4740 1.518721 7 S -823.4680 637.54000 1.000000 498.70 8 SM -1397.0000 -637.54000 -1.000000 -823.4680 9 S -108.71200 BK7 -1.518721 304.60 10 S -744.4740 -36.80037 -1.000000 241.52 IMG S -616.1092 -1.000000 ASPHERES: # Type K A В 0.000000000 -0.34051249E-10 0.23079226E-15 0.00000000E+00 PARAXIAL DATA AT INFINITE CONJUGATES. SH1 (Princ.Plane 1) 1873.65195 EFT. 613.44135 FNO 1.20000 SH2 (Princ.Plane 2) 576.58537 EPD (Entr.Pup.Dia.) 511 201 Schmidt-Cassegrain Telescope, Long: Sect. 43.13.7 APE-Y # TYPE RADTIIS DISTANCE GLASS INDEX Infinity 0.10000E+21 Infinity 12.00000 1.000000 OBJ S 0 00 12.00000 N-BK7 1.518726 100.00 STO>S 2 A Infinity 689.26280 1.000000 100.02 -367.86853 3 AM -1013.1842 -1.000000 101.94 4 AM -371.5625 547.66795 1.000000 30.05 IMG S -151.4390 1.000000 8.57 ASPHERES: # Type 2 EVEN 0.90565428E+08 0.14520388E-10 -0.49775246E-18 0.00000000E+00 -1.0000000000 0.00000000E+00 0.00000000E+00 0.00000000E+00 -3.0973174770 0.00000000E+00 0.00000000E+00 0.00000000E+00 3 EVEN PARAXIAL DATA AT INFINITE CONJUGATES: EFL. 2000.00000 SH1 (Princ.Plane 1) SH2 (Princ.Plane 2) -3263.06921 FNO 10.00000 -1452.32632 EPD (Entr.Pup.Dia.) 200 000 Schmidt-Cassegrain Telescope, Short: Sect. 43.13.7 APE-Y AP # TYPE RADIUS DISTANCE GLASS INDEX Infinity 0.10000E+21 Infinity 11.67789 Infinity 389.26284 OBJ S 1.000000 0.00 11.67789 N-BK7 389.26284 1.518726 100.00 1>S 1.000000 2 A STO AM -1013.1196 -367.86853 -1.000000 100.01 547.57478 4 AM -371.4679 1.000000 30.05 TMG S 1.000000 -149.7523 8.57 ASPHERES. # Type 2 EVEN 0.90565430E+08 0.16987886E-10 -0.25868864E-17 0.00000000E+00 3 EVEN -1.000000000 0.0000000E+00 0.00000000E+00 0.00000000E+00 4 EVEN -3.1441615440 0.00000000E+00 0.00000000E+00 0.00000000E+00 PARAXIAL DATA AT INFINITE CONJUGATES:

2000.00000

10.00000

200.000

SH1 (Princ.Plane 1)

SH2 (Princ.Plane 2) -1452.41897

-3564.28972

#### Schmidt-Cassegrain Telescope, Flat-field: Sect. 43.13.7 APE-Y # TYPE RADIUS DISTANCE GLASS INDEX 1.000000 OBJ S Infinity 0.10000E+21 0.00 11.67789 N-BK7 1>S Infinity 2 A 389.26284 Infinity 1.000000 103.60 STO AM -800.0000 -220.00000 327.25515 -1.000000 100.20 -800.0000 Infinity 1.000000 47.28 4 AM IMG S 3.82 ASPHERES: # Type В 2 EVEN 0.90565413E+08 0.26338628E-09 -0.42146256E-15 0.00000000E+00 3 EVEN -1.000000000 0.00000000E+00 0.00000000E+00 0.00000000E+00 4 EVEN -0.18766917E+02 0.00000000E+00 0.00000000E+00 0.00000000E+00 PARAXIAL DATA AT INFINITE CONJUGATES: EFL 727.27273 3.63636 EPD (Entr.Pup.Dia.) 200.000

Schmidt-Cas	ssegrain Telesco	Sect. 43.1	3.7				
# TYPE	RADIUS	DISTANCE	GLASS	INI	DEX APE-Y		
OBJ S	Infinity	0.10000E+21		1.0000	0.00		
STO>S	Infinity	10.00000	N-BK7	1.5187	726 100.00		
2 A	Infinity	697.00000		1.0000	000 100.01		
3 AM	-650.0000	-211.25000		-1.0000	105.77		
4 SM	-650.0000	174.98912		1.0000	000 39.52		
IMG S	Infinity			1.0000	000 4.44		
ASPHERES:							
# Type	K		A		В	C	
2 EVEN	0.30970071E+08	0.11705115	E-08	0.34088591E-1	4 0.000000	00E+00	
3 EVEN	0.0061284814	0.00000000	E+00	0.0000000E+0	0.000000	00E+00	
	ATA AT INFINIT		•	(- 1			
EFL		500.0000			Plane 1)		
FNO		2.5000		SH2 (Princ.	Plane 2)	-325.00000	
EPD (En	tr.Pup.Dia.)	200.00	0				

Sigler Teles	cope:	Sect. 43.13.9	1				
# TYPE OBJ S STO>SM 2 S 3 SM 4 S 5 S 6 S 7 S	-836.4113 103.4033 Infinity 103.4033 103.4033 -103.4033	16.37130 183.00170	GLASS BK7 BK7		INDEX 1.000000 -1.000000 -1.518726 1.518726 1.000000 1.518726 1.000000	6.55	
8 S 9 S IMG S	103.4033 -103.4033 Infinity	8.18560 172.14122	BK7		1.518726 1.000000 1.000000	14.48 14.55 4.78	
EFL FNO	DATA AT INFINIT	CONJUGATES -1066.8732 -7.1124 150.000	4 9	SH1 SH2	(Princ.Plane (Princ.Plane		-4791.62225 1239.01446

### Houghton Telescope: Sect. 43.13.10

# TYPE	RADIUS	DISTANCE	GLASS	INDEX	APE-Y	
OBJ S	Infinity	0.10000E+21		1.000000	0.00	
STO>S	5364.0423	16.00000	K10	1.503493	100.00	
2 S	579.8176	5.60000		1.000000	100.83	
3 S	641.3256	20.00000	N-SK2	1.609942	101.43	
4 S	3403.7815	1700.30474		1.000000	103.07	
5 SM	-1600.0000	-799.19495		-1.000000	126.65	
IMG S	Infinity			-1.000000	13.91	
PARAXIAL EFL FNO	DATA AT INFINI	TE CONJUGATES 800.0007 4.0000	8	(Princ.Plan	. ,	1727.93383
EPD (	Entr.Pup.Dia.)	200.000	0	 (	,	

Houghton–Cassegrain Telescope:			Sect. 43.13.12						
#	TYPE	RADIUS	DISTANCE	GLASS		INDEX	APE-Y		
OBJ	S	Infinity	0.10000E+21			1.000000	0.00		
STO>	S	1926.6457	20.00000	N-BK7		1.518726	100.00		
2	S	-1514.1602	1.99992		:	1.000000	99.68		
3	S	-979.3603	10.00000	N-BK7		1.518726	99.67		
4	S	6331.8708	435.00000		:	1.000000	99.23		
5	SM	-1212.6496	-420.00000		- 3	1.000000	103.14		
6	SM	-537.4139	599.89103		:	1.000000	35.35		
IMG	S	Infinity			-	1.000000	17.21		
PARA	XIAL D	ATA AT INFINI	TE CONJUGATES	:					
E	EFL		1970.0029	5	SH1 (1	Princ.Plan	e 1)	-2648.66597	
F	FNO		9.8500	1	SH2 (1	Princ.Plan	e 2)	-1370.00162	
E	EPD (Ent	tr.Pup.Dia.)	200.000	0					

Houghton-	-Cassegrain Tele	scope, Flat-fiel	d:	Sect. 43	.13.12			
# TYPE	RADIUS	DISTANCE	GLASS		INDEX	APE-Y		
OBJ S	Infinity				00000	0.00		
STO>S	16948.0008	22.50000	N-BK7	1.5	18726	100.00		
2 S	-694.1898	0.64536		1.0	00000	100.14		
3 S	-637.9974	5.00000	N-BK7	1.5	18726	100.14		
4 S	-14064.2159	1112.30000		1.0	00000	100.32		
5 SM	-1200.0000	-338.50000		-1.0	00000	119.71		
6 SM	-1200.0000	461.12343		1.0	00000	58.15		
IMG S	Infinity			1.0	00000	18.56		
PARAXIAL	DATA AT INFINI	TE CONJUGATES	:					
EFL		1063.1890	6	SH1 (Pri	.nc.Plar	ne 1)	530.44526	
FNO		5.3159	5	SH2 (Pri	nc.Plar	ne 2)	-602.02804	
EPD (1	Entr.Pup.Dia.)	200.000	0					

#### Buchroeder-Houghton Telescope: Sect. 43.13.11 RADIUS DISTANCE GLASS INDEX APE-Y OBJ S Infinity 0.10000E+21 1.000000 0.00 20.00000 N-BK7 STO>S 1532.8939 1.518726 100.00 99.95 2 S Infinity 3.43367 1.000000 -1516.7135 1.518726 16.00000 N-BK7 99 86 3 S 1516.7135 4 S 3 43367 1 000000 100 07 20.00000 N-BK7 5 S Infinity 1.518726 100.29 -1516.7135 1565.51251 -1579.7600 -789.71154 6 S 1.000000 100.68 -1579.7600 125.81 7 SM -1 000000 IMG S Infinity -1.000000 13.81 PARAXIAL DATA AT INFINITE CONJUGATES: EFL. 789.97607 SH2 (Princ.Plane 1) SH1 (Princ.Plane 1) 1609.69118 FNO 3.94988 0.25341 EPD (Entr.Pup.Dia.) 200.0000 Lurie-Houghton Telescope: Sect. 43.13.13 DISTANCE GLASS INDEX # TYPE RADTHS APE-Y OBJ S 1.000000 Infinity 0.10000E+21 0 00 23.52942 BK7 11.05215 STO>S 1234.9357 1.518726 100.00 1519.9065 -746.5408 -858.5993 1.000000 99.63 2 S 3 S 19.60785 BK7 1.518726 99.64 870.00410 4 S 1.000000 100.69 -1999.7981 -810.29040 Infinity 193.89954 116.34 47.12 17.45 5 SM -1.000000 1.000000 6 SDM IMG S Infinity 1.000000 DECENTER / TILTS : ZDE XDE YDE ADE BDE CDE TLM TSEQ 0.0000 0.0000 BEN XYZABC 0 0000 0 0000 0.0000 45.0000 PARAXIAL DATA AT INFINITE CONJUGATES: EFL 1000.00000 SH1 (Princ.Plane 1) 909.95411 5.00000 SH2 (Princ.Plane 2) FNO -806.10125 EPD (Entr.Pup.Dia.) 200.0000 Maksutov Telescope: Sect. 43.13.14 APE-Y AP CP DP TP MP GLB RADIUS DISTANCE GLASS # TYPE INDEX OBJ S Infinity 0.10000E+21 1.000000 0.00 1.000000 100.00 644.00774 STO>S Infinity 104.39 2 S -364.5742 43.32423 N-BK7 1.518726 3 S -389.7307 1023.04527 110.19 4 SM -1694.7572 -873.29461 -1.000000 122.11 IMG S Infinity -1.000000 5.59 PICKUPS : 4 PIK THI -3 0.0000 PARAXIAL DATA AT INFINITE CONJUGATES: 1641.78300 809.16036 SH1 (Princ.Plane 1) 4.04580 SH2 (Princ.Plane 2) -64.14902 EPD (Entr.Pup.Dia.) 200.0000

#### Bouwers-Cassegrain with Weak Corrector Lens: Sect. 43.13.14

#	TYPE	RADIUS	DISTANCE	GLASS		INDEX	APE-Y	AP	CP I	DΡ	TP	MP	GLB
OBJ	S	Infinity	0.10000E+21			1.000000	0.00						
STO:	>S	17311.0000	10.16000	N-BK7		1.518726	100.00						
2	S	-17311.0000	280.97000			1.000000	100.02						
3	S	-458.7357	40.63700	N-BK7		1.518726	100.30						
4	S	-507.9703	487.68822			1.000000	103.44						
5	SM	-1219.1100	-450.00000			-1.000000	108.00						
6	SM	-477.3945	551.20192			1.000000	32.22						
IMG	S	-433.9679				1.000000	13.96						
		DATA AT INFINIT											
1	EFL		2000.0000	0	SH1	(Princ.Plane	1)	-28	362.8	888	306		
]	FNO		10.0000	0	SH2	(Princ.Plane	2)	-14	148.6	539	907		
1	EPD (E	Entr.Pup.Dia.)	200.000	0									

#### Schmidt-Bouwers: Sect. 43.13.14 APE-Y 0.00 # TYPE RADIUS DISTANCE GLASS INDEX Infinity 0.10000E+21 6869.7508 10.00000 OBJ S 1.000000 10.00000 N-BK7 1.518726 100.00 1>A 44678.1609 96975.7532 20090.2398 2 S 1.00000 10.00000 N-SF1 STO S 1.723088 99.97 351.35332 100.04 4 S 103.66 5 S -463.1522 20.00000 N-BK7 1.518726 260.00000 -150.00000 200.00252 -465.7098 1.000000 6 S -551.7190 -631.4152 -1.000000 107.84 7 SM 1.000000 48.98 8 SM IMG S Infinity 1.000000 3.15 ASPHERES: K В # Type A 1 EVEN -0.0021174267 -0.16244243E-08 -0.54083694E-14 0.00000000E+00 PARAXIAL DATA AT INFINITE CONJUGATES: 449.99583 SH1 (Princ.Plane 1) 424.73313 -249.99149 FNO 2.24998 SH2 (Princ.Plane 2) EPD (Entr.Pup.Dia.) 200.0000

Maksı	utov, Con	npact:	Sect. 43.13.1	4				
# '	TYPE	RADIUS	DISTANCE	GLASS	INDEX	APE-Y		
OBJ :	S	Infinity	0.10000E+21		1.000000	0.00		
STO>	S	-171.4400	9.44000	K5	1.524587	62.50		
2	S	-189.8800	142.06000		1.000000	63.89		
3	SM	-402.3400	-142.06000		-1.000000	68.26		
4	SM	-189.8800	76.25000		1.000000	21.02		
5	S	40.7000	3.63000	K5	1.524587	17.32		
6	S	92.5000	43.80000		1.000000	17.09		
7	S	-75.6400	2.42000	K5	1.524587	9.84		
8	S	26.5600	82.76000		1.000000	9.39		
9	S	89.9700	5.05000	K5	1.524587	9.39		
10	S	-35.3500	2.42000	LF5	1.584824	9.39		
11 :	S	-89.9700	15.62445		1.000000	9.39		
IMG	S	Infinity			1.000000	10.49		
		A AT INFINI	TE CONJUGATES	-		- 1		
_	FL		999.7668		SH1 (Princ.Pl			
F	NO		7.9981		SH2 (Princ.Pl	ane 2)	-983.59976	
E	PD (Entr	.Pup.Dia.)	200.000	0				

Klevtsov:	Sect.	43.14.7					
# TYPE	RADIUS	DISTANCE	GLASS	INDEX	APE-Y		
OBJ S	Infinity	0.10000E+21		1.000000	0.00		
STO>SM		-389.61831			100.00		
2 S	-140.0733	-24.17787	N-LAK8	-1.713179	38.68		
3 S	-151.3247	-4.28145		-1.000000	33.93		
4 S	1336.5742	-7.12762	KF3	-1.514665	33.93		
5 SM	-710.9795	7.12762	KF3	1.514665	32.94		
6 S	1336.5742	4.28145		1.000000	32.72		
7 S	-151.3247	24.17787	N-LAK8	1.713179	32.71		
8 S	-140.0733	469.63798		1.000000	34.52		
IMG S	-186.5782			1.000000	10.64		
EFL FNO	TA AT INFINI	TE CONJUGATES 1520.3462 7.6017 200.000	3	(Princ.Plane		-1872.92011 -1050.94211	
Telephoto Le	RADIUS	Sect. 43.14.8	GLASS	INDEX	APE-Y		

Telephoto Len	s:	Sect. 43.14.8	3			
# TYPE OBJ>	RADIUS Infinity	DISTANCE 0.10000E+21	GLASS	INDEX 1.000000	APE-Y	
1 S 2 S	764.9290 -765.3200	13.03116	BK7	1.518726 1.000000	62.68 62.23	
4 SM	-152.0293 -251.1665	17.85269 -17.85269		1.518726 -1.518726	53.69 54.68	
	-75.7019			-1.000000 -1.518726	53.69 19.55	
8 S	-129.4359 -75.7019	54.07931	BK7	1.518726 1.000000 1.518726	18.28 18.54 15.11	
10 S 11 S		9.77337	K3	1.000000	14.82 15.46	
12 S 13 S	-54.2122 53.9933	0.65156 6.51558	LASF3	1.000000 1.812742	17.28 19.13	
14 S IMG S	87.2410 Infinity	81.31956		1.000000	18.95 28.46	
EFL FNO	A AT INFINI	TE CONJUGATES 644.9345 6.4493 100.000	5 5	(Princ.Plane (Princ.Plane	,	

858	43 Telescopes			
	Schupmann Me	dial Telescope	<b>e</b> :	Sect. 43.14.9
	# TYPE	RADIUS	DISTANCE	GLASS

# TYPE	RADIUS	DISTANCE	GLASS	INDEX	APE-Y		
OBJ S		0.10000E+21		1.000000	0.00		
1>S	Infinity	0.00000		1.000000	0.00		
STO SD	546.1473	15.00000	N-BK7	1.518726	50.09		
3 S	-10234.4070	979.99425		1.000000	49.75		
4 SD	121.4471	10.00000	BK7	1.518726	4.74		
5 SMD	Infinity	-10.00000	BK7	-1.518726	4.74		
6 S	Infinity	0.00000		-1.000000	4.74		
7 S	Infinity	-284.79426		-1.000000	5.17		
8 SD	127.5798	-5.00000	BK7	-1.518726	13.34		
9 S	200.6849	-1.99854		-1.000000	13.73		
10 SD	63.6818	-5.00000	BK7	-1.518726	13.78		
11 SM	123.6401	5.00000	BK7	1.518726	14.60		
12 S	63.6818	1.99854		1.000000	13.75		
13 SD	200.6849	5.00000	BK7	1.518726			
14 S	127.5798	300.41668		1.000000			
IMG SD	Infinity			1.000000	6.27		
	/						
	/ TILTS :						
#	XDE	YDE	ZDE	ADE	BDE	CDE TLM TSEQ	
2	0.0000	0.0000	0.0000	0.1948	0.0000		
4	0.0000	-3.3837	0.0000	0.8852	0.0000	0.0000 NAX XYZAI	
5		0.0000	0.0000	-45.0000	0.0000	0.0000 BEN XYZAI	
8	0.0000	-5.7459	0.0000	1.6906		0.0000 NAX XYZAI	
10	0.0000		0.0000				
13	0.0000	-0.0181	0.0000	1.6106	0.0000	0.0000 NAX XYZAI	
15	0.0000	0.0000	0.0000	3.4448	0.0000	0.0000 NAX XYZAI	3C
PARAXTAL	DATA AT INFINI	TE CONJUGATES	3:				
EFL		-1000.000		SH1 (Princ.Pl	ane 1)	-4235.16932	
FNO		-9.982		SH2 (Princ.Pl			
	ntr.Pup.Dia.)			(	/		
212 (2		100.00					

Schunmann Medial Tele	scope with Reflective Corrector:	Sect. 43.14.9

#	TYPE	RADIUS	DISTANCE	GLASS	INDEX	APE-Y			
OBJ	S	Infinity	0.10000E+21		1.000000	0.00			
STO:	>SD	1195.2312	15.62500	N-BK7	1.518726	75.00			
2	SD	-49425.2769	2236.50000		1.000000	74.77			
3	SDM	-1570.7495	-1200.00000		-1.000000	9.76			
4	SD	321.7179	-11.25000	BK7	-1.518726	38.93			
5	SM	632.0885	11.25000	BK7	1.518726	39.63			
6	S	321.7179	1201.77983		1.000000	38.84			
IMG	SD	Infinity			1.000000	9.73			
		-							
DEC	ENTER /	TILTS :							
#		XDE	YDE	ZDE	ADE	BDE	CDE	TLM	TSEQ
1		0.0000	0.0000	0.0000	0.0000	0.0000	0.0000	DAR	XYZABC
2		0.0000	0.0000	0.0000	-0.0065	0.0000	0.0000	DAR	XYZABC
3		0.0000	0.0000	0.0000	-2.3000	0.0000	0.0000	BEN	XYZABC
4		0.0000	0.0000	0.0000	0.6000	0.0000	0.0000	NAX	XYZABC
7		0.0000	0.0000	0.0000	-1.2328	0.0000	0.0000	NAX	XYZABC
PAR	AXIAL D	ATA AT INFINI	TE CONJUGATES	3:					
]	EFL		-2249.9999	98	SH1 (Princ.Pla	ane 1)	-6437.154	83	
1	FNO		-15.0000	0.0	SH2 (Princ.Pla	ane 2)	3451.855	45	
]	EPD (En	tr.Pup.Dia.)	150.000	0.0					
		-							

### Ross Corrector for an F6/1200mm Parabolic Primary:

### Sect. 43.15.2

#	TYPE	RADIUS	DISTANCE	GLASS	INDEX	APE-Y	
OBJ	S	Infinity	0.10000E+21		1.000000	0.00	
STO:	>AM	-2400.0000	-1000.00000		-1.000000	100.00	! Parabolic primary
2	SDM	Infinity	122.00000		1.000000	31.54	! fold mirror
3	S	123.4400	3.04800	N-BK7	1.518726	20.00	
4	S	60.4500	9.13000		1.000000	20.00	
5	S	217.4200	8.89000	N-BK7	1.518726	20.00	
6	S	-217.4200	64.18011		1.000000	20.00	
IMG	S	Infinity			1.000000	10.77	
ASPI	HERES:						
#	Type		K	A	В		C
1	EVEN	-1.000000000	0.00000000	E+00 0	.0000000E+00	0.000000	00E+00
DEC	ENTER ,	/ TILTS :					
#		XDE	YDE	ZDE	ADE	BDE	CDE TLM TSEQ
2		0.0000	0.0000	0.0000	45.0000	0.0000	0.0000 BEN XYZABC
PAR	AXIAL I	DATA AT INFINI	re conjugates	5:			
1	EFL		1200.8501	.8	SH1 (Princ.Pl	ane 1)	920.73749
1	FNO		6.0042	15	SH2 (Princ.Pl	ane 2)	-1136.64332
1	EPD (Er	ntr.Pup.Dia.)	200.000	0			

### Three-lens Corrector for an F6/1200mm Parabolic Primary:

### Sect. 43.15.2

#	TYPE	RADIUS	DISTANCE	GLASS	INDEX	APE-Y	
OBJ	S	Infinity	0.10000E+21		1.000000	0.00	
STO:	>AM	-2400.0000	-1020.00000		-1.000000	100.00	! Parabolic primary
2	SDM	Infinity	109.00000		1.000000	31.54	! fold mirror
3	S	31.6345	4.00000	BK7	1.518726	14.85	
4	S	32.4123	23.97219		1.000000	14.36	
5	S	49.1084	3.00000	BK7	1.518726	12.80	
	S	23.0498	22.10063		1.000000	11.99	
7	S	60.3302	4.00000	BK7	1.518726	13.05	
8	S	-174.1368	17.98919		1.000000	13.05	
IMG	S	Infinity			1.000000	10.77	
#	HERES: Type EVEN	_	0.0000000	A E+00 (	B 0.00000000E+00	0.0000000	C 00E+00
DECI	ENTER /	TILTS :					
#	J. (1221)	XDE	YDE	ZDE	ADE	BDE	CDE TLM TSEO
2		0.0000		0.0000	45.0000	0.0000	0.0000 BEN XYZABC
1	EFL FNO	ATA AT INFINIS	TE CONJUGATES 1269.9905 6.3499 200.000	0	SH1 (Princ.Pla		5285.69182 -1251.97457

# Jones Corrector for an F4/800mm Spherical Primary:

### Sect. 43.15.3

#	TYPE	RADIUS	DISTANCE	GLASS	INDEX	APE-Y	
OBJ	S	Infinity	0.10000E+21		1.000000	0.00	
STO:	>SM	-1600.0000	-586.87000		-1.000000	100.00	
2	S	294.5948	-11.00000	SF2	-1.652228	30.96	
3	S	124.5392	-11.00000	N-BK7	-1.518726	30.79	
4	S	-300.1518	-509.72456		-1.000000	29.95	
IMG	S	Infinity			-1.000000	14.09	
1	EFL FNO	TA AT INFINIT	CE CONJUGATES 2000.0000 10.0000 200.000	0	(Princ.Plane	,	-3430.39073 1489.59713

# Brixner Corrector for an F4/800mm Spherical Primary: Sect. 43.15.3

#	TYPE	RADIUS	DISTANCE	GLASS		INDEX	APE-Y			
OBJ	S	Infinity	0.10000E+21			1.000000	0.00			
STO:	>SM	-1600.0000	-579.40000			-1.000000	100.00			
2	S	637.4474	-11.00000	N-BK7		-1.518726	30.96			
3	S	-95.4508	-11.00000	F4		-1.620589	30.79			
4	S	-198.2834	-517.96542			-1.000000	29.95			
IMG	S	Infinity				-1.000000	14.09			
PARA	PARAXIAL DATA AT INFINITE CONJUGATES:									
I	EFL		1999.8765	4	SH1	(Princ.Plane	1)	-3412.67352		
I	FNO		9.9993	8	SH2	(Princ.Plane	2)	1481.07553		
EPD (Entr.Pup.Dia.) 200.0000										

# Jones–Bird Corrector for an F4/800mm Spherical Primary: Sect. 43.15.3

# TYPE OBJ S	RADIUS Infinity	DISTANCE 0.10000E+21	GLASS		INDEX 1.000000	APE-Y		
STO>SM	-1562.9600	-610.06000				100.00		
2 S	379.5399	-5.02000	N-BK7		-1.518726	26.28		
3 S	-159.6144	-0.60000			-1.000000	25.83		
4 S	-109.3709	-5.64000	N-F2		-1.624089	25.84		
5 S	-194.4133	-252.47411			-1.000000	25.44		
IMG S	Infinity				-1.000000	8.44		
PARAXIAL DATA AT INFINITE CONJUGATES:  EFL 1200.00001 SH1 (Princ.Plane 1) -1555.0839;  FNO 6.00000 SH2 (Princ.Plane 2) 947.1540.  EPD (Entr.Pup.Dia.) 200.0000								

### Two-lens Corrector for a Cassegrain Telescope: Sect. 43.15.4

#	TYPE	RADIUS	DISTANCE	GLASS	S INDEX	APE-Y		
OBJ	S	Infinity	0.10000E+21		1.000000	0.00		
STO:	>AM	-2000.0000	-712.50000		-1.000000	100.00	! parabolic primar	У
2	AM	-862.5000	716.95960		1.000000	33.76	! hyperb. secondar	y
3	S	Infinity	20.00000		1.000000	33.76		
4	S	-125.0627	8.00000	N-BK7	1.518726	22.83		
5	S	-74.4834	19.42596		1.000000	23.18		
6	S	-62.2029	6.00000	N-BK7	1.518726	21.45		
7	S	-116.7210	100.02811		1.000000	21.97		
IMG	S	Infinity			1.000000	22.23		
ASPI	HERES:							
#	Type	K		A	В		C	
1	EVEN	-1.0000000000	0.00000000	E+00	0.0000000E+00	0.0000000	0E+00	
2	EVEN	-4.0000000000	0.00000000	E+00	0.0000000E+00	0.0000000	0E+00	
PARA	AXIAL DA	ATA AT INFINIT	E CONJUGATES	:				
3	EFL		3162.2234	5	SH1 (Princ.Pl	ane 1) -	11413.86363	
]	FNO		15.8111	2	SH2 (Princ.Pl	ane 2)	-3062.10537	
1	EPD (Ent	r.Pup.Dia.)	200.000	0				

### Focal Reducer (0.5x) for a Ritchey-Chretien Telescope (Shapley Lens):

### Sect. 43.15.5

#	TYPE	RADIUS	DISTANCE	GLASS	INDEX	APE-Y		
OBJ	S	Infinity 0	.10000E+21		1.000000	0.00		
STO:	>AM	-1200.0000	-426.92308		-1.000000	100.00	! hyperb.	primary
2	AM	-494.5055	486.92310		1.000000	30.80	! hyperb.	secondary
3	S	Infinity	20.00000		1.000000	30.80		
4	S	31.2317	4.00000	N-PSK53	1.622229	11.36		
5	S	348.1540	2.00000	N-SF11	1.791155	11.12		
6	S	60.6459	4.00000	N-PSK53	1.622229	10.92		
7	S	136.3758	27.87610		1.000000	10.65		
IMG	S	Infinity			1.000000	7.49		
ASPI	HERES:							
	Type	К		A	В		C	
	EVEN	-1.0696266930	0.00000000		00000000E+00	0.0000000	0E+00	
	EVEN	-4.1566206430	0.00000000		00000000E+00	0.0000000		
PARA	AXIAL D	ATA AT INFINITE	CONJUGATES	:				
1	EFL		1000.0000	0	SH1 (Princ.Pla	ane 1)	23076.218	89
]	FNO		5.0000	0	SH2 (Princ.Pla	ane 2)	-972.086	31
1	EPD (En	ntr.Pup.Dia.)	200.000	0				

### Focal Extender (2x) for a Ritchey-Chretien Telescope (Barlow Lens):

### Sect. 43.15.6

# TYPE OBJ S STO>AM 2 AM 3 S 4 S 5 S 6 S IMG S	RADIUS Infinity ( -1200.0000 -494.5055 Infinity 117.6132 -122.0040 57.5211 Infinity	DISTANCE 0.10000E+21 -426.92308 486.92310 20.00000 8.00000 5.00000 119.42647	N-SF1 N-LAS	1	INDEX 1.000000 -1.000000 1.000000 1.791155 1.887609 1.000000		! hyperb.	primary secondary
ASPHERES	: к		2		В		a	
# Type			A		_		C	
1 EVEN	-1.0696266930	0.00000000			0000E+00	0.0000000		
2 EVEN	-4.1566206430	0.00000000	E+00	0.0000	0000E+00	0.0000000	00E+00	
EFL FNO	DATA AT INFINITE	CONJUGATES 3999.9984 19.9999 200.000	2	SH1 SH2			-71564.258 -3880.664	

# 43.18 Literature

- 43-1 G.B. Airy, On the Diffraction of an Annular Aperture, Philosophical Magazine, Series 3, Vol. 18, pp. 1–10, 132–133 (1841); a reprint is available from SPIE Milestone Series, Vol. MS 74 (SPIE, Washington, 1994), ISBN 0-8194-1215-5.
- **43-2** H. Bach and N. Neuroth, The Properties of Optical Glass (Springer, Berlin, 1995).
- **43-3** J.G. Baker, Proc. Amer. Philos. Soc. **82**, 339 (1940).
- 43-4 J.G. Baker, US Patent 2,458,132 (1945).

- **43-5** A.D. Beach, Compact Imaging System Including an Aspheric Quaternary Element, PCT WO 01/77734 A1 (2001).
- 43-6 K.M. Bystricky and P.R. Yoder Jr., Catadioptric lens with aberrations balanced by aspherizing one surface, Appl. Opt. 24, 1206 (1985).
- **43-7** M. Born and E.Wolf, Principles of Optics, 6<sup>th</sup> ed. (Pergamon Press, New York, 1980).
- **43-8** M. Brunn, Unobstructed All-reflecting Telescopes of the Schiefspiegler Type, USP 5,142,417 (1992).

- 43-9 L.G. Cook, Three-mirror Anastigmatic Optical System, USP 4,265,510 (1981).
- 43-10 L.G. Cook, Wide Field of View Focal Threemirror Anastigmat, USP 5,170,284 (1992).
- 43-11 L.G. Cook, Off-axis Three-mirror Anastigmat Having Corrector Mirror, USP 5,550,672
- 43-12 L.G. Cook, Fast-folded Wide-angle Large Reflective Unobscured System, USP 5,331,470 (1994).
- 43-13 H. Hirsch and E. Dietsch, German patent DE 19964079 C1 (1999).
- 43-14 D.C. Dilworth, Sky & Telescope, 425, Nov. 1977.
- 43-15 G.Z. Dimitroff and J.G. Baker, Telescopes and Accessories (The Harvard Books on Astronomy, Philadelphia, 1945), p. 105.
- 43-16 R. Duplov, Apochromatic telescope without anomalous dispersion glasses, Appl. Opt. 45, 5164 (2006).
- 43-17 E. Everhart and J.W. Kantorsky, Diffraction effects produced by obstructions in reflecting 43-38 D. Korsch, Reflective Optics (Academic telescopes of modest size, Astronomical Journal, Dec. 1959, p. 64.
- 43-18 J. Francis, New Twist on Tilted-Mirror Telescopes, Sky & Telescope, July 1999, p. 128.
- 43-19 J. Gregory, A Cassegrainian-Maksutov Telescope Design for the Amateur, Sky and Telescope, March 1957, pp. 236-239.
- 43-20 MK. Brass (Ed.), Handbook of Optics, Vol.II (McGraw-Hill, New York, 1995).
- 43-21 H. Haferkorn, Optik (VEB Deutscher Verlag der Wissenschaften, Berlin, 1981).
- 43-22 K.L. Hallam, Wide-angle Flat- field Telescope, USP 4,598,981 (1986).
- 43-23 D.G. Hawkins and E.H. Linfoot, Monthly Notices of the Royal Astronomical Society of London, vol. 105, Dec. 11, pp. 334-344 (1945).
- 43-24 E. Herrig, Kompakt-Schiefspiegler, German patent DE 196 49 841 C2 (1996).
- 43-25 M.Herzberger, Color correction in optical systems and a new dispersion formula, Opt. Acta 6, 197 (1959).
- 43-26 J.L. Houghton, "Lens System", USP 2,350,112 (May 1944)
- 43-27 J.M. Howard and B.D. Stone, Imaging a point with two spherical mirrors, Appl. Opt. **15**, 3045 (1998).
- 43-28 J.M. Howard and B.D. Stone, Imaging with three spherical mirrors, Appl. Opt. 39, 3216

- 43-29 J.M. Howard and B.D. Stone, Imaging with four spherical mirrors, Appl. Opt. 39, 3232 (2000).
- 43-30 Y. Iizuka, Catadioptric Telephoto Lens, USP 4,666,259 (1987).
- 43-31 F.A. Jenkins and H.E. White, Fundamentals of Optics (McGraw-Hill, New York, 1976).
- 43-32 R.S. Kebo, Four-mirror Afocal Wide Field of View Optical System, USP 4,804,258 (1989).
- 43-33 R.Kingslake, Lens Design Fundamentals (Academic Press, New York, 1978).
- 43-34 Kellner, Projecting lamp, USP 969,785 (Sept. 1910).
- 43-35 Yu.A. Klevtsov, New optical system for smallsize telescopes, J. Opt. Technol. 67, 176
- 43-36 A. König and H. Köhler, Die Fernrohre und Entfernungsmesser (Springer Verlag, Berlin,1959).
- 43-37 D. Korsch, Wide-field Three-mirror Collimator, USP 4,737,021 (1988).
- Press, New York, 1991).
- 43-39 D. Korsch, Aplanatic two-mirror telescope from near-normal to grazing incidence, Appl. Opt. 19, 499 (1980).
- 43-40 D. Korsch, Anastigmatic Three-mirror Telescope, USP 4,101,195 (1978).
- 43-41 A.Kutter, The Schiefspiegler (oblique telescope), Sky Publishing Corp., Harvard Observatory (1958).
- 43-42 M. Laikin, Lens Design (Marcel Dekker, New York, 2001).
- 43-43 U. Laux, Astrooptik (Verlag Sterne und Weltraum, Hüthig GmbH, 1999).
- 43-44 M. Lidwell, Catadioptric Systems for Pushbroom Sensors, Proc. SPIE 1191, 161 (1989).
- 43-45 E.H. Linfoot and E. Wolf, Diffraction Images in Systems with an Annular Aperture, Proc. Phys. Soc. B 66, 143 (1953).
- 43-46 N. Loveday, A Folded Newtonian with Dual Focal Length, Sky and Telescope, June 1981, pp. 543-548.
- 43-47 R.J. Lurie, Anastigmatic Catadioptric Telescopes, JOSA 65, 216 (1975).
- 43-48 D. Malacara, Handbook of Lens Design (Marcel Dekker, New York, 1994).
- 43-49 D.D. Maksutov, New Catadioptric Meniscus Systems, JOSA 34, 270 (1944).
- 43-50 R.G. Marsh and H.N. Sissel, A Comparison of Wide-angle, Unobscured, All-reflecting Optical Designs, Proc. SPIE 818, 168–182 (1987).

- **43-51** J. Maxwell, Tertiary-spectrum manipulation in apochromats, Appl. Opt. **31**, 2194 (1992).
- **43-52** J. Maxwell, Catadioptric Imaging Systems (Adam Hilger Ltd., London, 1972).
- **43-53** E.L. McCarthy, Optical System with Corrected Secondary Spectrum, USP 2,698,555 (1949).
- 43-54 R.I. Mercado, Design of apochromats and superapochromats, Proc. SPIE CR41: Lens Design, edited by Warren J.Smith (1992).
- **43-55** R.I. Mercado and L. Ryzhikov, Designs of Apochromats and Superachromatic Objectives, SPIE **3482**, 321–331 (1998).
- 43-56 MIL-Handbook Optical Design, MIL-HDSK-141 (Defense Supply Agency, Washington D.C., USA, 1962).
- 43-57 H. Kaspar, Carl Zeiss Superachromate für Hasselblad, Magazin für Photographie und Medientechnik, AGT Verlag Thum GmbH, May 1998, pp. 36–38.
- **43-58** K. Penning, Optisches Spiegelsystem zur Erzeugung reeller Bilder, German Patent 907709 (1954).
- **43-59** M. Paul, Rev. Opt. Theor. Instrum. **14**, 169 (1935).
- **43-60** I. Powell, Design of a 360mm focal length, F/3.6 spectrograph objective, Opt. Eng. **27**, 1042 (1988).
- **43-61** R. Riekher, Fernrohre und ihre Meister (Verlag Technik GmbH, Berlin, 1990).
- 43-62 John M. Rodgers, Catadioptric Optical System Including Concave and Convex Reflectors, USP 5,309,276 (1994).
- **43-63** F.E. Ross, Lens Systems for correcting Coma of Mirrors, Astrophysical Journal **81**, 156 (1935).
- **43-64** N.J. Rumsey, Telescopic System Utilizing Three Axially Aligned Substantially Hyperbolic Mirrors, USP 3,460,886 (1969).
- **43-65** H. Rutten and M.v. Venrooij, Telescope Optics (Willman–Bell Inc., 1988).
- **43-66** Schott, 2000 Optical Glass Catalog, published by Schott AG, Hattenbergstr. 10, 55122 Mainz, Germany
- **43-67** D.J. Schroeder, Astronomical Optics (Academic Press, New York, 2000).
- **43-68** G. Schröder and H. Treiber, Technische Optik (Vogel Buchverlag, 2002).
- **43-69** L. Schupmann, Über Medial-Fernrohre von kurzer Brennweite, Zeitschr. f. Instrumentenk., Oct. 1913, pp. 308–312.

- 43-70 L. Schupmann, Berechnung der Medial-Fernrohre mit einfacher Spiegellinse, Zeitschr. f. Instrumentenk., July 1921, pp. 212–219.
- **43-71** L.Schupmann, Optical correcting device for refracting telescopes, USP 620,978 (1899).
- 43-72 K. Schwarzschild, Untersuchungen zur geometrischen Optik I – III (Dietrich'sche Univ.-Buchdruckerei, Göttingen, 1905).
- **43-73** D.R. Shafer, Four-mirror unobscured anastigmatic telescopes with all-spherical surfaces, Appl. Opt. **17**, 1072 (1978).
- **43-74** R.D. Sigler, Glass selection for airspaced apochromats using the Buchdahl dispersion equation, Appl. Opt. **25**, 4311 (1986).
- 43-75 R.D. Sigler, All-spherical catadioptric telescope with small corrector lenses, Appl. Opt. 21, 2804 (1982).
- 43-76 R.L. Sinclair and R.H. Arsenault, Wide field-of-view three mirror telescope designed for improved manufacturability, Proc. SPIE, Vol. 1970: Systems-oriented optical design (1993), pp. 139–147.
- **43-77** W.J. Smith, Modern Optical Engineering (McGraw-Hill Inc., New York, 1990).
- **43-78** https://bhs.broo.k12.wv.us/homepage/alumni/dstevick/stevpaul.html
- **43-79** S.C. Tam, Optical system for target acquisition and ranging, Opt. Eng. **23**, 448 (1984).
- **43-80** H.F.A. Tschunko, Image performance of annular apertures, Appl. Opt. **18**, 3770 (1979).
- 43-81 J.J. Ulmes, Design of a catadioptric lens for long-range oblique aerial reconnaissance, Proc. SPIE, Vol. 1113: Reflective Optics II (1989).
- **43-82** K. Wenske, Spiegeloptik (Bibliographisches Institut, Mannheim, 1967).
- 43-83 W.B. Wetherell and M.P. Rimmer, General analysis of aplanatic Cassegrain, Gregorian and Schwarzschild Telescopes, Appl. Opt. 11, 2817 (1972).
- 43-84 R.N. Wilson, Reflecting Telescope Optics I (Springer Verlag, Berlin Heidelberg, 1996).
- 43-85 R.V. Willstrop, The Mersenne–Schmidt: a three-mirror survey telescope, Mon. Not. R. Astron. Soc. 210, 597 (1984).
- **43-86** R.V. Willstrop, The flat-field Mersenne–Schmidt, Mon. Not. R. Astron. Soc. **216**, 411 (1985).
- **43-87** R.W. Sinnot, A new approach to color correction, Sky and Telescope, Oct. 1985, p. 375.

- **43-88** R.N. Wilson, Corrector systems for Cassegrain Telescopes, Appl.Opt. **7**(2), 253 (1968).
- **43-89** D. Shafer, Infrared Collimator System, Appl. Opt. **32**, 7117 (1993).
- **43-90** M. Shenker, High speed catadioptric objective in which three corrector elements define two power balanced air lenses, USP 3,252,373 (1966).
- 43-91 V.Y. Terebizh, A wide field corrector at the prime focus of a Ritchey-Chretien telescope, Astron. Lett. 30, 200–208 (2004).
- **43-92** S.C.B. Gascoigne, Recent advances in astronomical optics, Appl. Opt. **12**, 1419–1429 (1973).
- **43-93** D.J. Jones and W.E. James, Prime focus correctors for the spherical mirror, Appl. Opt. **31**, 4384–4388 (1992).
- 43-94 I.R. Abel and M.R. Hatch, The pursuit of symmetry in wide-angle reflective optical designs, Proc. SPIE, Vol. 237: International Lens Design Conference (1980), pp. 271– 280.

- 43-95 O.N. Stavroudis, The development of the Schiefspiegler, Proc. SPIE 2268, 38–47 (1994).
- 43-96 R.N. Wilson et.al., A new 4-mirror optical concept for very large telescopes with spherical primary and secondary mirrors, giving excellent field and obstruction characteristics, Proc. SPIE 2199, 1052–1063 (1994).
- **43-97** E.W. Cross, Explorations in eccentric pupil telescopes, Proc. SPIE **1049**: Recent Trends in Optical Systems Design II (1989)
- **43-98** D.R. Shafer, Magic with Mirrors, Photonics Spectra, pp. 103–104, July (1987)
- **43-99** H.B. Chung and S.S. Lee, Aplanatic four spherical mirror system, Opt. Eng. **24**, 317 (1985).
- **43-100** D.R. Shafer, Optical design with only two surfaces, Proc. SPIE **237**: International Lens Design Conference (1980).